

## Active restraint systems : feedback control of occupant motion

**Citation for published version (APA):**

Hesseling, R. J. (2004). *Active restraint systems : feedback control of occupant motion*. [Phd Thesis 1 (Research TU/e / Graduation TU/e), Mechanical Engineering]. Technische Universiteit Eindhoven.  
<https://doi.org/10.6100/IR578949>

**DOI:**

[10.6100/IR578949](https://doi.org/10.6100/IR578949)

**Document status and date:**

Published: 01/01/2004

**Document Version:**

Publisher's PDF, also known as Version of Record (includes final page, issue and volume numbers)

**Please check the document version of this publication:**

- A submitted manuscript is the version of the article upon submission and before peer-review. There can be important differences between the submitted version and the official published version of record. People interested in the research are advised to contact the author for the final version of the publication, or visit the DOI to the publisher's website.
- The final author version and the galley proof are versions of the publication after peer review.
- The final published version features the final layout of the paper including the volume, issue and page numbers.

[Link to publication](#)

**General rights**

Copyright and moral rights for the publications made accessible in the public portal are retained by the authors and/or other copyright owners and it is a condition of accessing publications that users recognise and abide by the legal requirements associated with these rights.

- Users may download and print one copy of any publication from the public portal for the purpose of private study or research.
- You may not further distribute the material or use it for any profit-making activity or commercial gain
- You may freely distribute the URL identifying the publication in the public portal.

If the publication is distributed under the terms of Article 25fa of the Dutch Copyright Act, indicated by the "Taverne" license above, please follow below link for the End User Agreement:

[www.tue.nl/taverne](http://www.tue.nl/taverne)

**Take down policy**

If you believe that this document breaches copyright please contact us at:

[openaccess@tue.nl](mailto:openaccess@tue.nl)

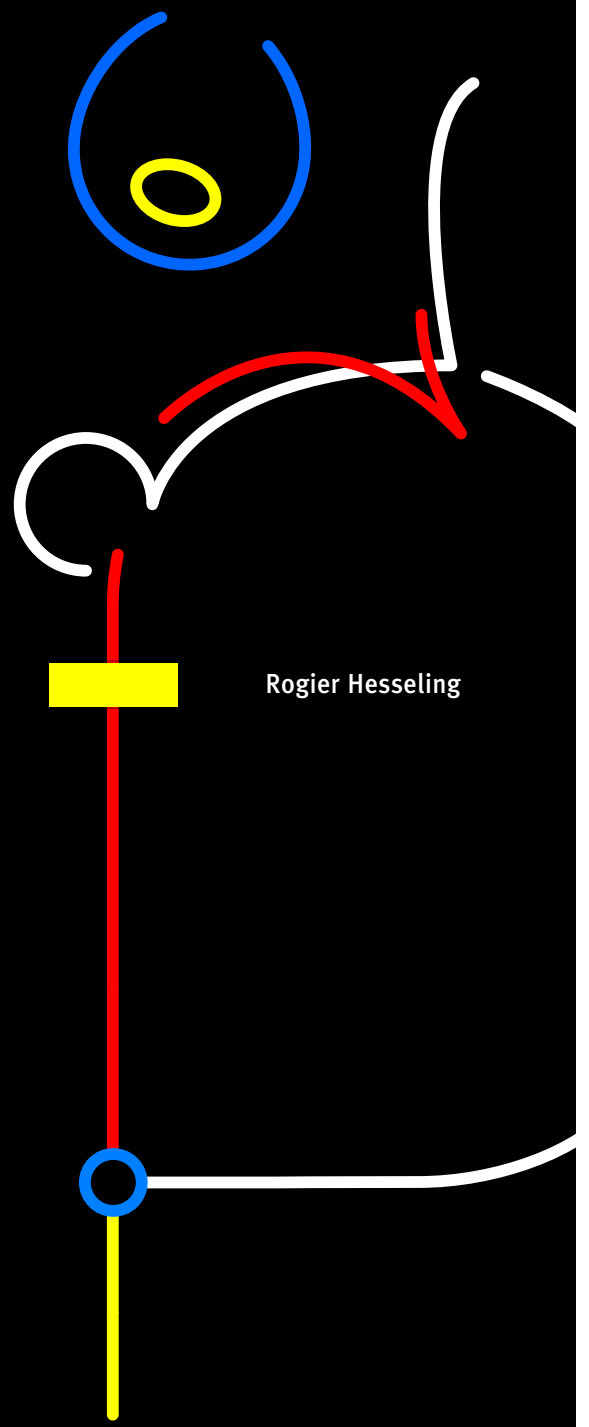
providing details and we will investigate your claim.

# Active Restraint Systems

## Feedback Control of Occupant Motion

Rogier Hesselting

Active Restraint Systems



Rogier Hesselting



# Stellingen

behorende bij the proefschrift

## Active Restraint Systems Feedback Control of Occupant Motion

1. Het dynamisch gedrag van de dummy, de gordel, de airbag en hun interacties kan als lineair worden beschouwd voor het regelaarontwerp.
  - Dit proefschrift
2. Nieuwe generaties restraint systemen zijn actieve restraint systemen.
  - Dit proefschrift
3. Gedetailleerde modellen geven blijk van matig inzicht in de essentie van het te modelleren systeem.
4. Ontwerpeisen zijn vaak moeilijk te formuleren als een wiskundig criterium. Het bereikte “optimum” is daarom niet altijd een optimaal ontwerp.
5. Regelaarontwerp wordt vaak ten onrechte gezien als een sluitpost van het ontwerp-proces.
6. Ter bevordering van de verkeersveiligheid is de eenheid meter per seconde te verkiezen boven de eenheid kilometer per uur.
7. Het bedrijfsleven mag aangeven welk onderzoek aan de universiteit gewenst is, maar mag dit niet dwingend voorschrijven.
8. Echte vrienden doen géén “toneelstukjes” bij promotiefeesten.
9. Gebruik van bijnamen relativeert het leven.
10. Sommige mensen zouden blij zijn als ze met de handen in het haar kunnen zitten.
11. Beter een goede buurvrouw dan een verre vriendin.

Rogier Hesseling  
Eindhoven, augustus 2004



# Active Restraint Systems

## Feedback Control of Occupant Motion

This research was conducted in co-operation with and financially supported by Bayerische Motoren Werke (BMW Group), Munich, Germany.

CIP-DATA LIBRARY TECHNISCHE UNIVERSITEIT EINDHOVEN

Hesseling, Rogier J.

Active Restraint Systems - Feedback Control of Occupant Motion / by Rogier J. Hesseling. – Eindhoven : Technische Universiteit Eindhoven, 2004

Proefschrift. – ISBN 90-386-2616-9

NUR 977

Subject headings: automotive safety / safety belt / airbag / active restraint systems / linear time-invariant control design models / approximate realization / feedback control

© 2004 by R.J. Hesseling.

All rights reserved. This publication may not be translated or copied, in whole or in part, or used in connection with any form of information storage and retrieval, electronic adaptation, electronic or mechanical recording, including photocopying or by any similar or dissimilar methodology now known or developed hereafter, without the permission of the copyright holder.

Cover design: Rogier Hesseling/Jan van Helvoirt/JWL Producties.

Reproduction: Universiteitsdrukkerij TU Eindhoven, Eindhoven, The Netherlands.

# Active Restraint Systems

## Feedback Control of Occupant Motion

PROEFSCHRIFT

ter verkrijging van de graad van doctor  
aan de Technische Universiteit Eindhoven,  
op gezag van de Rector Magnificus, prof.dr. R.A. van Santen,  
voor een commissie aangewezen door het College voor Promoties  
in het openbaar te verdedigen  
op woensdag 15 september 2004 om 16.00 uur

door

Rogier Jelke Hesseling

geboren te Amsterdam



Dit proefschrift is goedgekeurd door de promotoren:

prof.dr.ir. M. Steinbuch

en

prof.dr.ir. P.P.J. van den Bosch

Copromotor:

dr.ir. F.E. Veldpaus

# Contents

<b>Summary</b>	<i>vii</i>
<b>1 Introduction</b>	<b>1</b>
1.1 Vehicle safety . . . . .	1
1.2 A crash . . . . .	4
1.3 Towards active restraint systems . . . . .	9
1.4 Towards a design expedient . . . . .	12
1.5 Objective and contribution of the thesis . . . . .	12
1.6 Outline of the thesis . . . . .	13
<b>2 Modelling for control design</b>	<b>15</b>
2.1 Introduction . . . . .	15
2.2 The complex nonlinear model . . . . .	16
2.3 Linearizing the complex nonlinear model . . . . .	23
2.4 Modelling of the belt . . . . .	26
2.5 Modelling of the airbag . . . . .	30
2.6 Discussion . . . . .	38
<b>3 Control design for restraint system components</b>	<b>41</b>
3.1 Introduction . . . . .	41
3.2 Strategy . . . . .	43
3.3 Control of the chest acceleration by the belt . . . . .	45
3.4 Control of the head acceleration by the airbag . . . . .	54
3.5 Actuator saturation . . . . .	60
3.6 Discussion . . . . .	63
<b>4 Control design for the restraint system</b>	<b>65</b>
4.1 Introduction . . . . .	65
4.2 Interaction analysis . . . . .	66
4.3 Control of the chest and the head acceleration . . . . .	70
4.4 Discussion . . . . .	76
<b>5 Explorations</b>	<b>77</b>
5.1 Introduction . . . . .	77
5.2 Control of the chest deflection by the belt . . . . .	77

---

5.3	A small female dummy . . . . .	85
5.4	Adaptive restraint systems . . . . .	90
5.5	A first investigation towards a new control strategy . . . . .	92
<b>6</b>	<b>Conclusions and Recommendations</b>	<b>99</b>
6.1	Introduction . . . . .	99
6.2	Discussion . . . . .	100
6.3	Conclusions . . . . .	102
6.4	Recommendations . . . . .	103
	<b>Bibliography</b>	<b>107</b>
	<b>Samenvatting</b>	<b>117</b>
	<b>Kurzfassung</b>	<b>119</b>
	<b>Dankwoord</b>	<b>121</b>
	<b>Curriculum Vitae</b>	<b>123</b>

# Summary

Major drawbacks of transportation by motor vehicles are crashes and the consequences thereof like injuries and fatalities. The safety belt and the airbag, often referred to as the restraint system, have been introduced to reduce the number and severity of injuries. The restraint system should behave differently for different crashes and/or different occupants. State-of-the-art belt and airbag systems are “adaptive”, meaning that they have a limited set of modes of operation to adapt to different occupants and crashes. Examples of these modes of operation are different deformation characteristics of the load limiter in the belt system and different points of triggering the inflators of the airbag.

Design of such modes of operation focus on achieving a satisfactorily low risk of injury for classes of occupants and crashes. Examples of measures for the risk of injury are the maximum chest acceleration, the maximum chest deflection and the maximum head acceleration. Appropriate modes of operation are typically obtained by minimization of the risk of injuries, using complex nonlinear models to simulate a vehicle and occupant, subjected to a crash test. Such an approach is time-consuming and the obtained modes are a compromise.

In this thesis, an innovative view on (the design of) restraint systems is elaborated. The idea is to add sensors and actuators in order to allow feedback control of the restraint system. The airbag and/or the belt are manipulated during the crash to force one or more occupant variables, representing the risk of injuries, to follow an a priori defined reference signal. This reference signal represents the lowest possible risk of injuries. This view on restraint systems can be seen as a starting point for the development of future restraint systems, and as a basis for an effective design expedient for modes of operation of real world restraint system components.

The concept of active restraint systems has been elaborated using the numerical model of a mid-size male dummy as the “driver” of a mid-size passenger car, subjected to the US-NCAP frontal crash test. To manipulate the airbag, the size of the vent in the airbag and the mass flow into the airbag have been chosen. To manipulate the belt, the force in the belt section near the load limiter, has been chosen. The chosen occupant variables are the chest acceleration, the head acceleration and the chest deflection. Reference signals are pragmatically determined.

Controllers to manipulate the airbag or the belt, cannot be designed using the available numerical model, since that is nonlinear and far too complex. Therefore, linear time-invariant (LTI) control design models are derived to approximate the relevant dynamic

behavior of the restraint system, the dummy and their interactions. These control design models are obtained with the approximate realization method, using the responses of the occupant variables to stepwise perturbations in the manipulated variables of the restraint system. Low order feedback controllers are designed using “loopshaping” techniques, aiming at a stable closed loop system with satisfactory performance. Finally, the controllers are implemented and evaluated in the closed loop system with the complex nonlinear model.

In comparison with the original restraint system, control of the chest acceleration by manipulation of the belt force can reduce the risk of chest injuries by 60 %. Control of the head acceleration by manipulation of the vent size reduces the risk of head injuries by 50 %. Appropriate simultaneous control of the chest and the head acceleration reduces the risk of injury to the chest and head by 50 % or more.

The modelling and the control design strategy have also been applied successfully to arrive at a controller for the chest deflection by manipulation of the belt force. In addition, the strategies have been applied successfully to arrive at controllers for the chest and the head acceleration for the case of a small female dummy as the “driver”.

It has become clear that the dynamic behavior of the belt and/or the airbag, interacting with the dummy can be considered linear, at least for control design purposes. Besides that, low order feedback controllers are effective to enforce the desired behavior of the complex nonlinear model. Furthermore, it turned out that the control design problem for simultaneous control of the head acceleration and the chest acceleration by manipulation of the vent size and the belt force can be treated as a decoupled control design problem. The modelling and control design strategy have shown to be effective and efficient. Insight into appropriate modes of operation for adaptive restraint systems can be obtained from results of closed loop simulations.

## CHAPTER ONE

# Introduction

*A short introduction of vehicle safety is given and the encountered complexities involving (the design of) restraint systems are glanced at. Furthermore, an innovative view on “active” restraint systems is elucidated.*

### 1.1 Vehicle safety

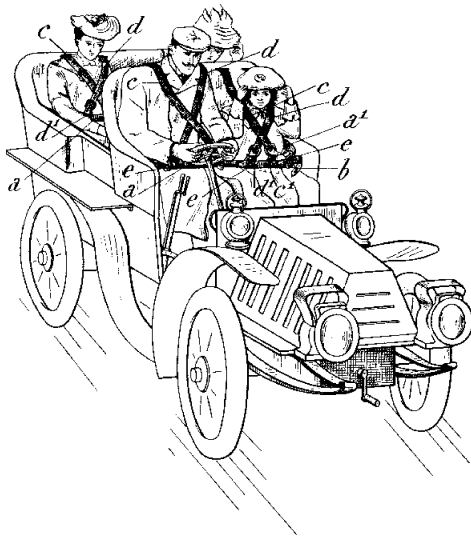
Motor vehicles are widely used for transport. Major drawback of this way of transportation are the number of crashes and the consequences thereof like crash costs, injuries and fatalities. For example, in 2001, costs of crashes were over 170 billion Euros [49]. In the same year, motor vehicle crashes were the leading cause of death and hospital admission for citizens under 50 years in the European Union, and 38 935 people died due to a crash [49].

A reduction of the number of crashes and the consequences thereof involves many aspects of economical, legal, medical, behavioral and engineering nature. An effective approach is the development of safe vehicles. To arrive at safe vehicles, various facilities have been introduced. One group of facilities, referred to as *active* safety facilities, aims to reduce the possibility that a crash occurs. Examples are the Electronic Brake Distribution (EBD) and the anti-lock braking system (ABS). The other group of facilities, referred to as *passive* safety facilities, aims to reduce the consequences in terms of injury severity in the event that a crash occurs. Examples are the crushing zone and the safety belt.

Within the group of passive safety facilities, the combination of vehicle components that restrain the occupant during a crash is called the restraint system. This system has to smoothly absorb the occupants kinetic energy to reduce the risk of severe or fatal injuries of vehicle occupants. The best known components are the safety belt and the airbag.

The first patent for an idea to restrain the occupant has been granted in 1903 [89]. The ‘bretelles protectrices pour voitures automobiles et autres’, shown in Figure 1.1(a), prevent the occupants from falling out of the car during a crash. State-of-the-art safety harnesses for Formula One cars are still based on the principles of that idea, Figure 1.1(b).

Once the goal of protection against falling out had been achieved, the next goal was to influence the occupants’ motion during a crash in order to prevent contact with the steering



(a) Leveau's idea of a safety belt in 1903, reproduced from [89]



(b) State-of-the-art safety harness for a Formula One car. Source: Sabelt Inc.

**Figure 1.1** The safety belt through the years

wheel or other vehicle interior parts. For that purpose, the three-point safety belt, developed by de Haven and Griswold in 1950 [5], has been introduced in the fifties. At that time, the first idea about a 'Safety Cushion Assembly for Automotive Vehicles', nowadays called an airbag, has been granted a patent [65], resulting in its first public appearance as an accessory for the 1973 Chevrolet Impala [15]. Over the last decades, the belt and airbag system have become more and more sophisticated by the introduction of additional components. An example is the so-called pre-tensioner to remove slack in the belt system as soon as a crash is detected.

Until the nineties, most of the restraint system components were "passive", meaning that they have only one mode of operation. However, research revealed that occupant characteristics like seating position, mass and age, influence the risk of severe or fatal injuries [30, 94]. In addition, it became clear that crash characteristics, like impact velocity, also influence the risk of injuries [172] and that different crashes may pose contradictory requirements on the restraint system. Besides that, forces applied by the restraint system on the occupant can cause severe or fatal injuries [9, 74].

Research and development nowadays focus on "adaptive" restraint system components with several modes of operation. Based on measurements of relevant occupant and/or crash characteristics, the most appropriate mode is chosen when the crash is detected. An example of this type is the choice of the point of time at which the airbag is inflated. Apart from that, pre-crash facilities like the reversible pre-tensioner [17] have recently been introduced to anticipate an oncoming crash.

### 1.1.1 Development of a restraint system

The development of real world restraint system components and their modes of operation is challenging, not only because crash and occupant characteristics play an important role, but also because vehicle characteristics which are not exactly known until the end of the development process of the vehicle, play a role. At the end of this process, changes to the vehicle or restraint system components are extremely expensive. In addition, aspects like cost, ergonomics, comfort, mass, durability and size are in conflict with each other and with the performance of the restraint system.

The goal of the development of a restraint system is a system that satisfactory performs for a wide spectrum of crashes and occupants and that satisfies criteria on cost, durability etcetera. To achieve that goal, numerical experiments or simulations, real world component tests and full scale crash tests are performed during the development process of the vehicle. Their importance during this process is illustrated in Figure 1.2.

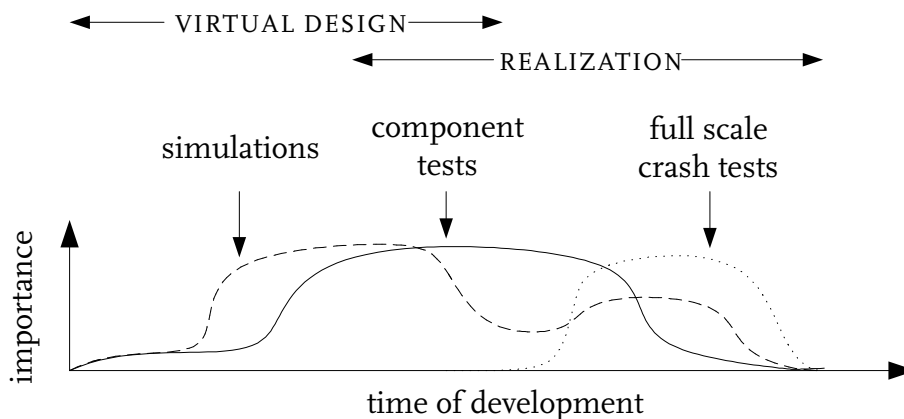


**Figure 1.2** Importance of simulations, component tests and full scale crash tests during the development process of a vehicle [80]

At the start of the vehicle development process, first economical and marketing issues are solved. Next, simulations are performed to evaluate innovative ideas and to roughly design appropriate modes of operation of the adaptive restraint system components. After that, the development of hardware is initiated and real world component tests are performed with (prototypes of) restraint system components to evaluate the components and to improve the quality of the simulation models. Finally, full scale crash tests with (prototypes of) the vehicle are performed and simulation models can be validated, if necessary.

The real world component tests involve components, assemblies or vehicle parts. Examples are the so-called tank test [122], where the inflator of the airbag is discharged into a closed volume to determine the actual mass flow, the seat belt assembly test [113] to evaluate whether the seat belt components can withstand the expected forces during a crash and the impactor test [112] to determine the acceleration of the dummy head, rep-



resented by an impactor [114], during impact on vehicle interior components like the steering wheel.

During the design process, the greater part of the simulations focus on the design of appropriate mode(s) of operation for the restraint system components. Typically, an appropriate mode of operation is determined using trial-and-error, e.g. [135, 159], in combination with optimization, e.g. [61, 68, 123, 130]. The relevant characteristics of the mode of operation, e.g. the point of time to inflate the airbag, are determined by the minimization of a cost function, representing one or more measures for the risk of injury. Due to the nonlinear nature of the investigated system, optimization is often performed using the response surface and stochastic method [23, 97, 105, 106].

For the design of a restraint system, trial-and-error is time-consuming and therefore unattractive. The optimization approach is more attractive, since it is straightforward and can deal with a complex numerical model. However, the number of (time-consuming) simulations is more than linearly related to the number of to-be-optimized characteristics. Typically, the number of simulations exceeds ten thousand. Apart from that, an obtained mode of operation represents a compromise, since it is not the most appropriate mode of operation for a specific combination of a crash and occupant, but is the most appropriate mode of operation for classes of crashes and occupants.

In this thesis, an innovative view [62, 63, 64] on restraint systems and their design is elaborated. Basically, it is the introduction of “active” restraint systems by adding actuators, sensors in order to apply feedback control. First, one or more relevant measures for the risk of injury are chosen. Second, a reference signal for these measures is defined, such that the risk of injuries is as low as possible, if the reference signal is followed. Finally, a feedback controller is designed to force the controlled variables to follow the reference signal. During a (simulation of the) crash, the controlled variables are continuously measured and the restraint system components are continuously manipulated. The innovative view can be seen as the basis for future restraint systems, and makes it possible to obtain the mode of operation of a restraint system component that achieves the lowest possible risk of injury for a specific combination of a crash and occupant.

## 1.2 A crash

Numerous physical phenomena take place during a crash. In this section, first relevant aspects of a crash, the occupant and the restraint system are elucidated, followed by a discussion of relevant phenomena during a crash. The focus is on normal passenger cars, since they are involved in more than 60 % of the total number of crashes resulting in fatal injuries [3].

### 1.2.1 Crashes

Roughly spoken, more than 50 % of the total number of fatal injuries occurs due to frontal crashes [116]. Hence, the focus here is on frontal crashes. To determine whether a car is safe, standardized crash tests [1] in a conditioned environment with crash dummies, are performed. In fact, legislative authorities have made crash tests compulsory to warrant that every new car has a minimum passive safety level. In addition, consumer and insurance institutes perform crash tests to classify the passive safety level of cars.

Analysis of real world crashes [151] has revealed that the severity of occupant injuries due to frontal crashes is significantly influenced by the relative velocity, the relative angle and the relative overlap of the crash partners [29, 151], as well as by the effective stiffness of the crash partners [172]. As a result of that, different crash tests have been defined. In Figure 1.3, the general configuration of a frontal crash test is shown. In this figure,  $\alpha$  represents the relative angle,  $v_0$  the relative velocity and  $\Delta L/L$  the relative overlap. The barrier can be a deformable or rigid barrier and can be located at the left or right side of the vehicle front. For most common crash tests, the angle  $\alpha$  is  $30^\circ$  or  $0^\circ$ , the overlap is 40 % or 100 % and the impact velocity varies from 28 km/h to 64 km/h.

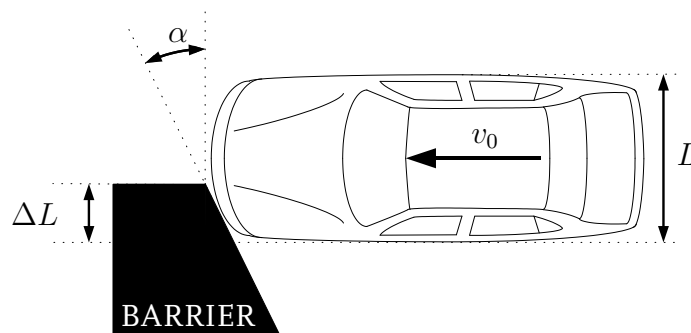


Figure 1.3 General configuration of a frontal crash test, reproduced from [2]

### 1.2.2 Occupants

Different occupants have different anthropometry and seating positions. Research has revealed that age, gender, size, mass and height of occupants significantly influence the risk of severe or fatal injuries and the injury tolerance [30, 52, 95]. Hence, different crash dummies have been developed for frontal crash tests. These crash dummies have a flexible rib-cage and consist of steel “bones” with layers of “flesh” and “skin”, connected by joints. They are designed to imitate as close as possible a human being, subjected to a crash test. Crash dummies are equipped with numerous sensors to measure accelerations, forces, torques and deflections. Examples of frontal crash dummies are the 3-year child crash dummy [71], the small female, mid-size male and large male crash dummy [100, 131, 140].

For most frontal crash tests, the mid-size male crash dummy, the so-called HYBRID III 50th percentile crash dummy [131], with a mass of 77.5 kg and a standing height of 1.75 m, is used. Here, “50th percentile” indicates that the value of the anthropometric measures are chosen such that 50 % of a certain population has a lower value. For most frontal crash tests, the dummy position represents a human in a normal seating position.

Injuries are caused by one or more of three principal injury mechanisms [35, 168], being compression of the body causing injuries if (elastic) tolerances are exceeded, impulsive loading causing injuries if viscous tolerances are exceeded and inertial loading causing internal structures to tear. To assess the risk of severe or fatal injuries, injury criteria with tolerance levels have been defined. The head and the thorax are the body parts most frequently involved in severe or fatal injuries due to a frontal crash [28, 30]. Important injury criteria for the risk of injury for these body parts are the Head Injury Criterion (HIC), the maximum acceleration of the head, the maximum acceleration of the chest and the maximum deflection of the sternum relative to the spine [50, 79]. The corresponding injury tolerances for a mid-size male crash dummy are 60 g for the maximum head and chest acceleration and 76 mm for the maximum chest deflection [48, 115].

### 1.2.3 Restraint Systems

Besides the belt and the airbag, vehicle parts like the knee bolsters and the seat also restrain the occupant. Although the seat does not significantly restrain the occupant during a frontal crash, the shape of its frame is important to prevent the pelvis to slide underneath the lap section of the belt [4]. Here, the focus is on the belt system and the airbag system for the driver of a mid-size passenger car. This combination will be used as the working example throughout the thesis. Other belt and airbag systems are described in [31, 70, 81] and in the references herein.

#### The belt system

The considered belt system is a three-point belt system, consisting of the belt, the buckle pre-tensioner, the load limiter and the D-ring, and is illustrated in Figure 1.4(a).

**The polyamide belt** has a length of approximately 2.5 m and a width of approximately 5 cm. Its elongation due to a loading of 11 kN is approximately 15 %. The belt is rigidly connected to the chassis at the downside of the B-pillar, goes over the pelvis to the buckle, cross-diagonally over the chest and is through the D-ring connected to the load limiter, in which the unused belt length is winded around a cylinder.

**The buckle pre-tensioner** consists of the buckle and the pre-tensioner. The buckle has to ensure that the chest section of the belt is cross-diagonally aligned over the chest and that the lap section of the belt is more or less horizontally aligned over the pelvis. The pyrotechnical pre-tensioner removes slack in the belt system by abruptly tightening the

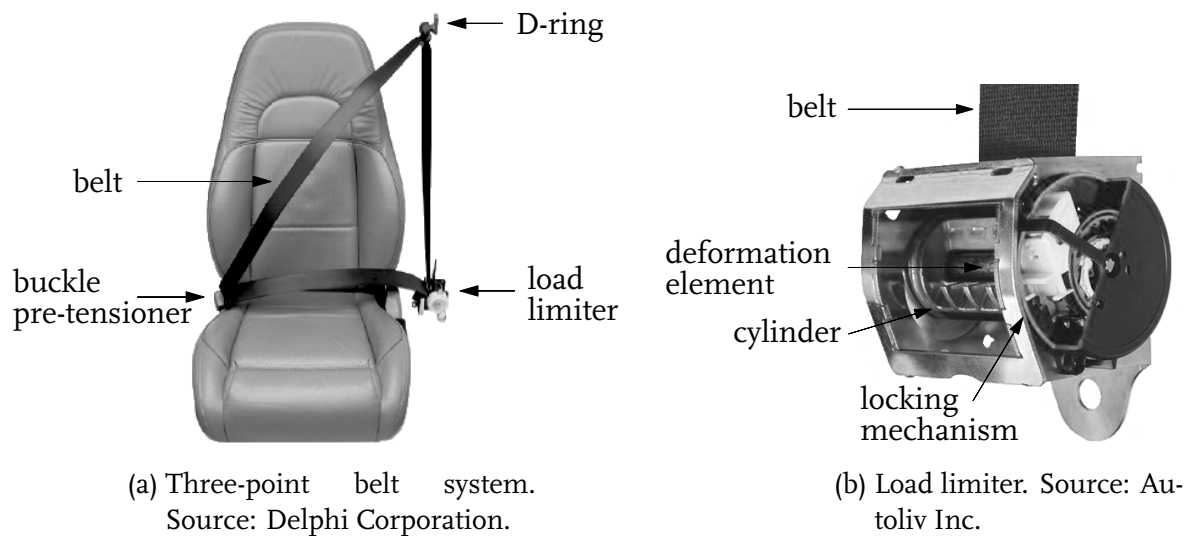


**Figure 1.4** Three-point belt system.

belt. The most important reason to combine the pre-tensioner with the buckle is the efficient removal of slack in the belt system with simultaneous tightening of the lap and chest section of the belt.

**The D-ring** is attached to the B-pillar. It has to properly align the belt over the chest and to allow a more or less free flow of the belt through the loop. For a proper belt alignment for small and tall occupants, the D-ring is height adjustable.

**The load limiter** limits the force applied to the occupant by the belt, and is shown in Figure 1.4(b). The rotation of the cylinder around which the unused belt is wound, is locked when its angular velocity exceeds a certain threshold, typically due to the abrupt tightening of the belt. From that point of time, the force in the section of the belt connected to the load limiter is limited by the deformation of certain load limiter components. The design of the belt system often focus on the (adaptation) of these deformation characteristics.

### The airbag system

The considered airbag system is a single chamber airbag, located in the steering wheel. The relevant components of the airbag system are the bag, the housing and the inflators, shown in Figure 1.5.

**The bag** is an inflatable cushion of porous polyamide with a more or less spherical shape, when deployed. It protects the driver from hitting the steering wheel or the dashboard. The deployed bag has a volume of approximately 50 liters. A circular vent with a diameter of approximately 50 mm is located at the downside of the (deployed) bag.

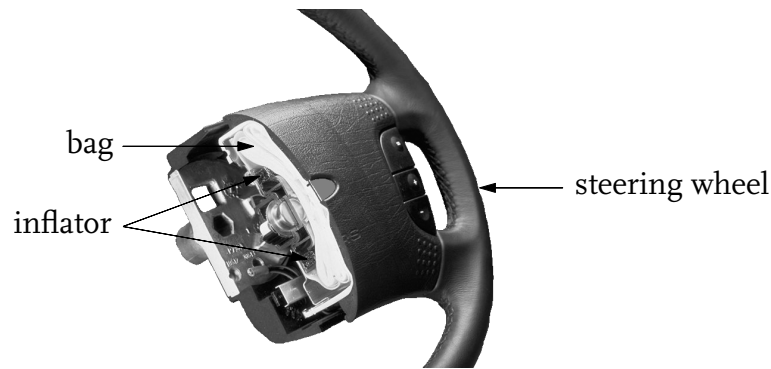


**Figure 1.5** The airbag system. Source: Autoliv Inc.

**The inflator** is a pyrotechnical device to generate a gas flow that has to inflate the bag. The considered inflator is a hybrid or multi-stage inflator, meaning that it actually consists of two inflators that can be triggered independently.

#### 1.2.4 A frontal crash test

In this section, relevant physical phenomena during a frontal crash test are discussed, focussing on the driver in a normal seating position. These phenomena are representative for a wide class of frontal crashes. In Figure 1.6, the kinematics of the driver during a frontal crash test is illustrated.

**The start of the crash** is the point of time  $t = t_0$  at which contact between the car and the crash partner is established.

**The free-flight phase** is the first phase of the crash and lasts until the belt significantly restrains the driver, typically at  $t \approx 20$  ms. During this phase, the occupant moves forward

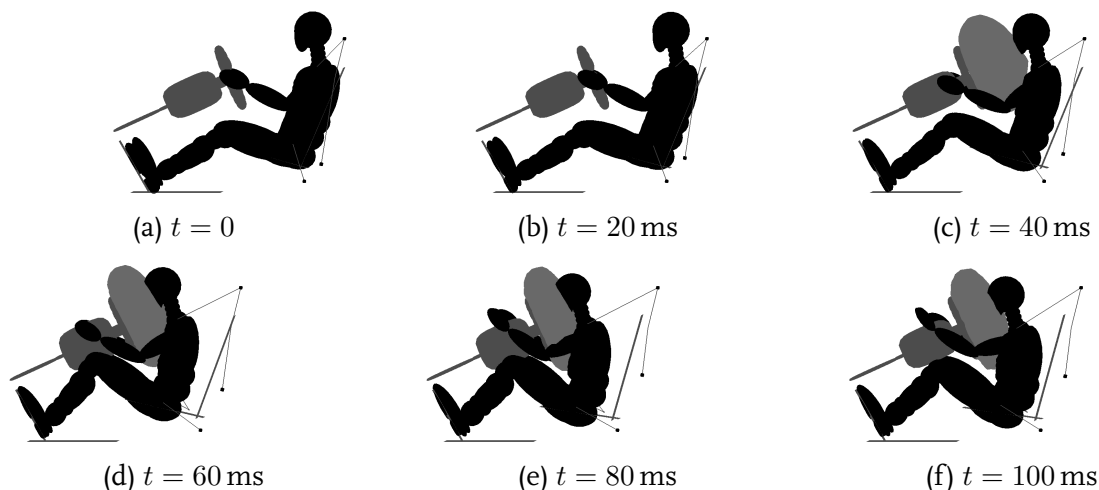


**Figure 1.6** Kinematics of the driver at regular time intervals during a frontal crash test

and is only restrained by the force due to the friction with the seat. As soon as the crash is detected, the pre-tensioner is triggered and the most appropriate mode of operation for the restraint system components is chosen.

**The ride down phase** is the phase of the crash, during which the driver significantly decelerates, due to forces applied by the restraint system components. From  $t \approx 20$  ms, the driver is restrained by the belt only and the thorax starts to rotate around the pelvis. From  $t \approx 40$  ms, the airbag additionally restrains the driver. For some cars and/or crashes, the knees of the driver contact the dashboard around  $t \approx 40$  ms. At  $t \approx 70$  ms, the vehicle velocity, and shortly thereafter, the driver velocity cross zero and the vehicle and the driver start to move backwards.

**The end of the crash** is the point of time  $t = t_e$  from which the driver does not significantly decelerate anymore. This point of time varies from 100 ms to 150 ms for frontal crash tests with a rigid barrier.

## 1.3 Towards active restraint systems

This thesis aims to contribute to the reduction of the severity of physical injuries, using restraint system components that can be continuously manipulated during the crash. Henceforth, such components are referred to as "active" restraint system components. In the sequel, the focus of this thesis is elucidated, followed by a general introduction into feedback control.

### 1.3.1 Focus of the thesis

The development of sensors and actuators for active restraint system components has been initiated [36], but they do not exist yet. Therefore, the focus here is on numerical simulation, which allows the use of (idealized) sensors and actuators. A variety of simulation packages for crash simulation exists, e.g. [47, 109, 153]. Here, the commercially available package MADYMO [153] is used.

The US-NCAP crash test [115] and the EURO-NCAP crash test [48] are appropriate for our purposes. Here, it is chosen for the frontal, full overlap, symmetric US-NCAP crash test of a mid-size passenger car. The car with a normally positioned mid-size male dummy as the "driver" has an impact velocity  $v_0$  of 56 km/h and an overlap  $\Delta L/L$  of 100%. It crashes with an angle  $\alpha$  of  $0^\circ$  into a rigid barrier.

State-of-the-art pre-crash sensing devices [27, 108] are able to classify an oncoming crash in terms of offset and impact velocity. Current research [165] indicates that a fairly accurate prediction of the acceleration of the safety cage during the crash may be possible in the (near) future. Throughout this thesis, it is assumed that the acceleration of the safety cage over the full crash duration is known at the start of the crash.

For our purposes, variables are desired that represent the risk of injuries and that can be measured or estimated relatively easy during a crash. As mentioned earlier, possible measures are the chest deflection, the acceleration of the head and the acceleration of the chest. Although the chest deflection is considered the best predictor of the severity of injuries to the chest [79], it can not be easily measured or estimated, whereas the measurement or estimation of the acceleration of the head and of the chest may be possible in the (near) future [22, 24]. Therefore, the focus is on the acceleration of the chest and of the head. The chest acceleration  $\ddot{c}$  is defined as the forward acceleration of the center of gravity of the dummy chest, whereas the head acceleration  $\ddot{h}$  is defined as the forward acceleration of the center of gravity of the dummy head [115]. The maximum of the acceleration is defined as the maximum level of the acceleration over a contiguous time span of 3 ms [115].

To reduce the risk of injuries, the forces applied by the restraint system components on the chest and the head are the key variables. Modern belt systems [34] are adaptive in the sense that the force in the belt section, connected to the load limiter, can be influenced by the change of deformation characteristics of load limiter components. Although the force in the belt section, near the load limiter strongly influences the force applied on the chest, these forces are not equal. Nevertheless, it seems reasonable to adopt the force in the belt section, connected to the load limiter, as the manipulated variable or input of the active belt system. Henceforth, this force is referred to as the belt force  $F$ .

Modern airbag systems [16, 26, 37] are adaptive in the sense that the point of time at which inflators are triggered, can be changed. Furthermore, numerous ideas to change the size of the vent during a crash have been granted a patent, e.g. [69, 166, 167]. This suggests that the manipulation of the size of the vent as a function of time may be possible in the (near) future. Therefore, it seems reasonable to adopt the size of the vent and the mass flow into the airbag as the manipulated variables or inputs of the active airbag system. Henceforth, the vent size and the mass flow are referred to as  $A$  and  $\phi$ , respectively.

Above, the focus of the main part of this thesis is given. At the end of this thesis, explorations are presented focussing on the chest deflection as a measure for the risk of chest injuries and on a small female dummy as the driver.

### 1.3.2 Feedback control

Consider the closed loop system in Figure 1.7. In this figure,  $\Theta$  is the Input-Output map (IO map) of the controlled system with input  $u = \mathcal{C}^{FB}(e)$  and output  $\tilde{y} = \Theta(u)$ ,  $\mathcal{C}^{FF}$  the IO map of the feedforward controller and  $\mathcal{C}^{FB}$  the IO map of the feedback controller. The IO maps relate their output via functional operators to their inputs. Furthermore,  $r$  represents the reference signal,  $e$  the error signal,  $u$  the input signal consisting of a feedforward component  $u^{FF}$  and a feedback component  $u^{FB}$ ,  $y$  the measurement of the output signal and  $d$  the external disturbance signal, e.g. noise.

In our case,  $\Theta$  represents the numerical model of a vehicle and dummy, subjected to a

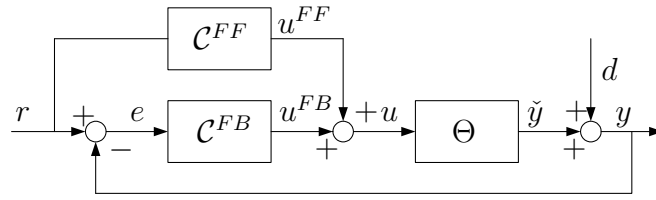


**Figure 1.7** Closed loop system

crash, whereas  $\mathcal{C}^{FF}$  and  $\mathcal{C}^{FB}$  represent the control laws to manipulate the active restraint system components. For example,  $r$  may represent the reference signal for the chest acceleration,  $\tilde{y}$  the actual chest acceleration,  $y$  the measured chest acceleration and  $u$  the belt force.

By appropriately designing the feedforward and feedback controllers, the output  $y$  can be forced to follow the reference signal  $r$ , and criteria concerning stability, performance and robustness of the closed loop system can be ensured. A feedforward component can be used to improve the performance and is typically applied for control problems where detailed knowledge of the dynamic behavior of the to-be-controlled system is available and/or where repetitive disturbances are present. In our case, a detailed model is available, but it can not be easily translated into the required inverse model for feedforward purposes. Besides, crashes do not show repetitive aspects. Hence, the focus is on feedback control without feedforward.

For the case without feedforward and without disturbances, i.e. for  $u^{FF} = 0$  and  $d = 0$ , the error  $e = r - y$  satisfies the feedback equation:

$$e = r - \Theta(\mathcal{C}^{FB}(e)) = r - \Lambda(e) \quad (1.1)$$

where  $\Lambda(e)$  is the result of the series connection of the IO map of the feedback controller  $\mathcal{C}^{FB}$  followed by the IO map of the controlled system  $\Theta$ , and is called the loop IO map.

Feedback is most effective if the loop IO map has a “large gain” [20, 84]. From Equation 1.1, it follows easily that if the gain is large, i.e. if  $\Lambda(e) \gg e$ , then with  $y = \Lambda(e)$ :

$$y \approx r \quad (1.2)$$

Equation 1.2 shows the linearizing effect of feedback on the closed loop system. No matter how nonlinear the controlled system is, the relation from the reference signal  $r$  to the output  $y$  remains approximately linear, as long as the feedback equation has a unique solution  $e$ .

Another advantage of feedback is disturbance rejection. For the case without feedforward and reference signal  $r$ , but with an external disturbance signal  $d$ , i.e.  $u^{FF} = 0, r = 0$  and  $d \neq 0$ , it can be shown [20, 84] that with a large gain of the loop IO map  $\Lambda(e)$ :

$$\|y\| \ll \|d\| \quad (1.3)$$

with  $\|\cdot\|$  some signal norm. This means that the effect of the external disturbance  $d$  to the controlled output  $y$  is small.



To enforce the desired behavior of the closed loop system, the role of the feedback controller is to achieve that the loop IO map has a large gain. However, the loop gain can not be infinitely increased, for example, due to (physical) limits on the actuators. In addition, a large gain may easily result in an unstable closed loop system, meaning that the feedback equation does not have a unique solution  $e$ .

## 1.4 Towards a design expedient

This thesis also aims to contribute to the design of modes of operation for real world restraint system components. As mentioned earlier, typical approaches, like trial-and-error in combination with optimization, are unattractive for the design of these modes, since they are time-consuming and require a high number of simulations. Results of simulations with the closed loop system including the active restraint system components, give insight into the desired behavior of the restraint system components. For example, deformation characteristics of a load limiter can be determined from results of a closed loop simulation in which the belt force is manipulated to control the chest acceleration. Therefore, the strategies to arrive at controllers for active restraint system components can be seen as a design expedient.

The design expedient has to comply with several desires. The design of the modes typically aims to reduce the risk of injuries, formulated in terms of one or more injury measures. Besides that, it often focus on several combinations of dummies and/or crash tests and requires a high number of simulations. This means that the design expedient has to be generalizable to cases in which different dummies, crash tests and/or measure(s) for the risk of injury are considered. In addition, the design expedient is easy-to-use and requires a low number of simulations. Since the design expedient will be applied to crash tests with a priori known characteristics, the acceleration of the safety cage over the full duration of the crash may be assumed to be a priori known.

## 1.5 Objective and contribution of the thesis

The basic hypothesis of this thesis can be formulated as:

- **active restraint systems can reduce the risk of physical injuries.**

To evaluate this hypothesis, appropriate reference signals for the head and chest acceleration are defined, such that the control problem boils down to the design of feedback controllers to force the head and chest acceleration to follow the reference signal by the manipulation of the belt force, the vent size and/or the mass flow. The objectives of this research are formulated as:

- Develop a strategy to reveal the dynamic behavior of the dummy, interacting with

the belt and the airbag, as far as this behavior is relevant for control design purposes.

- Develop a strategy to design controllers to manipulate the belt and the airbag.
- Assess the proposed strategies for cases of different dummies and measures for the risk of injury.

Development of sensors and actuators for real world active restraint system components is not a topic of this research. In fact, idealized actuators to manipulate the belt and the airbag and idealized sensors to measure the occupant injuries are used.

The strategies for modelling and for control design, have to fulfil a number of requirements. First, their application has to result in appropriate modes of operation for real world restraint system components. Second, they have to be generalizable to different dummies and different measures for the risk of injury. Third, they have to be easy-to-use and require a low number of simulations.

This thesis aims to contribute to the research and development in the field of vehicle safety by treating restraint systems from a new point of view. This point of view makes it possible to obtain the restraint system characteristics that achieve the lowest possible risk of injuries for a certain crash test. Furthermore, this thesis outlines a basis for future restraint system components that can be continuously manipulated during the crash. This thesis aims to contribute to the field of control by adopting low order, simple models to approximate the local dynamic behavior of a complex, nonlinear model in order to design a low order controller for the nonlinear model.

## 1.6 Outline of the thesis

A flowchart of the development process of real world restraint system components is shown in Figure 1.8. It depicts the typical approach to arrive at modes of operation of real world restraint system components, as well as the to-be-followed approach to arrive at active restraint system components. The approach to arrive at active restraint system components is shown by the grey boxes. The mentioned sections in the grey boxes with rounded angles discuss the pursued strategies in general terms, whereas the sections in the grey right-angled boxes contain the application of the strategies to the working example.

In Chapter 2, the modelling of the relevant dynamic behavior for control design purposes is discussed. The complex nonlinear model, used as throughout this thesis, is introduced first. Next, the strategy to reveal the relevant dynamic behavior for control design purposes is elucidated in general terms. Finally, the strategy is applied to arrive at control design models for the belt and for the airbag, successively.

Chapter 3 deals with the design of a controller for the belt or for the airbag, for the case that only one component of the restraint system is manipulated. First, the control design

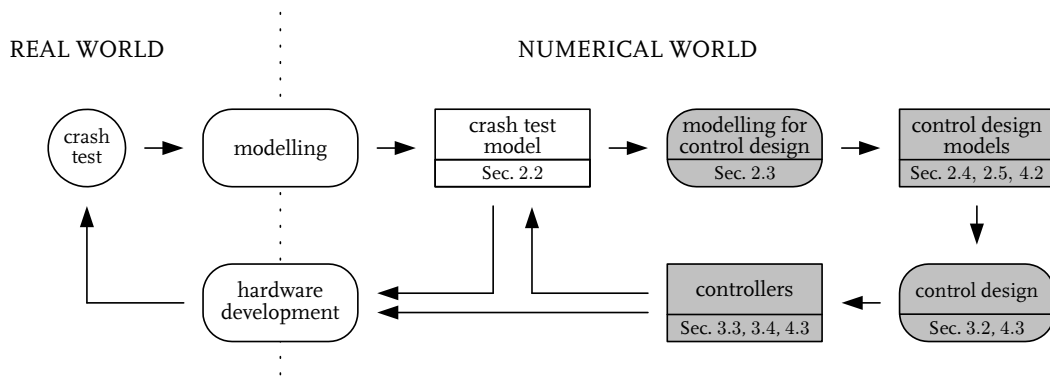


**Figure 1.8** Flowchart of the development process of restraint system components

strategy is discussed in general terms first, followed by the application of the strategy to arrive at a controller for the belt and for the airbag, successively.

Chapter 4 discusses the design of a controller for the belt and a controller for the airbag, for the case that both components are manipulated. First, interactions are analyzed, followed by the discussion of the control design strategy. After that, the strategy is applied to arrive at a controller for each restraint system component.

Chapter 5 contains explorations to assess the suitability of the proposed modelling and control design strategies as a design expedient in the cases of a different dummy and a different measure for the risk of injuries. Furthermore, a first investigation towards the application of predictive control is given. Finally, in Chapter 6, conclusions are drawn and recommendations for future research are given.

# Modelling for control design

*Numerical models to simulate a crash test often are complex and highly non-linear. Therefore, they are not suitable for control design purposes. A strategy is presented to arrive at simple models, suitable for control design purposes. To derive these simple models, input and output measurements of a complex non-linear numerical model are used.*

## 2.1 Introduction

A (typical) numerical model of a mid-size passenger car and mid-size dummy, subjected to the frontal US-NCAP crash test, is available and used throughout this thesis. The model consists of 86 rigid bodies and connecting joints, more than 130 (nonlinear) springs and dampers and two finite element models with a total of more than 7 000 elements. One simulation with this model takes approximately 45 minutes on a Silicon Graphics Origin Workstation with a 195 MHz R10.000 processor.

The available model is highly nonlinear, complex and time-consuming. This means that the dynamic behavior of the dummy interacting with the restraint system, as far as it is relevant for the design of a controller for an active restraint system component, can not be easily obtained from the available model. Therefore, a control design model is desired that approximates the relevant dynamic behavior of the dummy, the inner-vehicle components and their interactions. The desired control design model preferably is linear, time-invariant and of low order. The use of such models for the design of a controller for a (nonlinear) complex system can be very worthwhile, e.g. [7, 33, 41, 125]. Besides that, they enable the use of powerful linear control design and analysis techniques. The strategy to arrive at the desired control design model has to be straightforward and as general as possible, such that it can be used when a different combination of a crash, dummy and/or when other manipulated and controlled variable(s) are considered.

In principle, two modelling strategies exist, being the theoretical and the experimental modelling strategy [19]. The theoretical strategy is based on first principles of physics to derive a set of equations describing the relevant dynamic behavior of a system. It is often applied to model injury mechanisms [168], dynamic behavior of isolated restraint system

components [8, 11, 163] or a complete vehicle. The experimental strategy is based on experimentally obtained data to reveal relationships between system variables. It is typically applied to determine mathematical relationships between restraint system characteristics and measures for the risk of injury, e.g. [61, 68, 99, 170]. In that case, simulations with a numerical model of the crash are performed to obtain “experimental” data.

The models resulting from the theoretical strategy are unattractive for our purposes, since they only describe a part of the relevant dynamic behavior and/or are far too complex for control design purposes. The application of the experimental modelling strategy is unattractive, because the obtained relationships are far from simple. Furthermore, it is questionable whether the relationships are physically meaningful. Besides that, the number of simulations required to arrive at accurate relationships often exceeds thousand.

Although the combination of the dummy and the vehicle, subjected to a crash, is a nonlinear system, it might behave locally as an approximately linear system. This is the main motivation to try to linearize the dynamic behavior, as far as it is relevant for control design purposes. A linearization tool from the simulation package MADYMO is available [137], but can not deal with finite element models. This leaves us with the only option to use input and output measurements of the complex nonlinear model.

The complex nonlinear model, used as the working example throughout the thesis, is introduced in Section 2.2. The linearization strategy is presented in Section 2.3. In Section 2.4 and 2.5, the modelling strategy is applied to derive control design models of the belt and the airbag, respectively. Finally, the proposed strategy is evaluated in Section 2.6.

## 2.2 The complex nonlinear model

The numerical MADYMO model of a mid-size passenger car with the HYBRID III 50th percentile dummy as the “driver”, is seen as the representation of the real world dummy and vehicle, subjected to the frontal US-NCAP crash test. This model, illustrated in Figure 2.1, is referred to as  $\mathcal{M}_p$ , where the lower index “p” denotes that the restraint system components are passive, meaning that they are not manipulated.

The model  $\mathcal{M}_p$  only incorporates the dummy and those vehicle components that may contact the dummy during the considered crash test. Except for the airbag and the windscreen, these vehicle components, the dummy and their interactions are modelled by rigid bodies, kinematic joints, massless planes and massless springs and dampers for force interactions [155]. The airbag and the windscreen are modelled by a lumped-mass finite element model with the mass equally distributed over the nodes of the elements. The gas in the airbag is treated as a mixture of ideal gases and the pressure and temperature are assumed to be uniform throughout the airbag. Furthermore, contacts are modelled as force interactions by springs and dampers.

In the sequel, the structure and the quality of the model  $\mathcal{M}_p$  are discussed. After that, changes to this model, necessary for manipulation of the restraint system components, are discussed.

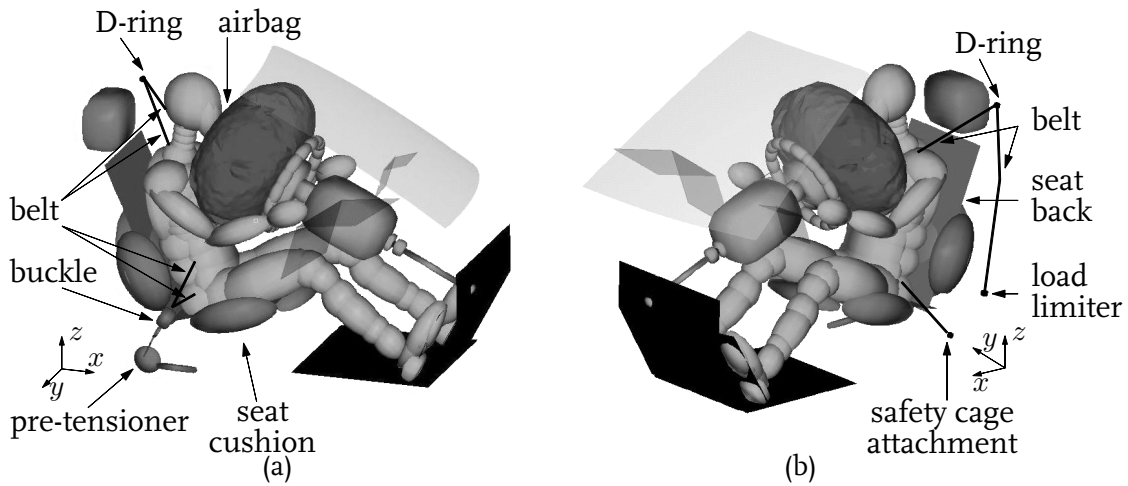


**Figure 2.1** The complex nonlinear model  $\mathcal{M}_p$

### 2.2.1 Structure

The safety cage is seen as a rigid body. This seems to be justified, since it marginally deforms during the real world crash test. Typical for a simulation of a frontal crash test, only the acceleration in the positive  $x$ -direction is prescribed to the safety cage. In Figure 2.2, the vehicle acceleration  $\ddot{x}_{\text{veh}}(t)$ , measured at the left longitudinal girder at the back side of the vehicle, is shown.

The shown time history is the acceleration profile of the considered vehicle, subjected to the considered crash test. Nevertheless, it has strong similarities with the acceleration profile for other mid-size passenger vehicles, subjected to the same crash test [160]. The shape of the acceleration signal mainly depends on the (plastic) deformation characteristics of the car front structure and the engine [54]. Simplified models of a car [54, 76], subjected to a frontal crash test, indicate that small changes to the front structure slightly influence the acceleration of the safety cage. Besides that, the energy that is to be absorbed by the front structure remains the same, if this structure is changed. Apart from that, the effect of changes to the front structure is not significant compared to the effect of changes in crash characteristics like the relative angle and/or overlap, see Figure 1.3.

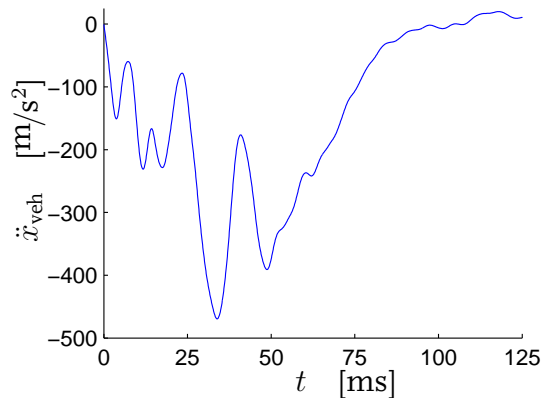


**Figure 2.2** Vehicle acceleration  $\ddot{x}_{\text{veh}}(t)$

**The dummy** is modelled as a combination of 37 rigid bodies, connected by kinematic joints plus more than 80 massless, nonlinear springs and dampers for force interactions. This commercially available model [154] will not be discussed in more detail.

**The safety belt** is modelled as a series structure of massless, one-dimensional elements. Each element consists of a nonlinear spring parallel to a damper. One end of the structure is attached to the safety cage. From that point, the structure goes over the pelvis through the buckle, cross-diagonally over the chest, through the D-ring to the load limiter, to which its other end is attached. At the nodal points of the belt model, contact with a rigid body can be described by a simple friction model [155].

**The load limiter**, see Figure 2.1(b), is modelled as a nonlinear element  $\mathcal{L}$ , representing the (plastic) deformation characteristic of the real world load limiter, see Figure 2.3(a). A rigid body has to be defined to connect the nodal point of the last belt element with the element  $\mathcal{L}$ . This body can only translate in the direction of the displacement  $x_1$ , referred to as the belt outlet. The reaction force  $F_{\mathcal{L}}$  as a function of  $x_1$  is shown in Figure 2.3(b). For  $0 \leq x_1 \leq 3$  cm, indicated by I, the reaction force is low to represent phenomena like slack in the real world load limiter. For  $3 \text{ cm} \leq x_1 \leq 13$  cm, indicated by II, the reaction force increases and remains high to restrain the dummy. For  $x_1 \geq 13$  cm, indicated by III, the reaction force decreases, since for these values of  $x_1$ , the dummy is expected to have moved forward so far that a contact with the airbag has been established.

**The buckle pre-tensioner**, see Figure 2.1(a), is modelled as a stiff, one-dimensional, massless spring  $K$ , see Figure 2.4. A rigid body with a mass equal to the real world buckle mass, connects the belt elements with the spring. This body can translate in the direction of the displacement  $x_2$ . Initially, the displacement  $x_2$  is fixed and the spring is stretched. The release of the body at  $t = 6$  ms imitates the tightening of the belt by the pre-tensioner.

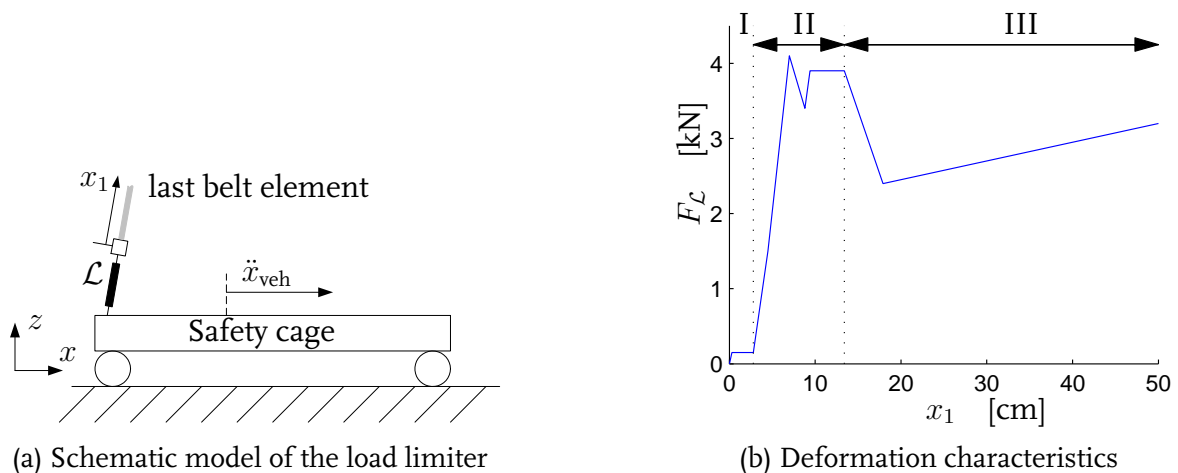


**Figure 2.3** The load limiter

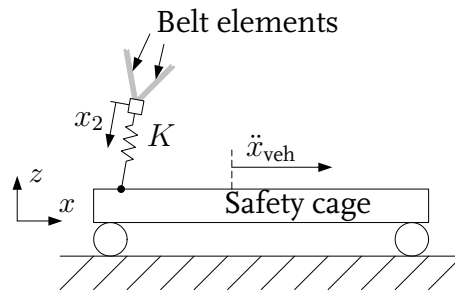


**Figure 2.4** Schematic model of the buckle pre-tensioner

**The bag** of the airbag system is modelled as a finite element model of 2 824 flat membrane elements with three nodes per element. A hole with an area of approximately  $17 \text{ cm}^2$  represents the vent. The gas flow through the vent is assumed to be isentropic. Porosity of the bag material is modelled as a pressure dependent outflow.

The modelling of the deployment of an airbag is difficult. Recently, approaches to achieve an accurate description of the deployment have been proposed [77, 173], but they are not implemented in the model  $\mathcal{M}_p$ . To achieve a correct state of the airbag at the moment of first contact with the dummy, the vent “opens” at  $t = 26 \text{ ms}$ . The vent size as a function of time for the passive restraint system,  $A_p(t)$  is shown in Figure 2.5(a).

**The inflators** in the model  $\mathcal{M}_p$  deliver two a priori known mass flows  $\phi_1(t)$  and  $\phi_2(t)$  with known temperature. Geometric characteristics of the inflators like location are irrelevant, since the pressure and temperature of the gas in the bag are assumed to be uniform. The inflators are triggered at  $t = 6 \text{ ms}$  and  $t = 12 \text{ ms}$ , according to the points of time at which the real world inflators are triggered for the considered crash test. The total mass flow for the passive restraint system  $\phi_p(t) = \phi_1(t) + \phi_2(t)$  is shown in Figure 2.5(b).

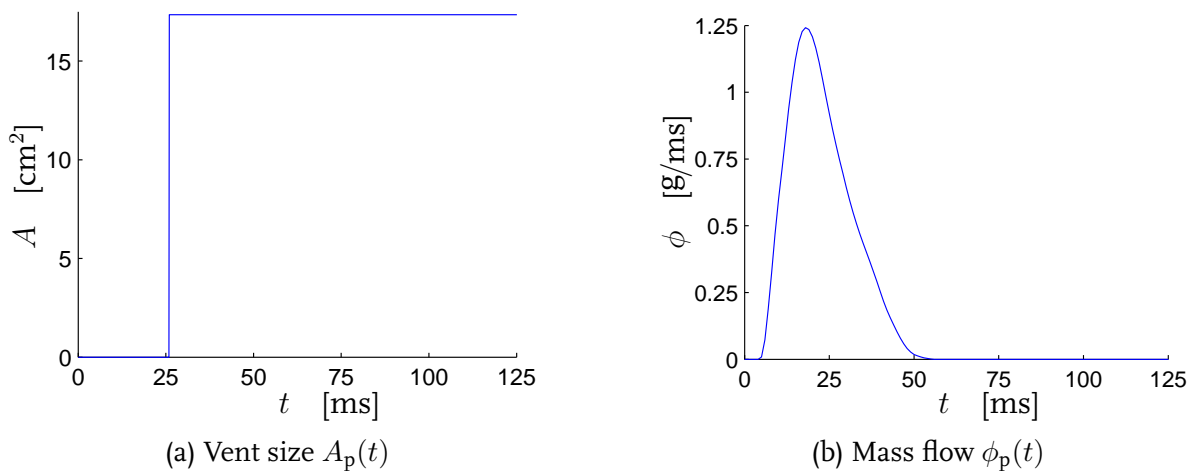


**Figure 2.5** Vent size  $A_p$  and mass flow  $\phi_p(t)$  as a function of time



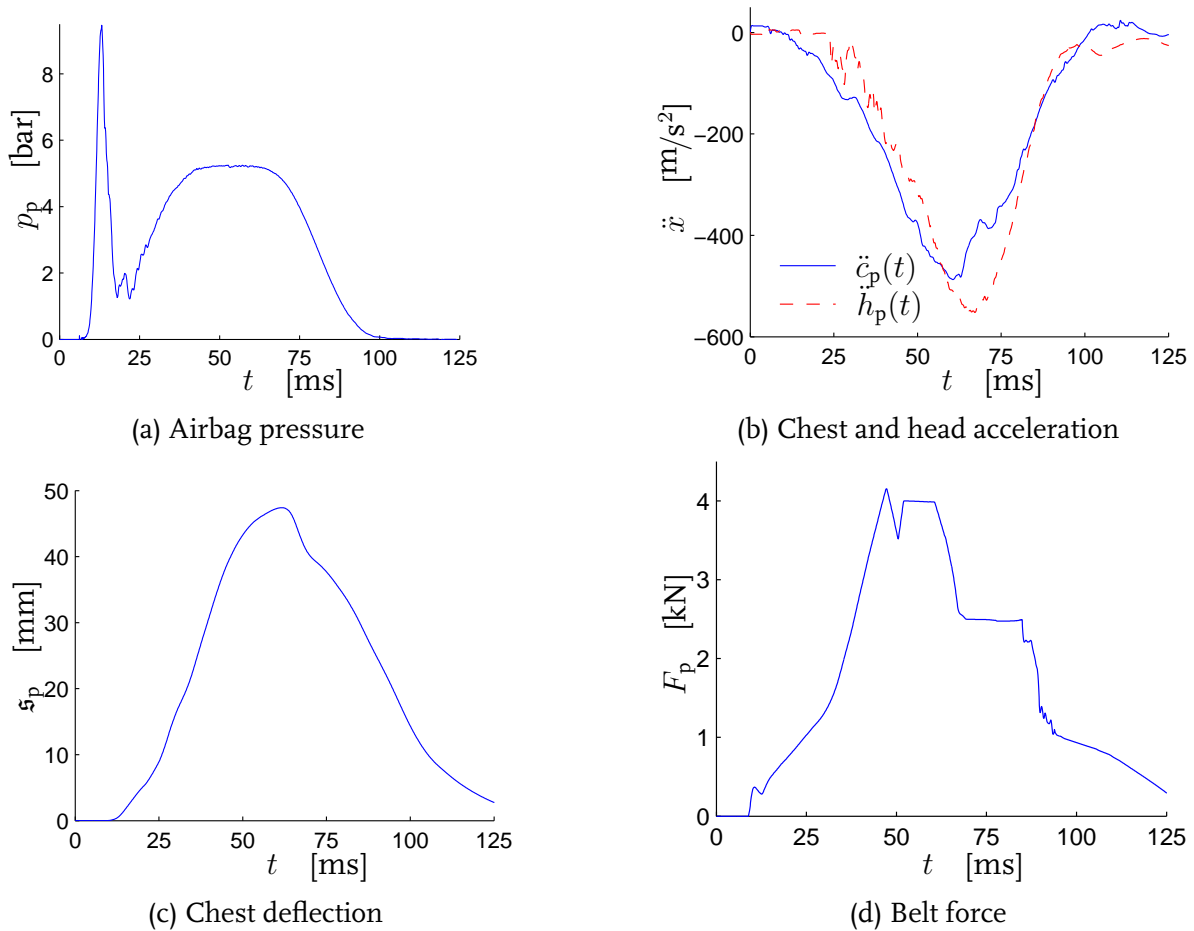


**Figure 2.6** Relevant results of the simulation with the model  $\mathcal{M}_p$

### The crash test simulation

Some results of the simulation of the considered crash test using model  $\mathcal{M}_p$  are shown in Figure 2.6. The maximum chest acceleration, head acceleration and chest deflection are 49 g, 55 g and 47 mm, whereas the tolerance level is 60 g, 60 g and 76 mm, respectively.

The (typical) time history of the pressure of the gas in the bag is shown in Figure 2.6(a). The peak at  $t = 13$  ms is due to MADYMO peculiarities concerning the modelling of a (deploying) airbag. The bag is considered to be fully deployed at  $t \approx 40$  ms. From  $t = 45$  ms until  $t = 70$  ms, the pressure is more or less constant, and for  $t > 90$  ms, the airbag is “empty”.

Figure 2.6(b) shows typical time histories of the head acceleration  $\ddot{h}_p(t)$  and the chest acceleration  $\ddot{c}_p(t)$  for a mid-size dummy of a mid-size passenger vehicle, subjected to the considered crash test, cf [72]. The head starts to decelerate later than the head, due to the neck. The dip in the head acceleration at  $t \approx 26$  ms is caused by a short impact of the airbag on the head. This phenomenon is called bag slap [150]. From  $t \approx 35$  ms until the end of the crash, the head and chest are permanently in contact with the airbag.

Figure 2.6(c) shows the (typical) chest deflection  $s(t)$ . For  $t < 50$  ms, the shape of the time history is similar to that of the belt force  $F_p(t)$ . Because of the forces applied by the

airbag, the drop of the belt force does not cause a similar drop in the chest deflection.

At  $t = 6$  ms, the pre-tensioner is triggered to remove slack in the belt system, resulting in the activation of the load limiter at  $t \approx 8$  ms. Figure 2.6(d) shows the reaction force of the element  $\mathcal{L}$  (see Figure 2.4), i.e. the belt force  $F_p(t)$ . Its rather peculiar shape is related to the shape of the deformation characteristic of the load limiter, cf Figure 2.3(b). At  $t \approx 85$  ms, the reaction force drops, since the dummy starts to move backwards, relative to the vehicle.

The absolute acceleration of the head and of the chest are less than  $25 \text{ m/s}^2$  for  $t \geq 100$  ms. Therefore, it seems reasonable to assume that the crash test may be considered to be ended at  $t = t_e = 100$  ms. It is emphasized that for other vehicles, crashes, dummies and/or restraint systems, the point of time at which the crash may be considered to be ended, can be different.

### 2.2.2 Quality

The quality of the model  $\mathcal{M}_p$  is judged by its robustness to parameter changes and by a comparison of its results with results from the real world crash test. Both aspects are shortly elucidated in the sequel.

In Figure 2.7, the time histories of the chest and the head acceleration as well as the chest deflection are shown. The lower indices “ $\mathcal{M}_p$ ” and “rw” refer to the simulation and the real world crash test, respectively. The shape of the time histories is similar, but the real world results seem to be shifted over a time interval of at least 10 ms. The maximal difference for the measures for the risk of injuries is 12 %.

The observed differences are more or less typical [127, 152, 174] and are caused by various reasons. First of all, a numerical model like  $\mathcal{M}_p$  still is a relatively simple model of the real world system. Secondly, even during a frontal crash test, a vehicle does not only move in the forward direction, but it also pitches. Thirdly, the contact of the belt with the dummy is modelled by a limited number of force interactions, whereas that contact actually yields a more distributed loading.

To judge the numerical robustness of the model  $\mathcal{M}_p$ , the Monte Carlo method [97, 132] can be applied, exemplified in [38, 102]. An extensive set of simulations is performed and for each simulation, one or more parameters are changed within a (small) range around their default. Next, the scatter in the results is analyzed, indicating whether the model is numerically robust. In the robustness study of the model  $\mathcal{M}_p$  [143], parameters like the time step, the ambient pressure and the position of the dummy are perturbed. The analysis of the results show that their scatter is of the same order of magnitude as the scatter in the perturbed parameters. This observation indicates that the model  $\mathcal{M}_p$  is numerically robust, at least for (small) changes of the considered parameters.

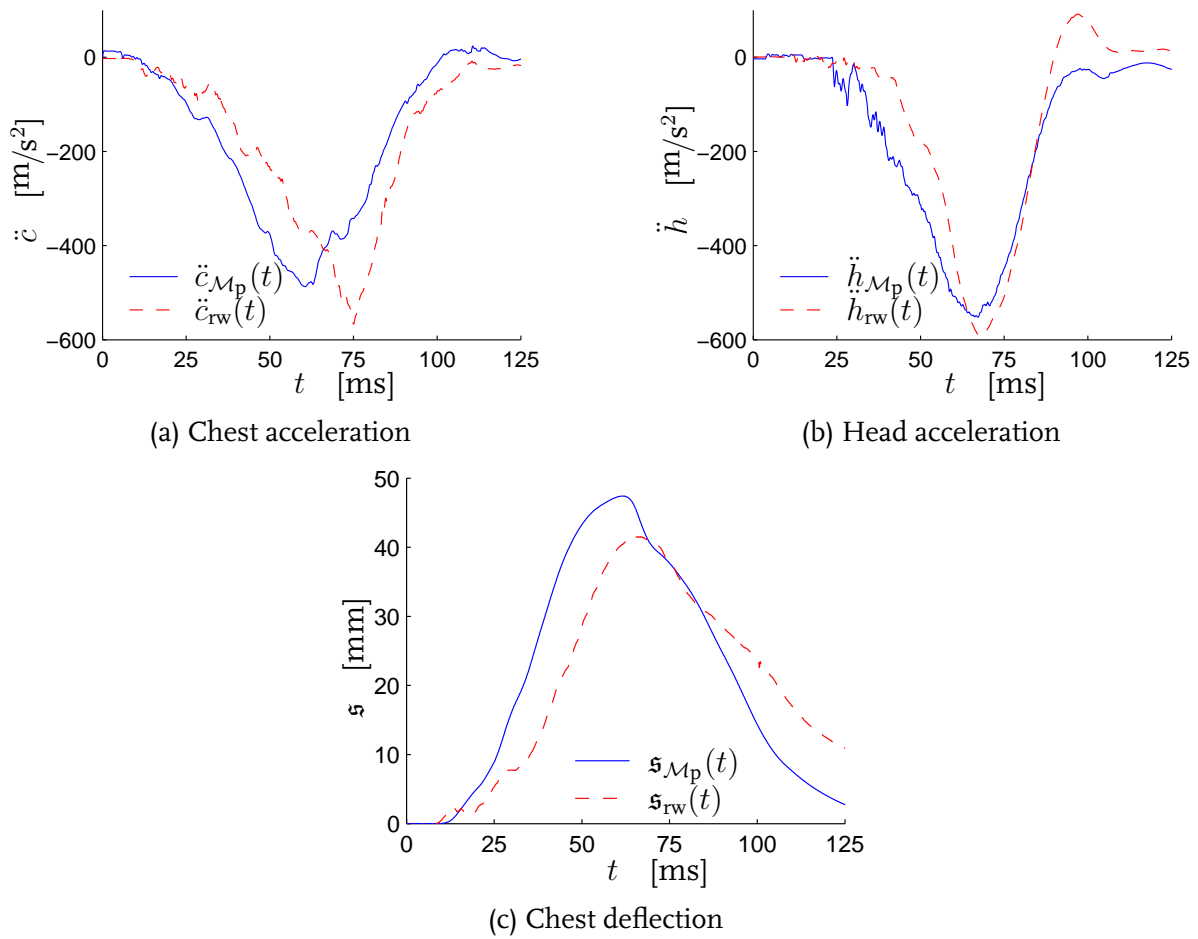


**Figure 2.7** Relevant results of the real world crash test and the crash test simulation

### 2.2.3 Changes for control purposes

For control purposes, it has to be possible to manipulate the belt force  $F$ , the mass flow  $\phi$  and the vent size  $A$  during a simulation. Especially to manipulate the belt force, the model has to be modified. The element  $\mathcal{L}$ , see Figure 2.3(a), is replaced by an actuator [156, pp. 349–350], that applies a force in the same direction and at the same location.

To allow the use of standard control facilities of MATLAB/SIMULINK, the model is coupled with MATLAB/SIMULINK [98]. The coupling, in the form of a direct executable, is commercially available [138, 153] and is not discussed here. The required modifications to actually couple a MADYMO model to a SIMULINK model are described in [156]. The coupled model with the “active” restraint system components is referred to as  $\mathcal{M}$ .

To judge whether the modifications yield undesired changes, the time histories of the chest and head acceleration, and of the chest deflection, obtained from a simulation with the models  $\mathcal{M}$  and  $\mathcal{M}_p$ , are compared. During the simulation with  $\mathcal{M}$ , the belt force, mass flow and vent size are prescribed, i.e.  $F(t) = F_p(t)$ ,  $\phi(t) = \phi_p(t)$  and  $A(t) = A_p(t)$ . The relevant time histories, obtained from the simulations differ only marginally.

## 2.3 Linearizing the complex nonlinear model

The goal of this chapter is to develop a strategy to arrive at an easy-to-handle, linear time-invariant (LTI) control design model of low order, since the available model  $\mathcal{M}$  is highly nonlinear and too complex. A schematic representation of the complex nonlinear model  $\mathcal{M}$  and the desired LTI control design model  $\mathcal{H}(s)$  with  $s$  the Laplace variable [82], is shown in Figure 2.8. In these figures,  $u$  may represent the belt force  $F$ , the mass flow  $\phi$  or the vent size  $A$ , whereas  $y$  may represent the chest acceleration  $\ddot{c}$ , the head acceleration  $\ddot{h}$ .



**Figure 2.8** Schematics of the complex nonlinear model and the control design model

The complex nonlinear model  $\mathcal{M}$  can be formulated as a set of nonlinear differential equations. The state  $\underline{x}_o(t)$  and output  $\underline{y}_o(t)$  of the model  $\mathcal{M}$ , corresponding to a given initial state  $\underline{x}_o(t_0)$ , vehicle acceleration  $\ddot{x}_{veh}(t)$  and input  $\underline{u}_o(t)$ , follow from<sup>1</sup>:

$$\begin{cases} \dot{\underline{x}}_o &= \underline{f}(\underline{x}_o, \underline{u}_o, t) \\ \underline{y}_o &= \underline{g}(\underline{x}_o, \underline{u}_o, t) \end{cases} \quad (2.1)$$

The perturbations  $\delta\underline{x}(t)$  of the state  $\underline{x}_o(t)$  and  $\delta\underline{y}(t)$  of the output  $\underline{y}_o(t)$ , due to a perturbation  $\delta\underline{u}(t)$  of the input  $\underline{u}_o(t)$  can be determined from:

$$\begin{cases} \delta\dot{\underline{x}} &= \underline{f}(\underline{x}_o + \delta\underline{x}, \underline{u}_o + \delta\underline{u}, t) - \underline{f}(\underline{x}_o, \underline{u}_o, t) \\ \delta\underline{y} &= \underline{g}(\underline{x}_o + \delta\underline{x}, \underline{u}_o + \delta\underline{u}, t) - \underline{g}(\underline{x}_o, \underline{u}_o, t) \end{cases} \quad (2.2)$$

If the behavior of the system is smooth and perturbations  $\delta\underline{u}(t)$  are small, Equation 2.2 may be approximated by:

$$\begin{cases} \dot{\underline{x}} &= A(\underline{x}_o, \underline{u}_o, t) \cdot \delta\underline{x} + B(\underline{x}_o, \underline{u}_o, t) \cdot \delta\underline{u} \\ \underline{y} &= C(\underline{x}_o, \underline{u}_o, t) \cdot \delta\underline{x} + D(\underline{x}_o, \underline{u}_o, t) \cdot \delta\underline{u} \end{cases} \quad (2.3)$$

Here,  $A, B, C$  and  $D$  denote the derivatives of the functions  $\underline{f}$  and  $\underline{g}$  with respect to  $\underline{x}_o$  and  $\underline{u}_o$ , meaning that:

$$\begin{cases} A(\underline{x}, \underline{u}, t) &= \frac{\partial \underline{f}(\underline{x}, \underline{u}, t)}{\partial \underline{x}} & B(\underline{x}, \underline{u}, t) &= \frac{\partial \underline{f}(\underline{x}, \underline{u}, t)}{\partial \underline{u}} \\ C(\underline{x}, \underline{u}, t) &= \frac{\partial \underline{g}(\underline{x}, \underline{u}, t)}{\partial \underline{x}} & D(\underline{x}, \underline{u}, t) &= \frac{\partial \underline{g}(\underline{x}, \underline{u}, t)}{\partial \underline{u}} \end{cases} \quad (2.4)$$

The matrices  $A, B, C$  and  $D$  depend explicitly on time  $t$ , meaning that the dynamic behavior for a known  $\underline{u}_o(t)$  and  $\underline{x}_o(t)$  is time-variant. It is therefore important to analyze

<sup>1</sup> For clarity of notation, the dependency of  $\underline{x}_o, \underline{y}_o$  and  $\underline{u}_o$  on time  $t$  is not explicitly mentioned here.

the output measurements in order to get insight into the time-scale in which dynamic behavior changes and into non-smooth behavior.

For our modelling purposes, simulations with  $\mathcal{M}$  are performed to obtain data. During the simulations, a small perturbation  $\delta u(t)$  is added to one of the inputs of  $\mathcal{M}$ , so  $u(t) = u_o(t) + \delta u(t)$  for the considered input. For our purposes, a trajectory of the input  $u_o(t)$  as close as possible to the controlled input  $u(t)$ , is desired. However, that trajectory is not (yet) available, since controllers to enforce the desired behavior of the closed loop system are not (yet) available. In fact, only one trajectory exists, namely that for the passive restraint system, meaning that perturbations have to be added to that trajectory. For nonlinear time-variant systems, this is an uncommon approach. To determine whether the obtained LTI models do make sense, the behavior of controllers, to be designed using the LTI models, has to be evaluated. In addition, LTI models for closed loop operating points are to be obtained, when controllers are available.

The preferred perturbation is an impulse, since powerful methods like approximate realization [142], to determine a suitable LTI model from impulse responses, exist. However, numerical models like the model  $\mathcal{M}$  can not properly deal with impulses. The alternative of harmonic perturbations is not attractive, since it requires an extensive set of simulations to cover the frequency range of interest. For this reason and to facilitate a quick and intuitive interpretation of the results, stepwise perturbations are used, i.e.  $\delta u(t) = \Delta u \cdot \varepsilon(t - \tau)$  where  $\Delta u$  is the step size and  $\varepsilon(t - \tau)$  is a unit step applied at time  $t = \tau$ .

To investigate whether linearization is justified, i.e. to get insight into the time-scale in which the dynamic behavior changes and to rule out non-smooth behavior, several step sizes  $\Delta u$ , positive as well as negative, are used. Furthermore, to investigate whether the relevant dynamic behavior depends on the operating point, several points of application  $\tau$ , i.e. points of time at which the step is applied, are used. The comparison of normalized responses  $\delta y(t)/\Delta u$  to perturbations applied at the same point  $\tau$ , indicates whether linearization is feasible. The comparison of the normalized responses for perturbations added at different points of application, gives insight into the operating point dependency.

The length of the time interval of the normalized response  $\delta y(t)/\Delta u$  that is to be used in the procedure to realize an LTI model is far from trivial. On the one hand, it has to be long enough to capture the relevant dynamic behavior. On the other hand, it can not be chosen too long, since the relevant dynamic behavior may change as a function of time.

Suppose that the relevant part of the normalized response to a step  $\Delta u \cdot \varepsilon(t - \tau)$  is sampled with sample time  $\Delta t$ , resulting in  $\{S_k\}_{k=0}^n = \{\delta y(k)/\Delta u | k = 0, 1, 2, \dots, n\}$ , where  $\delta y(k)/\Delta u$  is the normalized response at time  $t = \tau + k \cdot \Delta t$ . Then, a variety of techniques is available to arrive at an approximating LTI model, e.g. [90, 91, 124, 142, 161]. Here, a technique is desired that does not require a priori knowledge about the to-be-approximated dynamic behavior and that can deal with step responses. Most of the previously meant techniques comply with these desires. Especially attractive is the so-called minimal realization technique [19, 142]. The use of this technique to arrive at an LTI model of finite order is straightforward and simple. In our case, approximate realization is used to arrive

at a discrete-time LTI model from a single input  $u \in \mathcal{R}^1$  to a single output  $y \in \mathcal{R}^1$ , with state  $x \in \mathcal{R}^\rho$ :

$$\begin{cases} x(k+1) &= Ax(k) + Bu(k) \\ y(k) &= Cx(k) + Du(k) \end{cases} \quad (2.5)$$

Using the relevant part of the normalized response  $\{S_k\}_{k=0}^n$ , this LTI model is realized by the following steps<sup>2</sup> [59, 66, 83]:

1. Construct matrix  $T$  with  $T_{(i,j)} = S_{i+j-1}$  for  $i = 1$  and  $T_{(i,j)} = S_{i+j-1} - S_{i-1}$  for  $i + j - 1 \leq n$  with  $i \geq 2$  and  $i$  and  $j$  positive integers with  $i \leq a$  and  $j \leq a$ , and  $a = n/2$  if  $n$  is even and  $a = (n + 1)/2$  if  $n$  is odd.
2. Perform singular value decomposition on the matrix  $T$  to determine the orthogonal matrices  $U$  and  $V$  and the diagonal matrix  $\Sigma = \text{diag}(\sigma_1, \sigma_2, \dots, \sigma_a)$  with  $\sigma_1 \geq \sigma_2 \geq \dots \geq \sigma_a \geq 0$ , such that  $T = U \Sigma V^T$ .
3. Analyze the decrease of the singular values  $\sigma_m$  as a function of  $m$  to determine which singular values are significant, or in other words, have to be retained. Typically, a decrease  $|\sigma_\rho/\sigma_{\rho+1}| \geq 10$  indicates that the first  $\rho$  singular values are significant.
4. Determine the matrices  $\Sigma_{(1:\rho,1:\rho)} = \text{diag}(\sigma_1, \dots, \sigma_\rho)$ , and  $U_{(:,1:\rho)}$  and  $V_{(:,1:\rho)}$  and realize the discrete-time LTI model of Equation 2.5 by:

$$\begin{cases} A &= \Sigma_{(1:\rho,1:\rho)}^{-\frac{1}{2}} U_{(:,1:\rho)}^T & T_{(2:a,1:a-1)} & V_{(:,1:\rho)} \Sigma_{(1:\rho,1:\rho)}^{-\frac{1}{2}} \\ B &= \Sigma_{(1:\rho,1:\rho)}^{-\frac{1}{2}} U_{(:,1:\rho)}^T & T_{(1:a-1,1)} & \\ C &= & T_{(1,1:a-1)} & V_{(:,1:\rho)} \Sigma_{(1:\rho,1:\rho)}^{-\frac{1}{2}} \\ D &= & S_0 & \end{cases} \quad (2.6)$$

The given algorithm is an extension of the minimal realization algorithm [66] to realize an LTI model from impulse responses.

The quality of the realized LTI model can only be judged by a comparison of the unit step response of the LTI model  $y_{\mathcal{H}}(t)$ , with the normalized response, used to derive it. For that purpose, the following measure is used:

$$\kappa = \frac{\int_{\tau}^{t'} \left| \frac{\delta y(t)}{\Delta u} - y_{\mathcal{H}}(t) \right| dt}{\int_{\tau}^{t'} \left| \frac{\delta y(t)}{\Delta u} \right| dt} \quad (2.7)$$

with  $(\tau, t')$  the time interval from  $t = \tau$  until  $t' = \tau + n \cdot \Delta t$ . Here, the arbitrary criterion  $\kappa \leq 0.05$  is adopted to indicate whether an LTI model is accurate.

---

<sup>2</sup> Here, a MATLAB-like notation is used to refer to a selection of rows, columns or submatrices of a given matrix. For example, the first  $i$  rows of  $A$  are denoted by  $A_{(1:i,:)}$ , and the  $j$ -th column of  $A$  is denoted by  $A_{(:,j)}$ , whereas the  $i$ -th element of the  $j$ -th column is denoted by  $A_{(i,j)}$ .

## 2.4 Modelling of the belt

In this section, the interaction of the belt with the dummy is modelled. The modelling strategy from Section 2.3 is applied to arrive at an LTI control design model for the belt. The risk of chest injuries is dominantly influenced by the forces applied by the belt [56, 75]. Therefore, the focus is on an LTI model for the transfer from a perturbation  $\delta F(t)$  in the belt force to the response  $\delta\ddot{c}(t)$  in the chest acceleration. Stepwise perturbations are added to the passive belt force  $F_p(t)$ .

In the sequel, the result of the application of the modelling strategy is presented in four consecutive steps: experiment design, analysis of the obtained data, realization of the LTI model(s) and evaluation of the realized model(s).

### Experiment design

In the simulations with the complex nonlinear model  $\mathcal{M}$ , a perturbation  $\delta F(t) = \Delta F \cdot \varepsilon(t - \tau)$  is added to the passive belt force  $F_p(t)$ . The mass flow and the vent size are not perturbed, meaning that they are the same as for the passive system.

To determine appropriate points  $\tau$  at which the perturbation is applied, the behavior of the dummy interacting with the passive restraint system is considered. At  $t = 6$  ms, the belt is abruptly tightened by the buckle pre-tensioner and at  $t \approx 18$  ms, the slack in the belt system is removed. The airbag shortly impacts the chest at  $t \approx 25$  ms, whereas a more stable contact is established at  $t \approx 35$  ms. The knees do not contact the knee bolsters during the crash. At  $t \approx 90$  ms, the airbag is more or less “empty”. Therefore, it seems reasonable to assume that, during the time interval from  $t = 20$  ms until  $t = 90$  ms, the dynamic behavior of the complex nonlinear model  $\mathcal{M}$  for the considered transfer is more or less smooth, except for the point of time at which the airbag shortly impacts the dummy and that at which a more stable contact is established. Here, two points of application before  $t = 35$  ms and two points thereafter are chosen, being  $\tau_1 = 20$  ms,  $\tau_2 = 25$  ms and  $\tau_3 = 40$  ms,  $\tau_4 = 64$  ms. Furthermore, to avoid disturbances of the dynamic behavior of the model  $\mathcal{M}$  due to the short impact of the airbag at  $t \approx 25$  ms, the airbag is removed from  $\mathcal{M}$  for the simulations for  $\tau_1 = 20$  ms and  $\tau_2 = 25$  ms.

To determine appropriate step sizes  $\Delta F$ , normalized responses  $\delta\ddot{c}(t)/\Delta F$  for various sizes added at  $\tau = 20$  ms, are analyzed. They are shown in Figure 2.9. It can be observed that for  $\Delta F \leq 50$  N, the normalized responses hardly differ. Therefore, the sizes  $\Delta F$  will be chosen in the range up to 50 N. Here, five positive and negative sizes are chosen, being  $\Delta F_1 = \pm 10$  N,  $\Delta F_2 = \pm 20$  N,  $\Delta F_3 = \pm 30$  N,  $\Delta F_4 = \pm 40$  N and  $\Delta F_5 = \pm 50$  N. A total of 20 simulations with the model  $\mathcal{M}$  without the airbag is performed, and 20 simulations with the model  $\mathcal{M}$  with the airbag are performed.

### Experimental results

The normalized responses  $\delta\ddot{c}_{i,1}(t)/\Delta F_i$  to steps at  $\tau_1 = 20$  ms with various sizes  $\Delta F_i$  for  $i = 1, \dots, 5$  are shown in Figure 2.10.

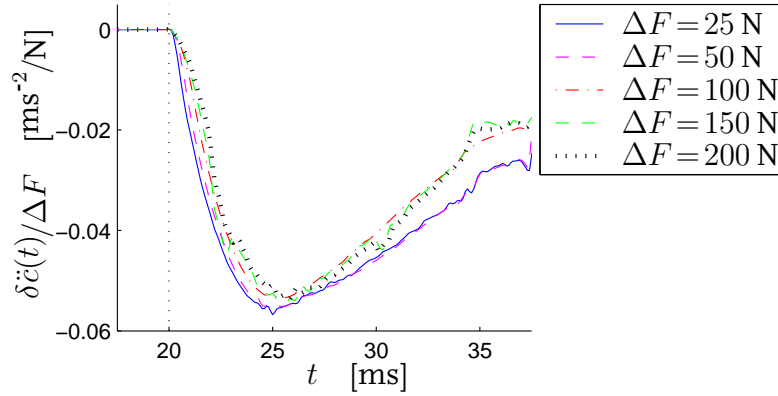


**Figure 2.9** Normalized responses to positive steps with various sizes at 20 ms

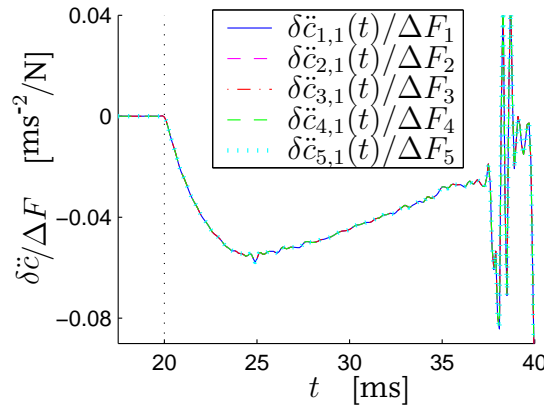


**Figure 2.10** Normalized responses to positive steps at  $\tau_1 = 20$  ms

As expected, the normalized responses hardly differ for  $t \leq 37$  ms, indicating dominantly linear dynamic behavior for (small) perturbations. This is not the case for  $t > 37$  ms. An analysis of the model  $\mathcal{M}$  shows that a reversal of the direction of the friction in the connecting joint of the left clavicle body and the left upper arm body causes this behavior. It is assumed that this friction does not drastically influence the relevant dynamic behavior. Therefore,  $\mathcal{M}$  is modified by eliminating this friction, and the simulations with  $\mathcal{M}$  are repeated. The newly obtained normalized responses  $\delta\ddot{c}_{i,1}(t)/\Delta F_i$  to positive and negative steps at  $\tau_1 = 20$  ms with size  $\Delta F_i$  with  $i = 1, \dots, 5$ , are shown in Figure 2.11.

These results justify the approximation of the relevant dynamic behavior for the considered transfer by a linear model, at least for small perturbations added at  $\tau_1 = 20$  ms. At  $t \approx 39$  ms, the normalized responses behave quite different. Since this occurs just after the dummy establishes a contact with the airbag, it is not analyzed and the normalized responses for  $t \in (20 \text{ ms}, 39 \text{ ms})$  are used for realization purposes.

For the other points of application  $\tau_2, \tau_3$  and  $\tau_4$ , the normalized responses also indicate that the transfer may be linearized for (small) perturbations. Henceforth, the averaged normalized responses for positive steps, denoted by  $\overline{\delta\ddot{c}_j}(t)$ , are used:

$$\overline{\delta\ddot{c}_j}(t) = \frac{1}{5} \sum_{i=1}^5 \frac{\delta\ddot{c}_{i,j}(t)}{\Delta F_i}. \quad (2.8)$$



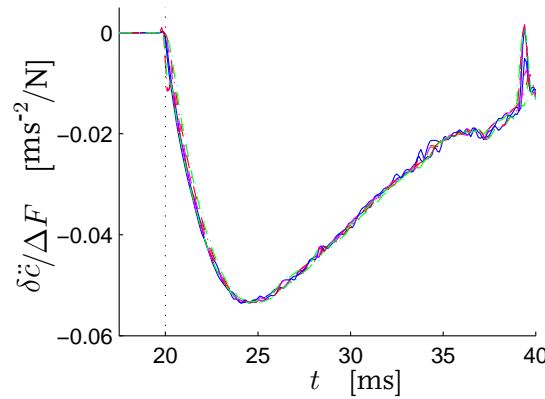


**Figure 2.11** Normalized responses to positive and negative steps at  $\tau_1 = 20$  ms

In Figure 2.12, the averaged normalized responses to steps at  $\tau_j$  with  $j = 1, 2, 3, 4$  are shown. They are shifted in time over a time interval of  $\tau_j$ . The responses  $\overline{\delta \ddot{c}_j}(t)$  for  $j = 1, 2$  are very similar, whereas the responses  $\overline{\delta \ddot{c}_j}(t)$  for  $j = 3, 4$  are clearly different. These observations suggest that the relevant dynamic behavior changes as a function of the operating point. Therefore, it is chosen to realize an approximating LTI model for each point of application. The length of the time interval of the responses is chosen as short as possible, but long enough to properly cover the first peak in the response.

### Realization

For the application of approximate realization, first the matrices  $T_j$  are constructed using the shown part of the averaged normalized responses  $\overline{\delta \ddot{c}_j}(t)$  with  $j = 1, 2, 3, 4$ . Then, singular value decomposition is performed. The largest five singular values are given in Table 2.1 and shown in Figure 2.13. These results make it plausible to neglect the third and higher singular values, meaning that the to-be-realized LTI models are of order two.

The system matrices  $A_j, B_j, C_j$  and  $D_j$  of these LTI models are computed using Equation 2.6. The feed through matrices  $D_j$ , directly obtained from  $\overline{\delta \ddot{c}_j}(\tau_j)$ , are given in Table 2.2. Their order of magnitude compared to the peak value of  $\overline{\delta \ddot{c}_j}(t)$ , seem to justify to neglect direct feed-through, i.e.  $D_j = 0$ .

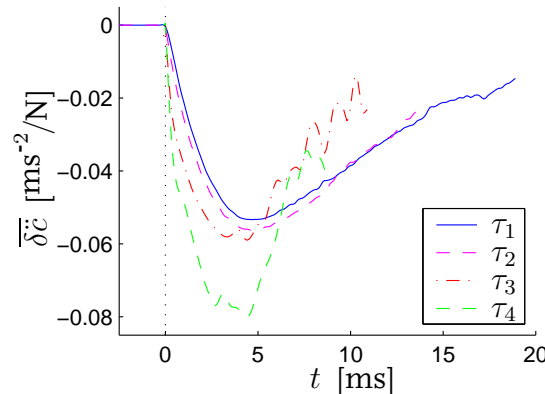


**Figure 2.12** Averaged normalized responses for the considered points of application

**Table 2.1** Singular values of  $T_j$

	$\sigma_1$	$\sigma_2$	$\sigma_3$	$\sigma_4$	$\sigma_5$
$\tau_1$	1.70	0.53	0.03	0.02	0.02
$\tau_2$	1.23	0.30	0.02	0.02	0.01
$\tau_3$	1.14	0.36	0.07	0.07	0.06
$\tau_4$	1.26	0.39	0.11	0.06	0.05

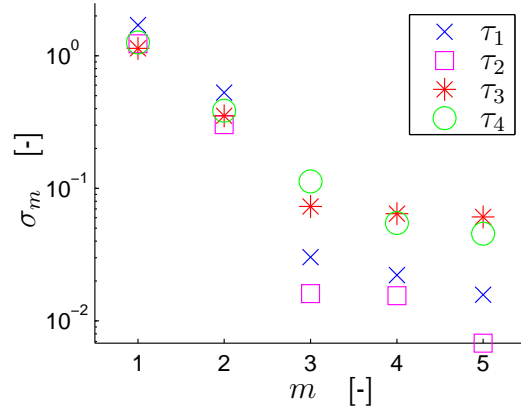


**Figure 2.13** Singular values of  $T_j$

**Table 2.2** Averaged normalized responses  $\overline{\delta\ddot{c}_j}(\tau_j)$

	$\tau_1$	$\tau_2$	$\tau_3$	$\tau_4$
$\overline{\delta\ddot{c}_j}(\tau_j)$ [ $\text{ms}^{-2}/\text{N}$ ]	$-3.6 \cdot 10^{-4}$	$-1.0 \cdot 10^{-3}$	$-2.2 \cdot 10^{-4}$	$-5.0 \cdot 10^{-4}$

The discrete-time models are transformed<sup>3</sup> into continuous-time models and reformulated into the standard transfer function:

$$\mathcal{H}(s) = \frac{K \cdot (s + z)}{\left(\frac{s}{\omega_n}\right)^2 + \frac{2\zeta}{\omega_n}s + 1} \quad (2.9)$$

where  $K$  is the gain,  $\omega_n$  the undamped eigenfrequency,  $\zeta$  the damping factor and  $z$  the system zero. These parameters are given in Table 2.3, whereas Figure 2.14 shows the Bode diagrams of the LTI models.

**Table 2.3** Model parameters of the realized LTI models

	$z/2\pi$ [Hz]	$K$ [ $\text{ms}^{-2}/\text{N}$ ]	$\omega_n/2\pi$ [Hz]	$\zeta$ [-]
$\tau_1$	-6	-0.017	39	0.72
$\tau_2$	-1	-0.024	36	0.88
$\tau_3$	-12	-0.011	72	0.88
$\tau_4$	-16	-0.013	75	0.78

## Evaluation

The model parameters of the realized LTI models for points  $\tau_1$  and  $\tau_2$  do not significantly differ. The same remark holds for the models for points  $\tau_3$  and  $\tau_4$ . However, the models for  $\tau_1$  and  $\tau_2$  significantly differ from the model for  $\tau_3$  and  $\tau_4$ . These observations suggest

<sup>3</sup> Transformation of the discrete-time models into continuous-time models is performed using the standard 'matched pole-zero' method [98].

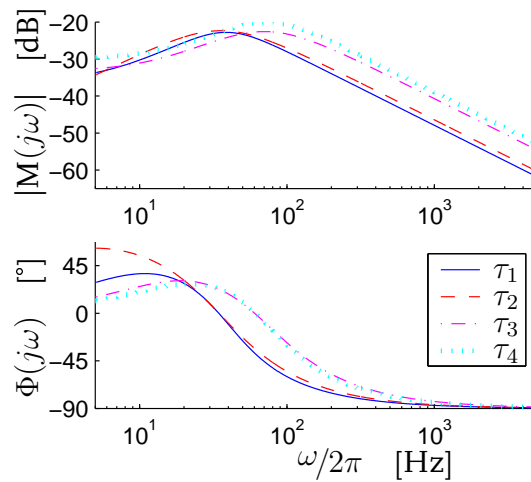


Figure 2.14 Bode diagrams of the realized LTI models

that the contact with the airbag has a significant influence on the relevant local dynamic behavior of the complex nonlinear model. Furthermore, it indicates that this behavior is more or less constant as long as the dummy is not in contact with the airbag. The same holds for the situation in which the dummy is in contact with the airbag.

Apparently, the contact of the dummy with the airbag results in an increase of the undamped eigenfrequency, a small reduction of the system gain and a significant change of the system zero. The fact that the order of the LTI models can be chosen as two may be explained by an analysis of a simplified model [92, 111] of the dummy thorax under frontal impact conditions. The simplified model describes the dummy thorax by two rigid bodies, representing the sternum and the thoracic mass, interconnected by springs and dampers and subjected to external forces, representing the forces applied by the belt and/or the airbag.

To judge the quality of the realized LTI models, the unit step response of the LTI models is compared to the averaged normalized responses, used to derive the LTI model. Figure 2.15 shows the averages  $\overline{\delta\tilde{c}_j}(t)$  together with the unit step responses  $y_{\mathcal{H}_j}(t)$  with  $j = 1, 3$ . The value of the quality measure  $\kappa$ , Equation 2.7, is 0.024, 0.026, 0.11, and 0.10 for  $\tau_j$  with  $j = 1, 2, 3, 4$ , respectively. For the points  $\tau_1$  and  $\tau_2$ , the quality is satisfactory, whereas for the points  $\tau_3$  and  $\tau_4$ , the quality is (too) low. Nevertheless, the shape of the responses in Figure 2.15(b) is very similar, as well as characteristics like peak value and rise time. Therefore, it seems that the relevant dynamic behavior is reasonably captured by the LTI model, and that is the most important aspect for control design purposes.

## 2.5 Modelling of the airbag

In this section, the relevant dynamic behavior of the airbag interacting with the dummy is modelled. The modelling strategy from Section 2.3 is applied to arrive at an LTI control design model for the airbag. Since almost all kinetic energy of the dummy head is absorbed by the airbag [56], the focus in this section is on the transfer from a perturbation

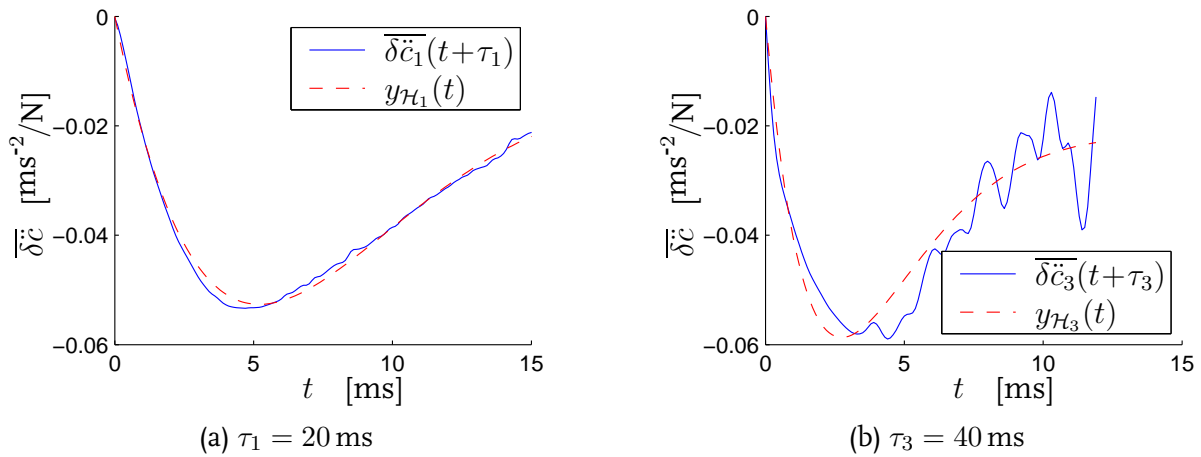


**Figure 2.15** The unit step response of the LTI models and the corresponding averaged normalized responses for  $\tau_1$  and  $\tau_3$

$\delta\phi(t)$  in the mass flow to the response  $\delta\ddot{h}(t)$  in the head acceleration and on the transfer from a perturbation  $\delta A(t)$  in the vent size to the response  $\delta\ddot{h}(t)$  in the head acceleration.

In Section 2.5.1, the approximation of the transfer from  $\delta\phi(t)$  to  $\delta\ddot{h}(t)$  and in Section 2.5.2, the approximation of the transfer from  $\delta A(t)$  to  $\delta\ddot{h}(t)$  is elucidated.

### 2.5.1 Modelling the transfer from the mass flow to the head acceleration

In this section, stepwise perturbations in the mass flow are added to the total mass flow of the passive inflators,  $\phi_p(t)$ . The results are presented in four consecutive steps: experiment design, analysis of the obtained data, realization of the LTI model(s) and evaluation of these LTI model(s).

#### Experiment design

A stepwise perturbation  $\delta\phi(t) = \Delta\phi \cdot \varepsilon(t - \tau)$  is added to the mass flow  $\phi_p(t)$ , whereas the belt force and the vent size are not perturbed, meaning that they are the same as for the passive system.

To determine points  $\tau$  at which the perturbation is applied, the behavior of the passive restraint system is considered. The airbag shortly impacts the head of the dummy at  $t \approx 25$  ms, and establishes a more stable contact with the dummy head at  $t \approx 35$  ms. At  $t \approx 40$  ms, the airbag is fully deployed and at  $t \approx 90$  ms, the airbag is “empty”. The knees of the dummy do not contact the knee bolsters and the head of the dummy does not contact the steering wheel. Therefore, it seems reasonable to assume that the relevant dynamic behavior is more or less smooth from  $t = 40$  ms until  $t = 90$  ms. In this time interval, two points of application are chosen, being  $\tau_1 = 50$  ms and  $\tau_2 = 60$  ms.

To determine appropriate step sizes  $\Delta\phi$ , the normalized responses  $\delta\ddot{h}(t)/\Delta\phi$  for various sizes of a step at 50 ms, are analyzed. They are shown in Figure 2.16. Although the normalized responses have been filtered in a causal and anti-causal manner with a second

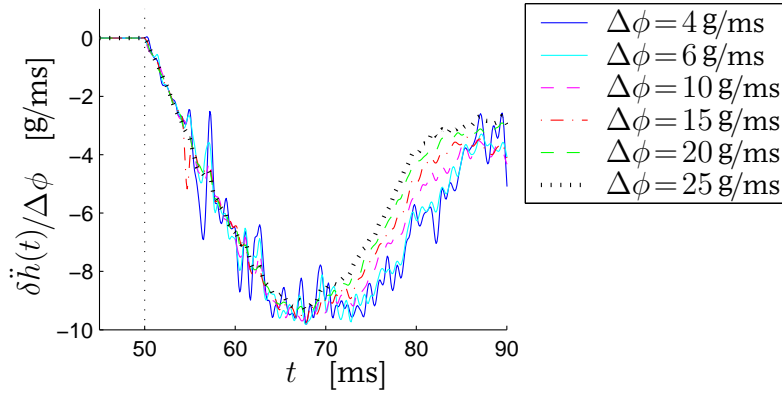


**Figure 2.16** Normalized responses to steps with various sizes at 50 ms

order, digital Butterworth filter [98] with a cut-off frequency of 1 kHz, they still suffer from (computational) noise. The normalized responses for  $\Delta\phi \leq 10$  g/ms are very close to each other. For  $\Delta\phi < 6$  g/ms, the signal-to-noise ratio is too low. Therefore, three step sizes are chosen, being  $\Delta\phi_1 = 6$  g/ms,  $\Delta\phi_2 = 8$  g/ms and  $\Delta\phi_3 = 10$  g/ms. The simulation package MADYMO interprets a mass flow  $\phi(t)$  lower than 0 as  $\phi(t) = 0$ . Since  $\phi_p(t) \leq 6$  g/ms for  $t > 48$  ms and  $\phi_p(t) = 0$  for  $t > 57$  ms, simulations with negative steps at 50 ms or 60 ms do not make sense. Hence, a total of 6 simulations with the model  $\mathcal{M}$  is performed.

### Experimental results

The normalized responses to steps at  $\tau_1 = 50$  ms and at  $\tau_2 = 60$  ms are shown in Figure 2.17. From these results, linearization of the investigated transfer seems to be justified, at least for each point of application  $\tau$ . Henceforth, the averaged normalized responses  $\overline{\delta \ddot{h}_j(t)}$  are used.

In Figure 2.18, the averaged normalized responses  $\overline{\delta \ddot{h}_1(t)}$  and  $\overline{\delta \ddot{h}_2(t)}$  are shown. Considering the relatively small differences in characteristics as the peak time, peak value and rise time, it seems justified to assume that the relevant dynamic behavior only slightly

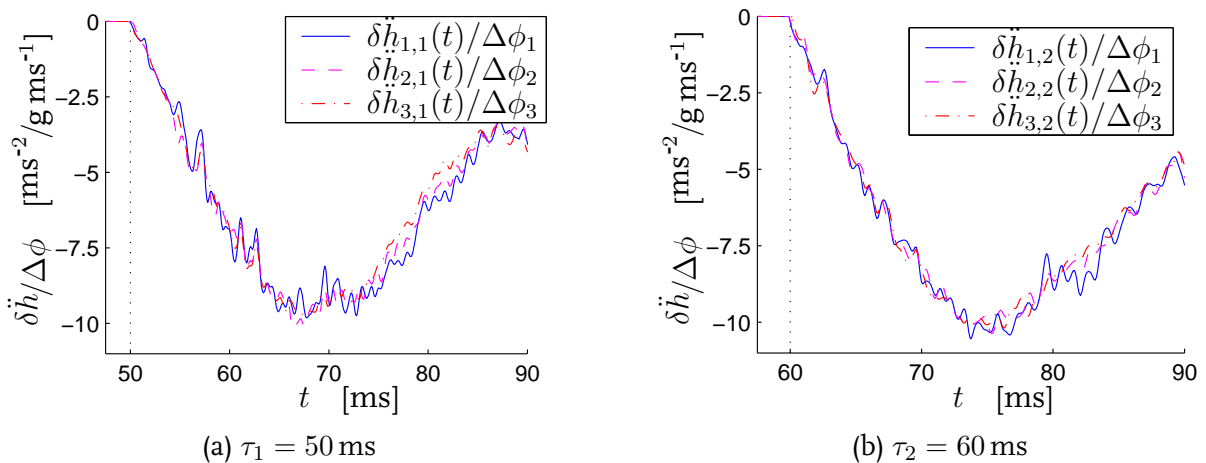


**Figure 2.17** Normalized responses to steps at  $\tau_1$  and  $\tau_2$

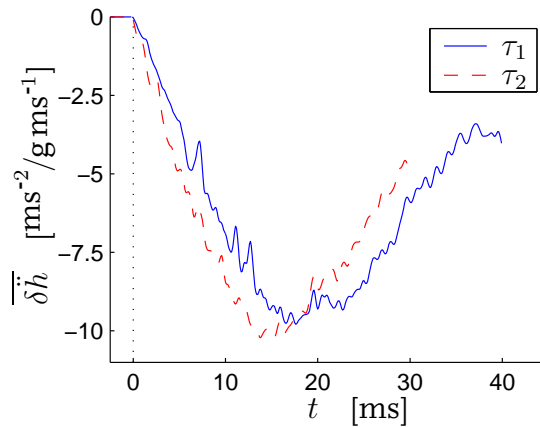


**Figure 2.18** Averaged normalized responses for the considered points of application

change as a function of the operating point. Nevertheless, it is chosen to approximate the relevant local dynamic behavior by an LTI model for each point  $\tau$ .

### Realization

Again, the concept of approximate realization is applied to derive LTI models. The matrices  $T_j$  are constructed using  $\overline{\delta \ddot{h}_j}(t)$  with  $j = 1, 2$ . Next, singular value decomposition is performed to determine the order of the to-be-realized LTI models. The largest five singular values are given in Table 2.4 and shown in Figure 2.19. They make it plausible to neglect the third and higher singular values, meaning that the to-be-realized LTI models are of order two.

Using Equation 2.6, the system matrices  $A_j, B_j, C_j$  and  $D_j$  of the LTI models are computed. The feed through matrices  $D_j$ , directly obtained from  $\overline{\delta \ddot{h}_j}(\tau_j)$ , are given in Table 2.5. Their magnitude compared to the peak value of  $\overline{\delta \ddot{h}_j}(t)$ , seems to justify to neglect direct feed through, i.e.  $D_j = 0$ .

The obtained discrete-time models are transformed into continuous-time models and

	$\sigma_1$	$\sigma_2$	$\sigma_3$	$\sigma_4$	$\sigma_5$
$\tau_1$	745	189	24	20	19
$\tau_2$	548	111	19	15	10

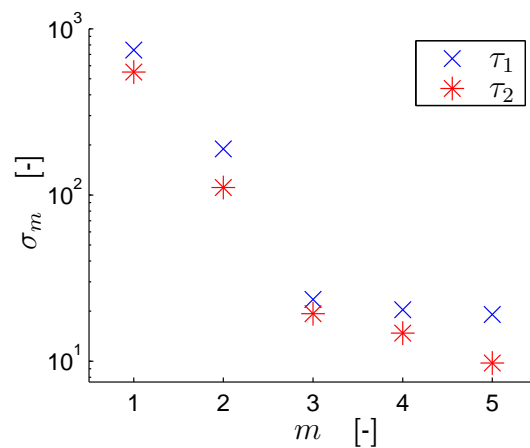


**Figure 2.19** Singular values of  $T_j$

**Table 2.5** Averaged normalized responses  $\overline{\delta\ddot{h}_j(\tau_j)}$ 

		$\tau_1$	$\tau_2$
$\overline{\delta\ddot{h}_j(\tau_j)}$	$[\text{ms}^{-2}/\text{g ms}^{-1}]$	0.035	-0.099

**Table 2.6** Model parameters of the realized LTI models

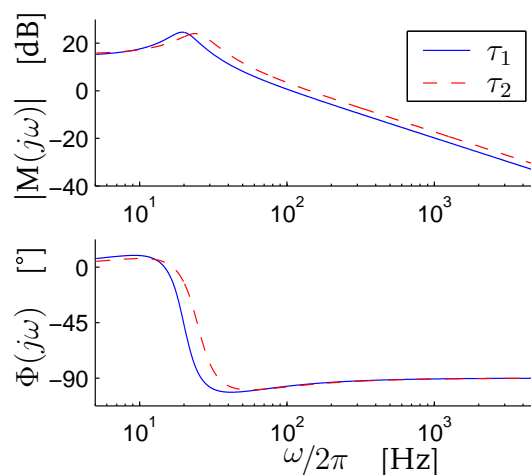
	$z/2\pi$ [Hz]	$K$ $[\text{ms}^{-2}/\text{g ms}^{-1}]$	$\omega_n/2\pi$ [Hz]	$\zeta$ [-]
$\tau_1$	-21	-1.60	20	0.22
$\tau_2$	-27	-1.39	25	0.26

reformulated into the standard transfer function of Equation 2.9. The model parameters are given in Table 2.6 and the Bode diagrams are shown in Figure 2.20.

### Evaluation

The model parameters of the realized LTI models for the considered points of application do not significantly differ, confirming the assumption that the relevant dynamic behavior changes slightly over the considered time interval.

To judge the quality of the realized LTI models, their unit step response is compared to the averaged normalized responses  $\overline{\delta\ddot{h}_j(t)}$  that are used to derive the models. Figure 2.21 shows these averages and the unit step responses  $y_{\mathcal{H}_j}(t)$  for  $\tau_j$  with  $j = 1, 2$ . The value of the quality measure  $\kappa$  is 0.043 and 0.032 for  $\tau_1$  and  $\tau_2$ , respectively. These values indicate that the LTI models are sufficiently accurate, at least for (small) perturbations at the considered points  $\tau$ .

**Figure 2.20** Bode diagrams of the realized LTI models

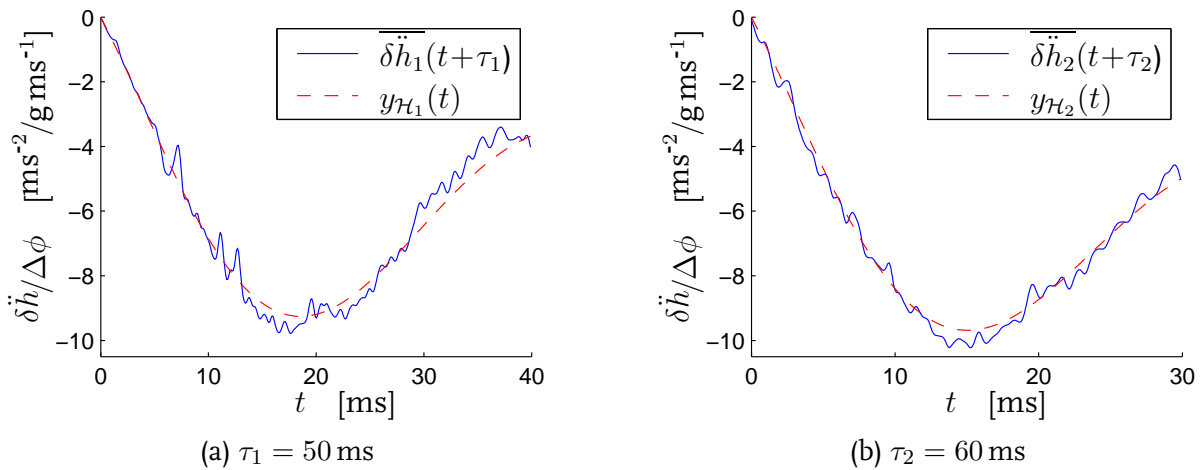


**Figure 2.21** The unit step response of the LTI models and the corresponding averaged normalized response for the considered points of application

## 2.5.2 Modelling the transfer from the vent size to the head acceleration

In this section, the focus is on the approximation of the transfer from a perturbation  $\delta A(t)$  in the vent size to the response  $\ddot{h}(t)$  in the head acceleration. In the sequel, the results are presented in the same four consecutive steps as previously.

### Experiment design

A perturbation  $\delta A(t) = \Delta A \cdot \varepsilon(t - \tau)$  is added to the vent size  $A_p(t)$ . The belt force and the mass flow are not perturbed, meaning that they are the same as for the passive system.

The points of application  $\tau$  from Section 2.5.1 are adopted here, i.e.  $\tau_1 = 50$  ms and  $\tau_2 = 60$  ms. To determine appropriate step sizes  $\Delta A$ , the normalized responses  $\delta \ddot{h}(t)/\Delta A$  to positive steps at 50 ms with various sizes, are analyzed. They are shown in Figure 2.22.

Although the normalized responses have been filtered in a causal and anti-causal manner with a second order, digital Butterworth filter with a cut-off frequency of 1 kHz, they still

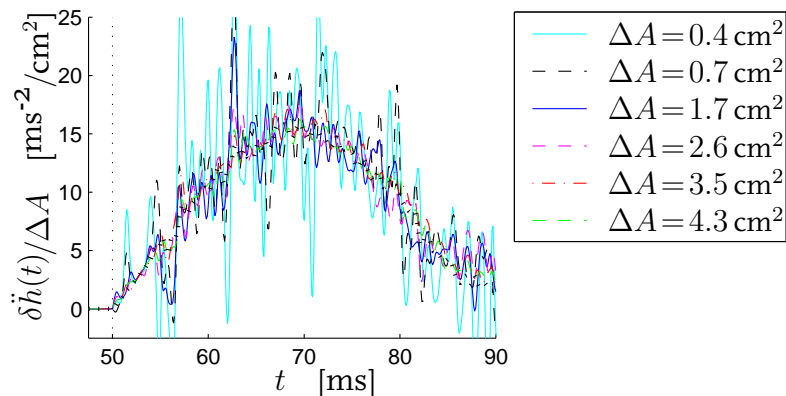


**Figure 2.22** Normalized responses to steps with various sizes at 50 ms



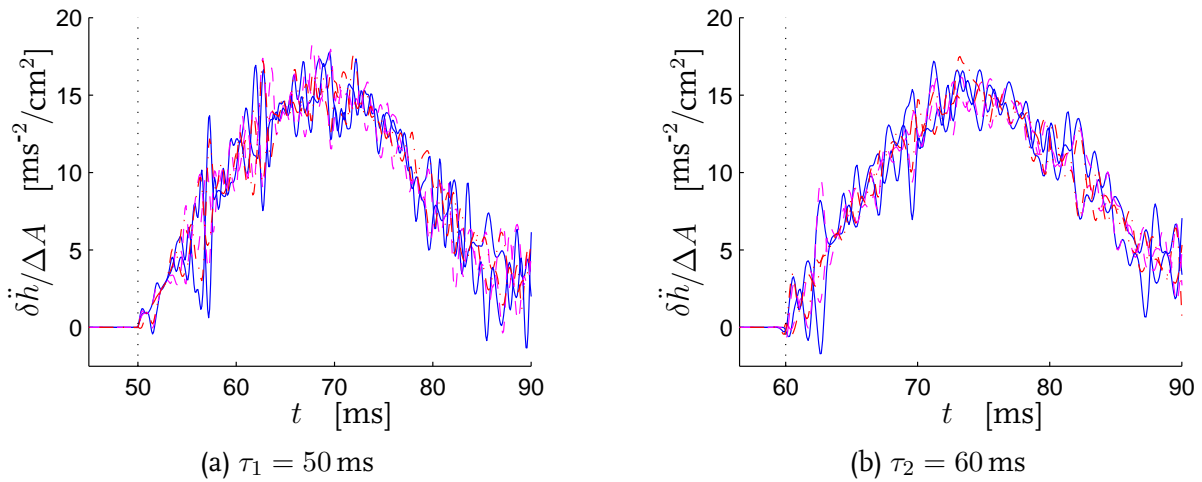


**Figure 2.23** Normalized responses to positive and negative steps at  $\tau_1$  and  $\tau_2$

suffer from (computational) noise. For  $\Delta A \leq 0.7$  cm<sup>2</sup>, the signal-to-noise ratio is far too low, whereas for  $\Delta A > 0.7$  cm<sup>2</sup>, the normalized responses are very close to each other. Here, positive and negative step sizes  $\Delta A_1 = \pm 1.4$  cm<sup>2</sup>,  $\Delta A_2 = \pm 1.7$  cm<sup>2</sup> and  $\Delta A_3 = \pm 2.1$  cm<sup>2</sup>, reflecting  $\pm 8\%$ ,  $\pm 10\%$  and  $\pm 12\%$  of the (constant) size of the “passive” vent, are chosen. A total of 12 simulations is performed.

### Experimental results

The normalized responses  $\delta \ddot{h}(t) / \Delta A$  to steps at  $\tau_1 = 50$  ms and  $\tau_2 = 60$  ms with positive and negative sizes are shown in Figure 2.23. The normalized responses to positive steps are close to the normalized responses to negative steps and approximation of the considered transfer by LTI models seems to be justified, at least at each point of application. Henceforth, the averaged normalized response  $\overline{\delta \ddot{h}}(t)$  for positive step sizes is used.

Figure 2.24 shows the averages  $\overline{\delta \ddot{h}}_j(t)$  for  $\tau_j$  with  $j = 1, 2$ , shifted over a time interval  $\tau_j$ . Considering the small differences in peak time and rise time, it seems justified to assume that the relevant dynamic behavior changes slightly as a function of the operating point.

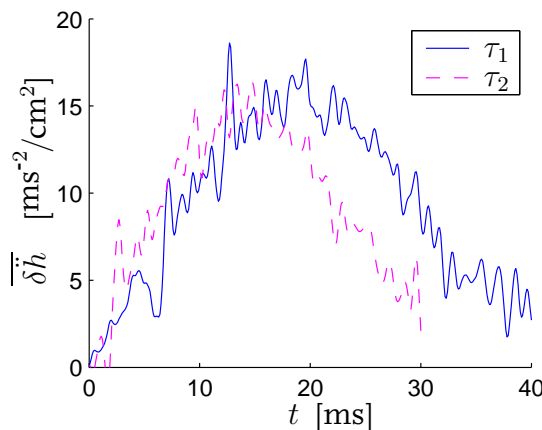


**Figure 2.24** Averaged normalized responses for the considered points of application

**Table 2.7** Singular values of  $T_j$

	$\sigma_1$	$\sigma_2$	$\sigma_3$	$\sigma_4$	$\sigma_5$
$\tau_1$	1316	377	108	71	69
$\tau_2$	881	232	73	48	47

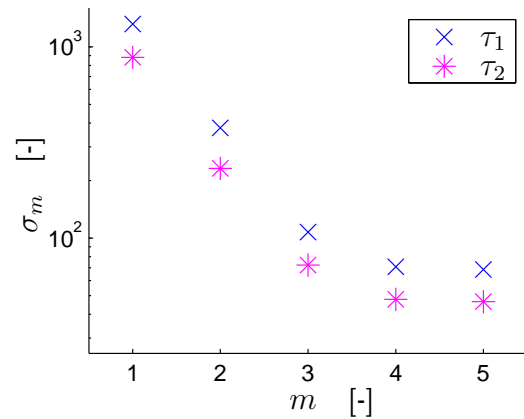


**Figure 2.25** Singular values of  $T_j$

It is chosen to approximate the relevant local dynamic behavior by an LTI model for each point  $\tau$ .

### Realization results

The matrices  $T_j$  are constructed using  $\overline{\delta\ddot{h}_j(t)}$  with  $j = 1, 2$  and singular value decomposition is performed to determine the order of the to-be-realized LTI models. The largest five singular values are given in Table 2.7 and shown in Figure 2.25. They make it plausible to neglect the third and higher singular values, meaning that the to-be-realized LTI models are of order two.

Using Equation 2.6, the system matrices  $A_j, B_j, C_j$  and  $D_j$  are computed. The feed through matrices  $D_j$  follow from  $\overline{\delta\ddot{h}_j(\tau_j)}$  and are given in Table 2.8. Comparing their magnitude to the peak value of  $\overline{\delta\ddot{h}_j(t)}$ , it is plausible to assume that  $D_j = 0$ .

The LTI models are transformed into continuous-time models and reformulated into the standard transfer function of Equation 2.9. The model parameters are given in Table 2.9, whereas the Bode diagrams of the transfer functions are shown in Figure 2.26.

### Evaluation

The small differences between the model parameters of the obtained LTI models for  $\tau_1$  and  $\tau_2$  indicate that the relevant local dynamic behavior of the complex nonlinear model only slightly changes as a function of the operating point.

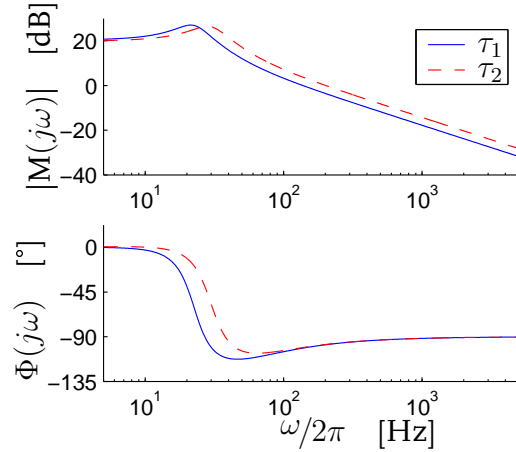
To judge the quality of the realized LTI models, their unit step response is compared to the averaged normalized responses, used to derive the models. Figure 2.27 shows these

**Table 2.8** Averaged normalized responses  $\overline{\delta\ddot{h}_j(\tau_j)}$

	$\tau_1$	$\tau_2$
$\overline{\delta\ddot{h}_j(\tau_j)}$ [ $\text{ms}^{-2}/\text{cm}^2$ ]	0.013	0.104

**Table 2.9** Model parameters of the realized LTI models

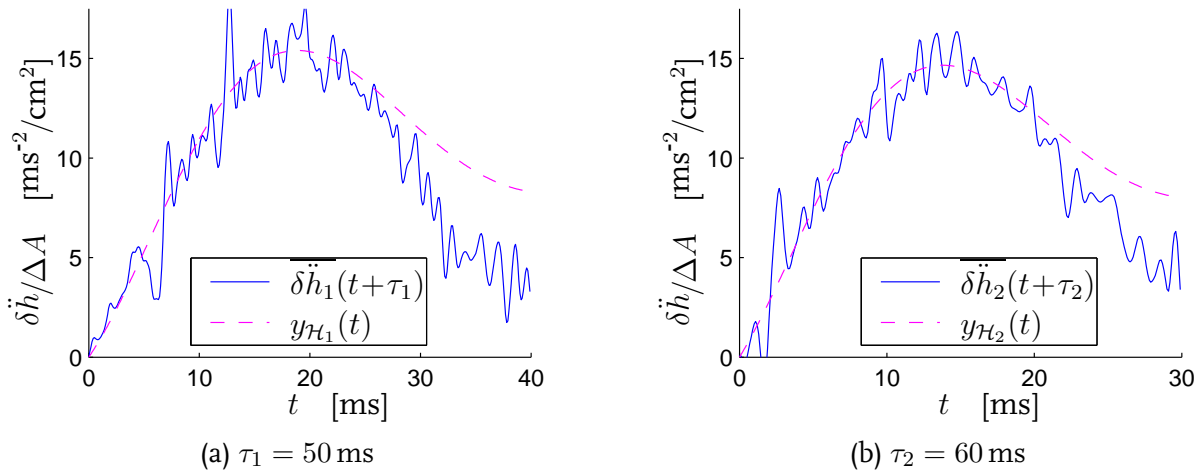
	$\tau_1$	$\tau_2$
$z/2\pi$ [Hz]	-41	-46
$K$ [ $\text{ms}^{-2}/\text{cm}^2$ ]	1.6	1.4
$\omega_n/2\pi$ [Hz]	23	30
$\zeta$ [-]	0.27	0.29

**Figure 2.26** Bode diagrams of the realized LTI models

averages together with the unit step responses  $y_{\mathcal{H}_1}(t)$  and  $y_{\mathcal{H}_2}(t)$ . The quality measure  $\kappa$  is 0.17 for  $\tau_1$  and 0.13 for  $\tau_2$ . These values exceed the criterion  $\kappa \leq 0.05$ . This may be explained by the (computational) noise and the less accurately predicted response for  $t > \tau_j + 20$  ms. Nevertheless, the shape of the unit step response and the averaged normalized responses is for the first part more or less the same, indicating that the (local) relevant dynamic behavior actually is reasonably described by the LTI models, at least for (small) perturbations.

## 2.6 Discussion

In the previous sections, a straightforward and fairly general applicable, data-based modelling strategy has been presented and the approach has been applied to the three most important transfers for (the design of) active restraint systems. Although many identification or approximation approaches exist, the approximate realization is robust and

**Figure 2.27** The unit step response of the LTI models and the corresponding averaged normalized response for the considered points of application

computational attractive. As for most applications, also here the most relevant issue during the modelling process is the design of experiments and the interpretation of the experiment results.

The choice of the point  $\tau$  at which a perturbation is added, is difficult, since detailed knowledge about non-smooth phenomena is not available. Furthermore, the determination of the length of the output response, used for realization purposes can be difficult, since the time scale of changes in the dynamic behavior has to be deduced from the output responses.

The strongest operating point dependency has been observed for the local behavior of the belt, interacting with the dummy. It is plausible that this is caused by the contact of the dummy with the airbag. Apart from that, the model parameters do not drastically change as a function of the operating point and the obtained LTI models are fairly accurate. This suggests that the local dynamic behavior of the nonlinear model does not drastically change as a function of the operating point. In addition, it gives some confidence in the use of the LTI models for the design of controllers.

Besides the hopeful results in this chapter, there are two arguments to expect that the use of LTI models for the design of controllers is effective. First, feedback control may have a linearizing effect on the behavior of the closed loop system. Second, if the dummy is properly restrained, undesired nonlinear and/or non-smooth phenomena as contacts of the dummy with vehicle parts like the steering wheel, will not occur. Still, the main uncertainty is the difference between the dynamic behavior along the used trajectory of operating points and that along the trajectory of operating points of the closed loop system. For this reason, closed loop results will be investigated and approximating LTI models will be realized in closed loop operating points of the complex nonlinear model. This will be done in the following chapter.



# Control design for restraint system components

*A strategy is presented to design a controller to manipulate the belt or the airbag to control one variable, representing the risk of injuries to the chest or to the head. The control design problem is formulated as a feedback tracking problem with the objective to force the controlled variable to follow an a priori defined reference signal. Specifications on the closed loop behavior are formulated and translated into control design criteria. Reference signals are constructed, such that they represent the lowest possible risk of injuries.*

### 3.1 Introduction

The control objective is to reduce one measure for the risk of injuries as much as possible by manipulation of the belt or the airbag during the crash. As mentioned in Chapter 1, the approach we follow in this work is to define a reference signal that represents the lowest possible risk of injuries. Such a reference signal is constructed for the head or chest acceleration and a feedback controller is designed to manipulate the belt force, the mass flow or the vent size to force the controlled variable to follow the reference signal. In this chapter, a control design strategy is presented to arrive at these controllers. One restraint system component is manipulated, whereas the other components are passive. Obtained results can function as a benchmark, whereas obtained insight into the closed loop system can be valuable for the case that both restraint system components are manipulated.

Feedback control has several advantages over feedforward control [40]. For our purposes, the advantage is threefold. First, the effect of model mismatches and uncertainties can be reduced. Second, the effect of disturbances on closed loop behavior can be reduced. Third, feedback control may have a linearizing and stabilizing effect on the closed loop system. These advantages are important, considering, for example, differences between the complex nonlinear model  $\mathcal{M}$  and the LTI control design models.

Feedforward control has some disadvantages for the problem at hand. To enforce the desired behavior of complex models like the model  $\mathcal{M}$  with feedforward only, is com-

plicated. The achieved performance strongly depends on the accuracy of knowledge of the dynamic behavior of the controlled system and of the disturbances. In our case, the model  $\mathcal{M}$  is accurate, but can not be translated easily into an inverse model for feed-forward purposes. Furthermore, accurate knowledge of disturbances for one crash and dummy is already limited, not to mention the knowledge of disturbances for wider classes of crashes and dummies.

Here, it is chosen for feedback control only. A control design strategy is desired to arrive at a linear feedback controller. The reason to investigate a linear controller is threefold. First, results of Chapter 2 show that for the most important transfer, the dynamic behavior from a small perturbation in the manipulated variables to the response in the controlled variables can be reasonably approximated by LTI models. Second, nonlinear controllers generally pose higher demands on control design and implementation than linear controllers. Third, the use of linear controllers for complex nonlinear systems can be very effective. Especially for process control, it is a widely applied approach, e.g. [44, 121, 129].

The question to be answered at this stage is whether linear feedback control is adequate or nonlinear control is necessary. The answer depends on various issues [40], like operating range, disturbances, modelling accuracy, etc. A theoretical framework to address the need for nonlinear controllers is given in [45, 120]. Unfortunately, that framework can not be used here, due to the lack of a manageable nonlinear model. This leaves us with the only option to experimentally investigate whether linear feedback control is adequate, and whether, for instance, gain scheduling [85, 133] is necessary.

For the design of a linear feedback controller  $\mathcal{C}$ , the control design problem is formulated as a feedback tracking problem. The objective is to regulate the manipulated variable, e.g. the belt force  $F(t)$ , to force the controlled output, e.g. the chest acceleration  $\ddot{c}(t)$ , to follow an a priori defined reference signal,  $r_{\ddot{c}}(t)$ , with a sufficiently small error,  $e_{\ddot{c}}(t) = r_{\ddot{c}}(t) - \ddot{c}(t)$ . A typical design technique for feedback tracking controllers is loopshaping [6, 42, 51]. Here, “classical” loopshaping technique is used, exemplified in [149]. Using an LTI control design model, a controller is designed to enforce the desired closed loop behavior. Typically, several transfer functions, each emphasizing specific aspects of the closed loop behavior, are used. For example, the sensitivity transfer function describes the transfer from the reference signal to the error signal, and gives insight into the error rejection in the closed loop system.

For our purposes, reference signals are (mis)used to translate the problem at hand into a tracking problem, comparable to the reference governor approach [12, 13, 14, 55]. Not only they have to represent the lowest possible value of the risk of injuries, but also they have to prevent undesired contacts of the dummy with inner-vehicle components. In addition, they should prevent actuator saturation. The model  $\mathcal{M}$  is nonlinear and far too complex to provide the required knowledge to derive appropriate reference signals. The specification of actuator saturation is almost impossible, since real world actuators do not (yet) exist. Therefore, it is chosen for a pragmatic approach to derive appropriate reference signals using simple, one-dimensional models of the dummy and the vehicle. Actuator saturation can be accounted for by imposing bounds on the manipulated variable in the

closed loop and iteratively adapting the reference signal until undesired contacts of the dummy are prevented.

Recently, so called pre-crash sensing devices [27, 108, 141, 165] have been introduced. They make it possible to classify an oncoming crash and tighten the belt before the crash takes place. Here, the use of such devices is anticipated. In fact, it is assumed that the vehicle acceleration over the full crash duration is known at the start of the crash, i.e. at  $t = t_0 = 0$ , and that the belt system can be manipulated from the start of the crash. As a result of that, tightening of the belt by the pre-tensioner at  $t = 6$  ms is unnecessary. For the airbag system, pre-crash sensing is less relevant, since occupants have to move forward to contact the airbag, meaning that the ideal point of time to trigger the inflators is not necessarily the earliest possible point of time [96, 144]. Here, triggering of the inflators is not changed, meaning that the inflators are triggered as if they are passive.

In Section 3.2, the control design strategy is elucidated in general terms. In Section 3.3 and 3.4, this strategy is applied to design controllers for the belt system and for the airbag system, respectively. Section 3.5 concerns actuator saturation. Finally, the control design strategy is evaluated in Section 3.6.

## 3.2 Strategy

The feedback controller  $\mathcal{C}$  is designed using LTI control design models and evaluated using the closed loop system with the model  $\mathcal{M}$ , illustrated in Figure 3.1. In this figure,  $r(t)$  denotes the reference signal,  $u(t)$  the manipulated variable,  $y(t)$  the controlled variable,  $e(t) = r(t) - y(t)$  the error, and  $\ddot{x}_{\text{veh}}(t)$  the vehicle acceleration.

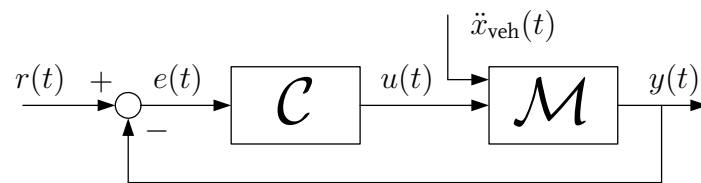


**Figure 3.1** Closed loop system for evaluation purposes

The control objective is to reduce the risk of injury as much as possible and to prevent undesired contacts. That goal will be achieved if the controlled variable  $y$  accurately follows an appropriate reference signal. For that purpose, specifications on the behavior of the closed loop system are defined and translated into criteria for control design. A simulation using the closed loop system with the controller and the complex nonlinear model shows whether these specifications are satisfied.

Three specifications concerning the behavior of the closed loop system with the model  $\mathcal{M}$  are formulated:



1. The closed loop system is stable. For closed loop systems with a model like  $\mathcal{M}$ , this specification is meaningless, since stability can not be proven. Instead, it is desired that the time histories of the manipulated and controlled variables are smooth.
2. The error  $e(t)$  is less than the maximum allowable error  $e_{\max}$ . Here, a maximum of 10 % of the (absolute) reference signal is chosen, i.e.  $e_{\max} = 0.1 \cdot \max_{t \in [t_0, t_e]} |r(t)|$ .
3. The controlled variable follows the reference signal sufficiently fast, formulated as the specification that 10 ms after an actuator is enabled, the error is less than 5 % of  $r_{\max}$ .

These specifications are translated into three control design criteria:

1. To ensure a stable and robust closed loop system with an LTI control design model, minimum values of the gain margin GM and the phase margin PM are required. Relatively large margins of  $\text{GM} > 3$  and  $\text{PM} > 45^\circ$  are adopted to account for uncertainties and for model mismatches between the model  $\mathcal{M}$  and the LTI control design models.
2. To achieve that the error  $e$  is less than  $e_{\max}$ , a bound is imposed on the modulus of the sensitivity transfer function  $S(s)$  with  $s = j\omega$ :

$$|S(s)| = \left| \frac{e(s)}{r(s)} \right| = \left| \frac{1}{1 + \mathcal{H}(s)\mathcal{C}(s)} \right| \leq -20 \text{ dB} \quad \text{for} \quad \omega \leq 2\pi f' \quad (3.1)$$

with  $f'$  the frequency at which the bound is imposed and  $\mathcal{H}(s)$  an LTI control design model. The frequency  $f'$  depends on characteristics of the closed loop system.

3. To achieve that the output follows the reference signal sufficiently fast, the 5 % settling-time  $t_{5\%}$ , defined as the elapsed time before the step response of an LTI model is bounded between 95 % and 105 % of the steady state response, is used. So,  $t_{5\%} \leq 10 \text{ ms}$ .

One of the key characteristics of a closed loop system with an LTI model is the bandwidth  $f_{\text{BW}}$ , defined as the 0 dB crossover frequency of the open loop transfer function  $\mathcal{H}(s) \cdot \mathcal{C}(s)$ . Typically, a controller is designed aiming at a high bandwidth to achieve high tracking performance. However, high bandwidth controllers pose high(er) demands on sensors and actuators and are more sensitive to noise and disturbances than low bandwidth controllers. Therefore, the aim is a low bandwidth controller. An indication of an appropriate bandwidth is obtained using [42]:

$$2\pi f_{\text{BW}} \approx \frac{3}{\zeta t_{5\%}}, \quad (3.2)$$

where  $\zeta$  is the damping factor. For a properly damped LTI closed loop system, i.e.  $\zeta = 0.7$ , this equation yields that a bandwidth of at least 70 Hz is required. It is emphasized that this relation only holds for LTI models of order two without a system zero, meaning that the computed bandwidth is to be seen as a rough indication.

The results of Chapter 2 suggest that the relevant dynamic behavior changes as a function of the operating point. However, these changes are relatively small. Therefore, the aim is one constant controller that satisfies the mentioned control design criteria for each of the considered LTI control design models.

### 3.3 Control of the chest acceleration by the belt

The control design strategy from the previous section is applied to design a controller to manipulate the belt force  $F$ . Here, the focus is on control of the chest acceleration  $\ddot{c}$ , since the risk of injuries to the chest is dominantly influenced by forces applied by the belt [56, 75]. The airbag is not manipulated, meaning that it behaves as if it is passive.

In the sequel, control of the chest acceleration is presented in four consecutive steps, concerning: control design criteria, controller design, design of the reference signal and evaluation of the controller and the reference signal in the closed loop system with the model  $\mathcal{M}$ . After that, the LTI control design models are compared with yet to-be-realized LTI models for closed loop operating points of the complex nonlinear model.

#### Control design criteria

The control design criteria, are the desired gain margin  $GM > 3$ , the desired phase margin  $PM > 45^\circ$ , the bound on the modulus of the sensitivity transfer function  $|S(j\omega)| \leq -20$  dB for  $\omega/2\pi \leq f'$ , and the 5% settling time  $t_{5\%} \leq 10$  ms.

To achieve sufficient error rejection, it is required that the modulus of the sensitivity transfer function does not violate the bound  $|S(j\omega)| \leq -20$  dB for  $\omega \leq 2\pi f'$  with  $f'$  a yet to-be-determined frequency. Typically, such a frequency is determined using available performance specifications [149] or frequency content of signals in the closed loop system. Unfortunately, such knowledge is limited for the problem at hand. Instead, an appropriate frequency  $f'$  is determined by an analysis of the spectral density of the chest acceleration  $\ddot{c}_p(t)$  for the case that the restraint system is passive. The cumulative spectral density of the chest acceleration  $\ddot{c}_p(t)$  is determined using Welch's averaged, modified periodogram [91, 98] and shown in Figure 3.2. From this result, it can be concluded that almost 95% of the total energy in the chest acceleration  $\ddot{c}_p(t)$  is covered by frequencies less than 100 Hz. Hence, the frequency  $f' = 100$  Hz seems to be appropriate.

#### Control design

In Section 2.4, it has been observed that the dynamic behavior of the dummy, interacting with the belt, is influenced by the contact of the dummy with the airbag. Therefore, the feedback controller is firstly designed focussing on the points of application at which the dummy does not contact the airbag, i.e.  $\tau_1 = 20$  ms and  $\tau_2 = 25$  ms. After that, it will be investigated whether the designed controller has to be adapted for the other points of application, i.e.  $\tau_3 = 40$  ms and  $\tau_4 = 64$  ms.

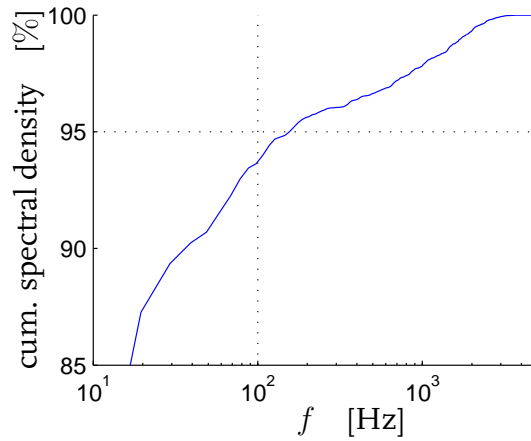


**Figure 3.2** Cumulative spectral density of the chest acceleration  $\ddot{c}_p(t)$

The differences between the model parameters of the LTI control design models for  $\tau_1$  and  $\tau_2$  are relatively small. Therefore, it seems reasonable to aim for one constant controller  $\mathcal{C}$ . The Bode diagrams of the considered LTI control design models, see Figure 2.14, show that a derivative controller part is not required to achieve the desired phase margin, but that an integral controller part is required to achieve the desired error rejection. Hence, the controller consists of a proportional plus an integral part. A second order low-pass filter is added to suppress (computational) noise, so:

$$\mathcal{C}(s) = P \cdot \left(1 + \frac{2\pi f_I}{s}\right) \cdot \left(\frac{(2\pi f_{LP})^2}{s^2 + 2\zeta_{LP}(2\pi f_{LP})s + (2\pi f_{LP})^2}\right) \quad (3.3)$$

For  $\zeta_{LP} = 0.7$  and  $f_{LP} = 1$  kHz, the filter effectively suppresses (computational) noise.

The Bode diagrams of the considered LTI control design models also show that a bandwidth  $f_{BW}$  of 70 Hz is too low to achieve the desired error rejection. The bandwidth is therefore increased by adapting  $P$  and  $f_I$ , until a controller is found that satisfies all control design criteria. This is the case for  $P = 93$  and  $f_I = 160$  Hz. Then, the bandwidth is 400 Hz for  $\tau_1$  and 463 Hz for  $\tau_2$ . The moduli of the sensitivity transfer functions  $S_j(s)$  with  $j = 1, 2$  and the relevant parts of the Nyquist plots of the open loop transfer functions  $\mathcal{H}_j(s) \cdot \mathcal{C}(s)$  with  $j = 1, 2$  are shown in Figure 3.3. Gain margins of 3.9 and 3.3 and phase margins of  $48^\circ$  and  $46^\circ$  for  $\tau_1$  and  $\tau_2$  are achieved, respectively.

To investigate whether the designed controller has to be adapted to satisfy the control design criteria for the points of application  $\tau_3$  and  $\tau_4$ , the Bode diagrams of the open loop transfer functions  $\mathcal{H}_3(s) \cdot \mathcal{C}(s)$  and  $\mathcal{H}_4(s) \cdot \mathcal{C}(s)$  with the designed controller with  $P = 93$  and  $f_I = 160$  Hz, are analyzed. They are shown in Figure 3.4. The 0 dB cross-over frequency is approximately 800 Hz for  $\tau_3$  and 900 Hz for  $\tau_4$ . At  $\omega/2\pi = 400$  Hz, the moduli are approximately 7 dB, equivalent to a factor 0.45, and the phases are approximately  $-120^\circ$ . Based on these observations, it seems reasonable to adapt only the controller gain  $P$  to satisfy the control design criteria for these points of application:

$$\mathcal{C}'(s) = P' \cdot \left(1 + \frac{2\pi f_I}{s}\right) \cdot \left(\frac{(2\pi f_{LP})^2}{s^2 + 2\zeta_{LP}(2\pi f_{LP})s + (2\pi f_{LP})^2}\right) \quad (3.4)$$

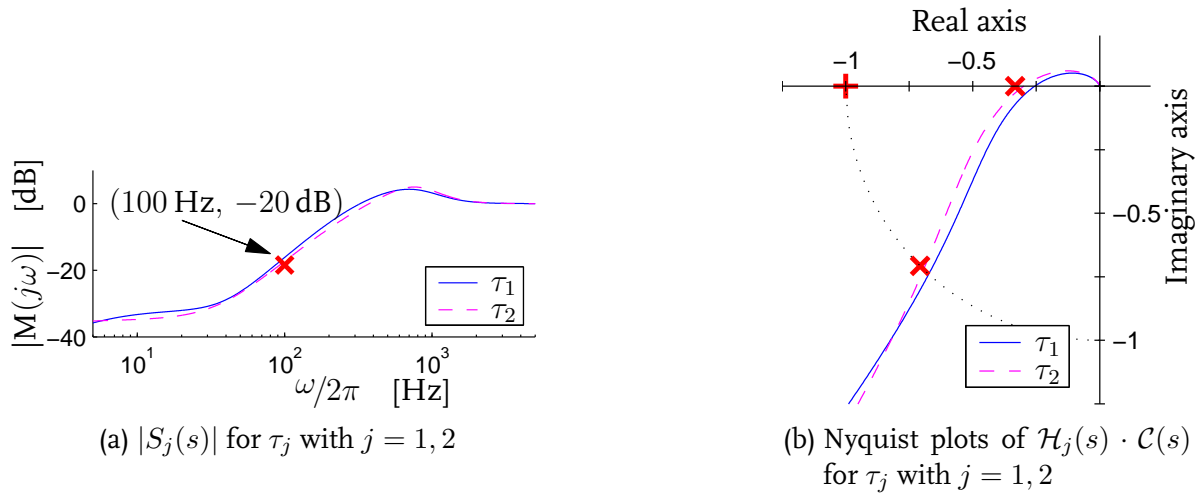


**Figure 3.3** Moduli of the sensitivity transfer functions and Nyquist plots of the open loop transfer functions

with  $P' = 0.45 \cdot P = 42$ . This approach is also known as gain scheduling [85, 133]. In Figure 3.5, the moduli of the sensitivity transfer functions  $S'_j(s) = 1/(1 + \mathcal{H}_j(s) \cdot \mathcal{C}'(s))$  with  $j = 3, 4$  and the relevant parts of the Nyquist plots of  $\mathcal{H}_j(s) \cdot \mathcal{C}'(s)$  with  $j = 3, 4$  are shown. Gain margins of 3.4 and 3.2 and phase margins of  $57^\circ$  and  $50^\circ$  are achieved for  $\tau_3$  and  $\tau_4$ , respectively.

To prevent numerical problems during simulations with the complex nonlinear model, the controller gain is adapted smoothly as a function of time. More specifically, it is chosen to linearly adapt the gain over the time interval from  $t = 30$  ms until  $t = 40$  ms. So, the controller actually is a nonlinear controller:

$$\mathcal{C}(s) = P(t) \cdot \left(1 + \frac{2\pi f_I}{s}\right) \cdot \left(\frac{(2\pi f_{LP})^2}{s^2 + 2\zeta_{LP}(2\pi f_{LP})s + (2\pi f_{LP})^2}\right) \quad (3.5)$$

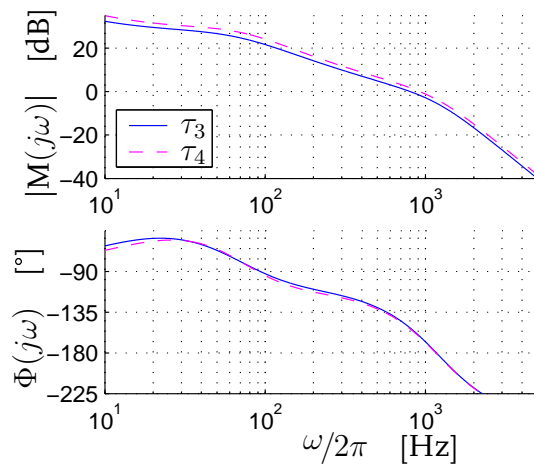


**Figure 3.4** Bode diagrams of the open loop transfer functions  $\mathcal{H}_3(s) \cdot \mathcal{C}(s)$  and  $\mathcal{H}_4(s) \cdot \mathcal{C}(s)$ , with  $\mathcal{C}(s)$  the controller of Equation 3.3 with  $P = 93$  and  $f_I = 160$  Hz

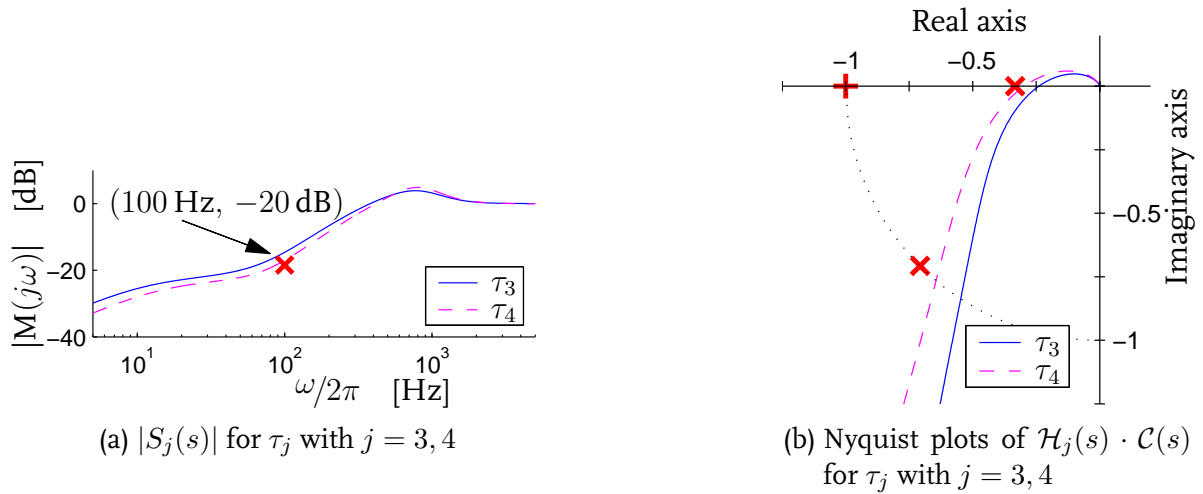


**Figure 3.5** Moduli of the sensitivity transfer functions and Nyquist plots

with:

$$P(t) = \begin{cases} 93 & t < 30 \text{ ms} \\ 93 - 51 \cdot \frac{(t-30)}{10} & \text{for } 30 \text{ ms} \leq t \leq 40 \text{ ms} \\ 42 & 40 \text{ ms} < t \end{cases} \quad (3.6)$$

### A reference signal

The reference signal  $r_{\tilde{c}}(t)$  for the chest acceleration should reflect the lowest possible maximum of the absolute chest acceleration and prevent undesired contacts of the chest with inner vehicle components. The contact most often leading to severe or fatal injuries is a high velocity impact on the steering wheel, typically occurring in the last phase of the crash. Besides that, the chest can not be pushed through the back of the seat. These desires are formulated as bounds that are to be accounted for:

1. the chest may not be pushed through the back of the seat,
2. the chest may not contact the steering wheel,
3. at the end of the crash, i.e. at  $t = t_e$ , the velocity of the chest is less than or equal to the velocity of the vehicle.

The choice of the point of time  $t = t_e$  is far from trivial. As discussed in Section 2.2, it seems reasonable to assume that this crash test may be considered to be ended at  $t = 100 \text{ ms}$ . Hence,  $t_e = 100 \text{ ms}$  is adopted. It is emphasized that for other vehicles, crashes, dummies and/or restraint systems, the point of time at which the crash may be considered to be ended, can be different.

It is a reasonable assumption that the lowest risk of injuries is achieved, if the maximum value of the absolute chest acceleration is as low as possible. This is the case, if the reference signal is constant from the start of the crash until the end of the crash, with an as low as possible absolute value of the constant. However, the chest will then be

pushed through the back of the seat in the first phase of the crash. The highest achievable absolute acceleration of the chest is equal to the vehicle acceleration  $\ddot{x}_{\text{veh}}(t)$ , as long as the chest does not lose contact with the back of the seat. This will be the case during the first phase of the crash, i.e. from  $t = t_0$  until a (yet) to-be-determined point of time  $t = t'$ . If the chest acceleration  $r_{\dot{c}}(t)$  remains at that level until the end of the crash, i.e. if  $r_{\dot{c}}(t) = \ddot{x}_{\text{veh}}(t')$  for  $t' < t \leq t_e$ , then the maximum value of the absolute chest acceleration is as low as possible:

$$r_{\dot{c}}(t) = \begin{cases} \ddot{x}_{\text{veh}}(t) & 0 \leq t < t' \\ \ddot{x}_{\text{veh}}(t') & t' \leq t < 97.5 \text{ ms} \\ \frac{\ddot{x}_{\text{veh}}(t')}{2} \cdot [1 + \cos(\frac{2\pi}{10}(t - 97.5))] & 97.5 \text{ ms} \leq t < 102.5 \text{ ms} \\ 0 & 102.5 \text{ ms} \leq t \end{cases} \quad \text{for} \quad (3.7)$$

with  $t'$  a yet to-be-determined point of time. To prevent numerical problems during simulations with the closed loop system, the reference signal is smoothed in the time interval from  $t = 97.5 \text{ ms}$  until  $t = 102.5 \text{ ms}$ .

To check whether the bounds on the motion of the chest are violated, the velocity and displacement of the chest, the seat and the steering wheel are estimated by integration of  $r_{\dot{c}}(t)$  and  $\ddot{x}_{\text{veh}}(t)$  with the initial conditions  $r_{\dot{c}}(t_0) = \dot{x}_{\text{veh}}(t_0) = v_0$  and  $r_c(t_0) = x_{\text{veh}}(t_0) = 0$ . Here, it is assumed that the seat and the steering wheel do not move, relative to the safety cage.

The point of time  $t = t'$  unambiguously determines the chest velocity and displacement, relative to the seat and to the steering wheel. Hence, it can not be guaranteed that a point of time  $t = t'$  exists for which the second bound and the third bound are not violated. Nevertheless, it is tried to find such a point of time  $t = t'$ , using trial-and-error. Based on the velocity difference  $(\dot{x}_{\text{veh}}(t_e) - \dot{x}_{\text{veh}}(t_0))$  over the time interval from  $t = t_0$  until  $t = t_e$ , a value  $r'_{\dot{c}} = -170 \text{ m/s}^2$  is expected. From the vehicle acceleration  $\ddot{x}_{\text{veh}}(t)$ , shown in Figure 3.6(a) as the solid line, an appropriate point of time  $t = t'$  may be found in the time interval from  $t = 0$  until  $t = 20 \text{ ms}$ . A point of time  $t' = 11 \text{ ms}$  with  $r'_{\dot{c}} = -195 \text{ m/s}^2$  is found, for which the bound on the chest displacement is not violated and the chest velocity at the end of the crash equals to the vehicle velocity.

In Figure 3.6(a), the reference signal  $r_{\dot{c}}(t)$  for the chest acceleration and the vehicle acceleration  $\ddot{x}_{\text{veh}}(t)$  are shown. In Figures 3.6(b) and 3.6(c), the corresponding velocities and displacements are shown. The displacement  $x_{\text{veh}}(t) + \ell_0$  is to be interpreted as the displacement of the steering wheel, and the displacement  $x_{\text{veh}}(t)$  as the displacement of the back of the seat. In Figure 3.6(c), it can be observed that the smallest distance between the front of the chest and the steering wheel is more than 10 cm, due to the desire that the bound on the chest velocity may not be violated.

In comparison with the maximum chest acceleration for the passive restraint system, the reference signal  $r_{\dot{c}}(t)$  suggests a reduction of the risk of injuries, represented by the maximum absolute chest acceleration, of approximately 40% compared to the original value. Such a reduction will be achieved if the reference signal is accurately followed and contact of the chest with the steering wheel is indeed prevented. That can only be

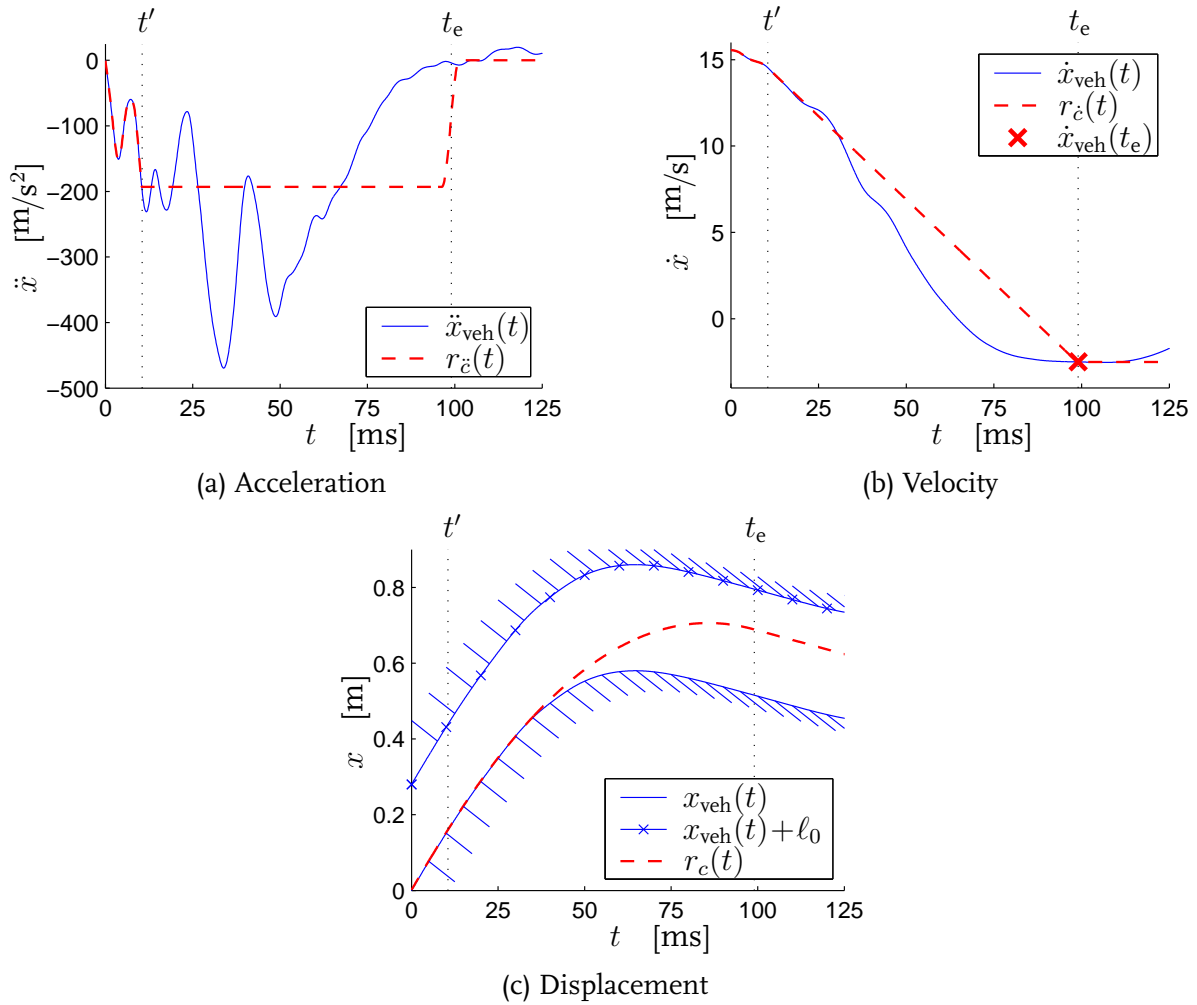


**Figure 3.6** Reference signal  $r_{\tilde{z}}(t)$  for the chest acceleration and vehicle acceleration  $\ddot{x}_{\text{veh}}(t)$ , as well as the corresponding velocities and displacements

investigated by a simulation of the closed loop system with the complex nonlinear model, which is done in the following section.

### Evaluation

The evaluation of the controller of Equations 3.5 and 3.6 and the reference signal  $r_{\tilde{z}}(t)$  is based on a simulation with the closed loop system with the model  $\mathcal{M}$ , see Figure 3.1. In Figure 3.7(a-c), some relevant results of the closed loop simulation are shown. In these figures, the results for the case that the restraint system is passive are shown also. The vehicle and dummy at  $t = t_e$ , shown in Figure 3.7(d) indicate that a distance of approximately 7 cm remains between the front of the chest and the steering wheel at  $t = t_e$ .

The smooth time histories of the chest acceleration and of the required belt force indicate that the closed loop system is stable. For  $t > 11$  ms, the error is less than 10% of the maximum absolute reference signal, indicating that the reference signals is followed sufficiently fast. The maximum allowable error  $e_{\text{max}}$  is not violated in the time interval

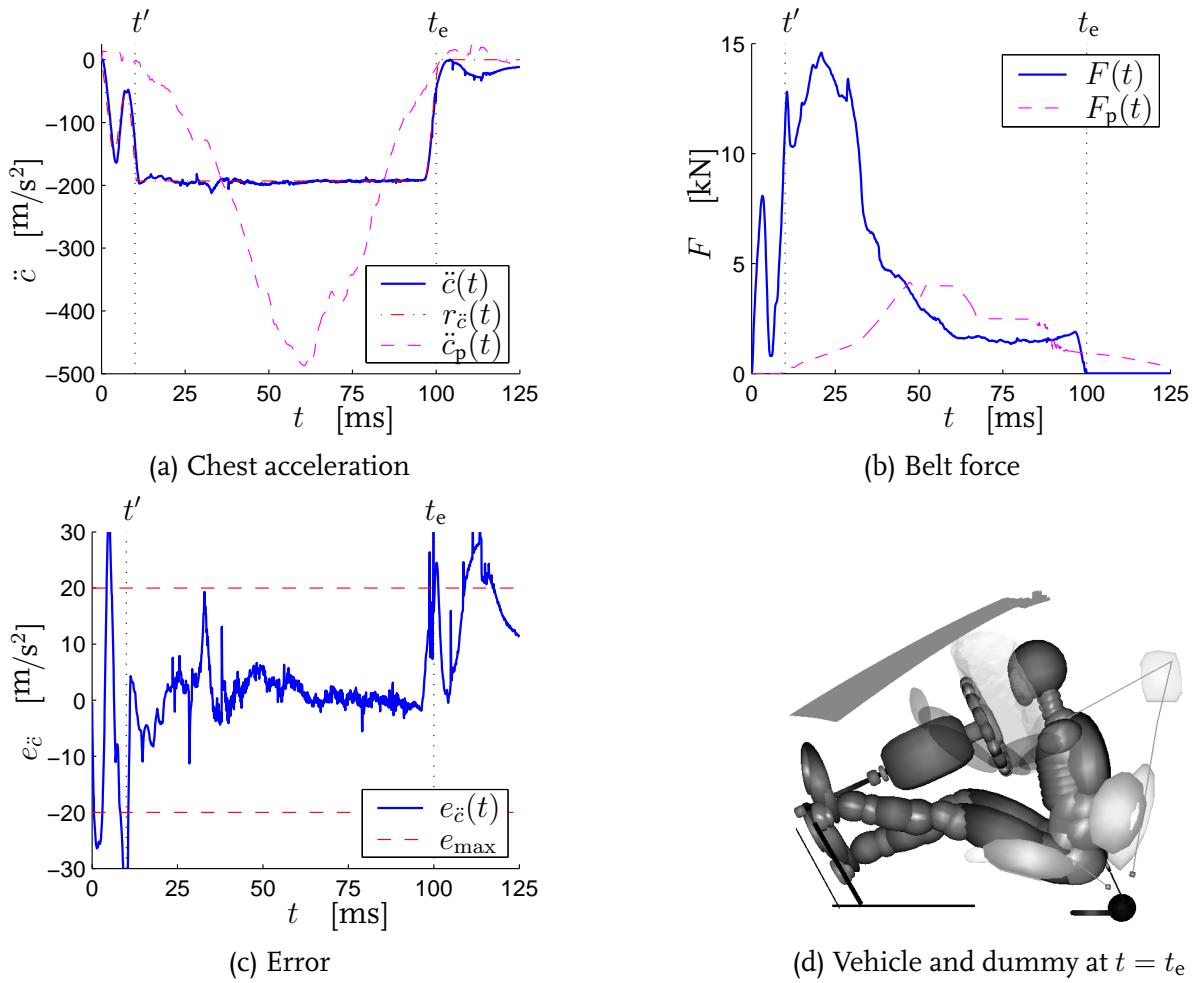


**Figure 3.7** Relevant results of the closed loop simulation for evaluation purposes

from  $t = 11$  ms until the end of the crash, indicating that the error rejection in the closed loop system is sufficient. From  $t = 25$  ms until the end of the crash, weak (computational) noise can be observed in the error signal, due to the contact of the dummy with the airbag.

A reduction of the maximum chest acceleration to approximately 40 % of its original value is obtained. Furthermore, the risk of injuries, represented by the maximum head acceleration and the maximum chest deflection is reduced to approximately 40 % and 90 % of their original value, respectively.

In Figure 3.7(b), it can be observed that the required belt force significantly drops at  $t \approx 32$  ms. This may be explained by the reversal of the direction of friction in the contact of the belt with the D-ring. In Figure 3.8(a), the manipulated belt force  $F(t)$  and the force  $F'(t)$  in the belt element that connects the D-ring with the dummy thorax, is shown. From  $t \approx 32$  ms, the friction force contributes to the required belt force, instead of counteracting it. Apart from that, additional forces are applied by the airbag from  $t = 35$  ms.

In Figure 3.8(b), trajectories of the centers of gravity of the dummy head, left clavicle, chest and pelvis, relative to the vehicle, in the  $(x, z)$ -plane of the vehicle are shown. Initial



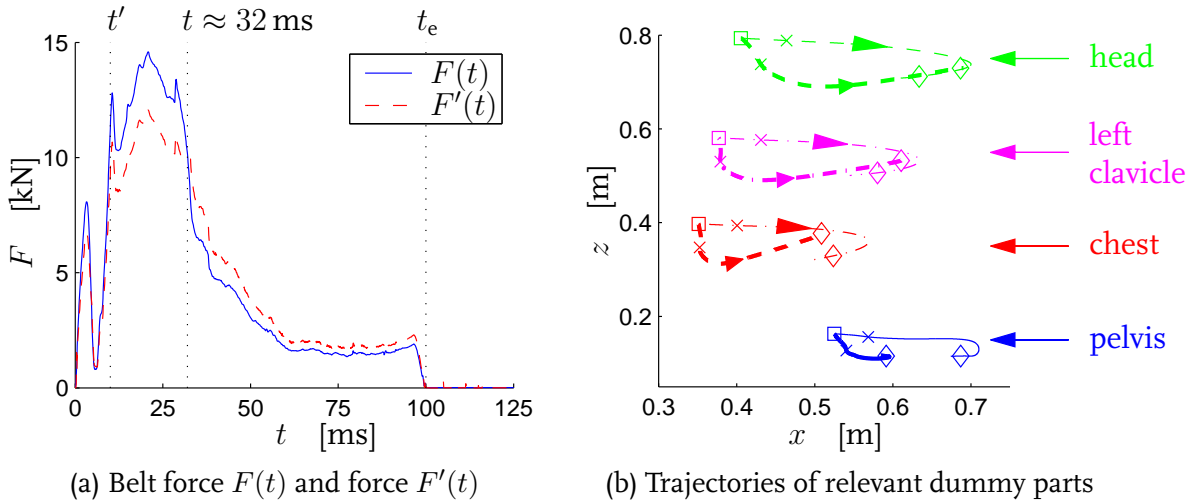


**Figure 3.8** Forces in the belt and trajectories of relevant dummy parts

positions are indicated with “□”, positions at  $t = 35$  ms with “×”, and positions at the end of the crash  $t = t_e$  with “◇”. Furthermore, thin lines denote the trajectories for the case that the restraint system is passive, and thick lines the trajectories for the case that the chest acceleration is controlled. Two interesting differences can be observed. First, for the case that the chest acceleration is controlled, the dummy moves downward before moving forward, due to forces applied by the lap section on the dummy. Second, the pelvis moves less forward, relative to the vehicle, for the case that the chest acceleration is controlled, yielding the upper part of the dummy to rotate more around the pelvis.

The closed loop results indicate that the LTI control design models are sufficiently accurate for design of a feedback controller. Nevertheless, in the sequel, LTI models for closed loop operating points of the complex nonlinear model are compared to the LTI control design models for open loop operating points.

### Closed loop identification

To derive approximating LTI models at closed loop operating points, the standard approach [67] for closed loop identification is applied. Simulations with the closed loop system with the model  $\mathcal{M}$  are performed, in which a step  $\delta F(t) = \Delta F_i \cdot \varepsilon(t - \tau)$  is added to the manipulated belt force at the point of application  $t = \tau$ , illustrated in Figure 3.9. The perturbed belt force  $\tilde{F}(t)$  and the perturbed chest acceleration  $\tilde{\ddot{c}}(t)$  are measured. Next, the approximate realization is applied to obtain LTI models for the transfer from  $\delta F(t)$  to  $\delta \tilde{F}(t)$  and for the transfer from  $\delta F(t)$  to  $\delta \tilde{\ddot{c}}(t)$ . Finally, properly combining [67] the realized LTI models yields one LTI model  $\mathcal{H}'(s)$  that approximates the transfer from a perturbation  $\delta F(t)$  in the belt force to the response  $\delta \tilde{\ddot{c}}(t)$  in the chest acceleration along closed loop operating points of the model  $\mathcal{M}$ .

Here, only the time interval in which the dummy is restrained by the belt is considered. The position of the dummy at  $t = 15$  ms for the case that the belt system is manipulated, resembles that at the points of application  $\tau_1 = 20$  ms and  $\tau_2 = 25$  ms for the case that the belt system is passive. Therefore, one point of application  $\tau = 15$  ms is chosen. Step sizes

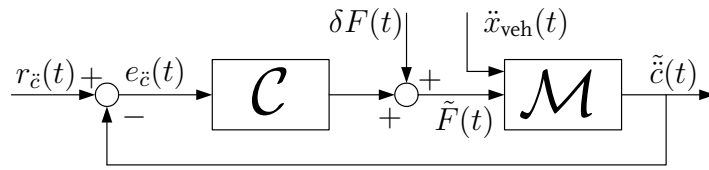


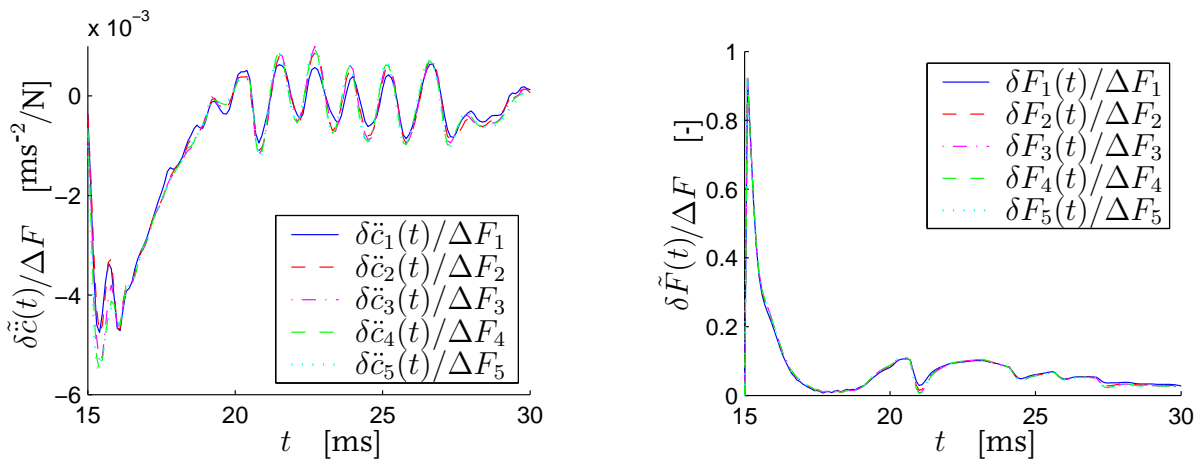
**Figure 3.9** Closed loop system with the model  $\mathcal{M}$  for closed loop identification purposes

$\Delta F$  are adopted from Section 2.4. The averaged normalized response in the belt force  $\delta \tilde{F}(t)/\Delta F$  and the averaged normalized responses in the chest acceleration  $\delta \tilde{c}(t)/\Delta F$  are shown in Figure 3.10(a) and Figure 3.10(b), respectively.

The normalized responses show that (stepwise) disturbances are significantly suppressed within a time interval of 4 ms, suggesting that the closed loop system with the complex nonlinear is satisfactorily fast. Furthermore, the normalized responses lay close to each other, suggesting that the considered transfers may be approximated by LTI models. Next, approximate realization is applied to determine an LTI model for each transfer.

Figure 3.11 shows the modulus of  $\mathcal{H}'(s)$ , as well as the moduli of the LTI control design models  $\mathcal{H}_1(s)$  for  $\tau_1 = 20$  ms and  $\mathcal{H}_2(s)$  for  $\tau_2 = 25$  ms of Section 2.4.

This comparison indicates that the dynamic behavior of the complex nonlinear model at open loop operating points, differs from the dynamic behavior at closed loop operating points. However, differences seem to be limited to approximately 5 dB in the moduli for frequencies less than the bandwidth  $f_{\text{BW}} = 400$  Hz. Such model mismatches can be appropriately dealt with by the feedback controller, as shown previously.



(a) Normalized responses in the controlled chest acceleration

(b) Normalized responses in the manipulated belt force

**Figure 3.10** Normalized responses to steps in the belt force with various sizes at 15 ms

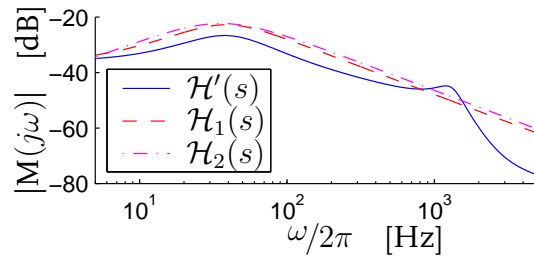


Figure 3.11 Moduli of the LTI models  $\mathcal{H}_1(s)$ ,  $\mathcal{H}_2(s)$  and  $\mathcal{H}'(s)$

### 3.4 Control of the head acceleration by the airbag

In this section, the control design strategy of Section 3.2 is applied to arrive at controllers for the airbag. Here, the focus is on manipulation of the mass flow or the vent size to control the head acceleration, since the risk of head injuries is significantly influenced by the airbag [56, 75]. The belt system is not manipulated, meaning that it behaves as if it is passive.

In Section 3.4.1, control of the head acceleration by manipulation of the mass flow is presented, followed by control of the head acceleration by manipulation of the vent size in Section 3.4.2.

#### 3.4.1 Manipulating the mass flow

In the sequel, control of the head acceleration  $\ddot{h}$  by manipulation of the mass flow  $\phi$  is presented in four consecutive steps, concerning: control design criteria, design of the controller, design of the reference signal and evaluation.

##### Control design criteria

The control design criteria are the desired gain margin  $GM > 3$ , the desired phase margin  $PM > 45^\circ$ , the bound on the modulus of the sensitivity transfer function  $|S(j\omega)| \leq -20$  dB for  $\omega/2\pi \leq f'$ , and the lower bound on the bandwidth  $f_{BW}$ .

To achieve enough error rejection, the modulus of the sensitivity transfer function may not violate the bound  $|S(j\omega)| \leq -20$  dB for  $\omega \leq 2\pi f'$  with  $f'$  a yet to-be-determined frequency. To determine an appropriate frequency  $f'$ , the spectral density of the head acceleration  $\ddot{h}_p(t)$  for the case that the restraint system is passive, is analyzed. The cumulative spectral density is shown in Figure 3.12. From this result, it can be concluded that more than 95% of the total energy in the head acceleration  $\ddot{h}_p(t)$  is covered by frequencies less than 50 Hz. Hence, the frequency  $f' = 50$  Hz seems appropriate.

##### Control design

In Section 2.5, it has been observed that the relevant dynamic behavior of the dummy, interacting with the airbag, does not significantly change as a function of the operat-

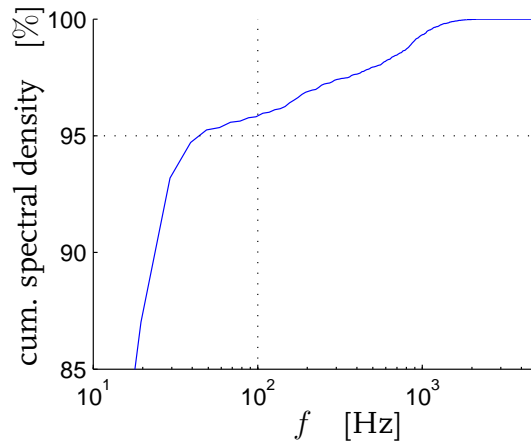


**Figure 3.12** Cumulative spectral density of the head acceleration  $\ddot{h}_p(t)$

ing point, at least for the considered points of application  $\tau_1 = 50$  ms and  $\tau_2 = 60$  ms. Therefore, the aim of control design is one constant feedback controller  $\mathcal{C}(s)$ . The Bode diagrams of the considered LTI control design models, see Figure 2.20, indicate that a derivative controller part is not necessary to achieve the desired phase margin, but that an integral controller part is required to achieve enough error rejection. Hence, the controller consists of a proportional plus an integral part, combined with a second order low-pass filter with  $f_{LP} = 1$  kHz and  $\zeta_{LP} = 0.7$  to effectively suppress computational noise:

$$\mathcal{C}(s) = P \cdot \left( 1 + \frac{2\pi f_I}{s} \right) \cdot \left( \frac{(2\pi f_{LP})^2}{s^2 + 2\zeta_{LP}(2\pi f_{LP})s + (2\pi f_{LP})^2} \right) \quad (3.8)$$

Aiming at a low bandwidth, a controller that satisfies all control design criteria, is found for  $P = 2.0$  and  $f_I = 50$  Hz. In that case, a bandwidth of 200 Hz for  $\tau_1$  and 281 Hz for  $\tau_2$  is obtained. The moduli of the sensitivity transfer functions  $S_j(s)$  with  $j = 1, 2$  and the relevant part of the Nyquist plots of the open loop transfer functions  $\mathcal{H}_j(s) \cdot \mathcal{C}(s)$  with  $j = 1, 2$  are shown in Figure 3.13. Gain margins of 6.7 and 4.7 and phase margins of  $55^\circ$  and  $54^\circ$  are achieved for  $\tau_1$  and  $\tau_2$ , respectively.

### A reference signal

The reference signal  $r_{\ddot{h}}(t)$  for the head acceleration should reflect the lowest possible risk of injuries to the head and prevent an undesired contact of the head with the steering wheel. The head acceleration can only be controlled by the airbag, from the point of time  $t = 35$  ms, at which the head establishes a stable contact with the airbag. At that point of time, the dummy has moved forward, suggesting that it is not necessary to account for the possibility that the head is pushed through the head rest. Hence, the reference signal has to prevent contact of the head with the steering wheel has to be prevent and at the end of the crash, i.e. at  $t = t_e$ , and ensure that the velocity of the head is less than or equal to the velocity of the vehicle. In line with the choice of the point of time  $t = t_e$  in the previous section, the point of time  $t = t_e = 100$  ms is adopted.

It is a reasonable assumption that the lowest possible risk of injuries to the head is

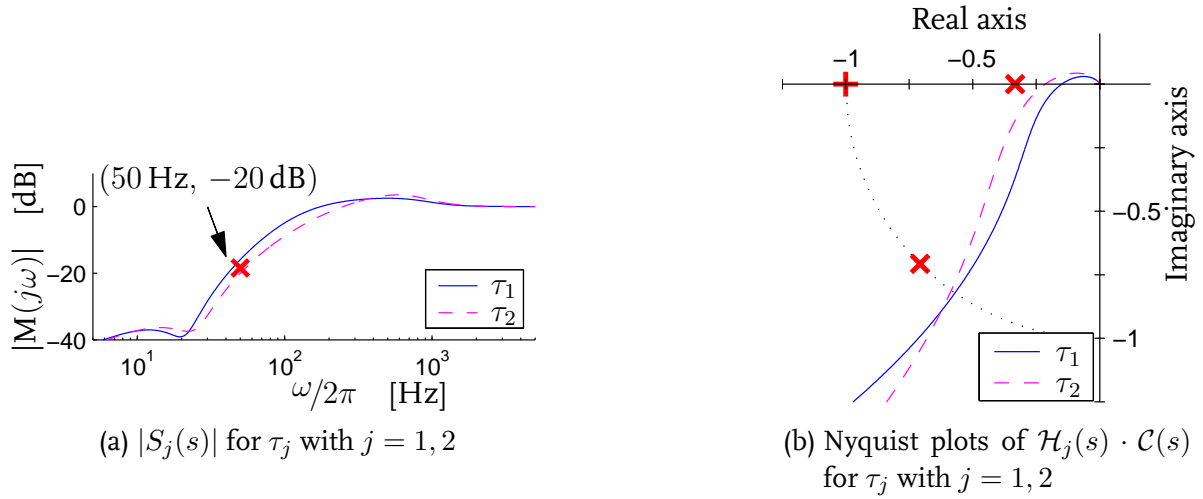


**Figure 3.13** Moduli of the sensitivity transfer functions and Nyquist plots of the open loop transfer functions

achieved, if the maximum value of the absolute head acceleration is as low as possible. This will probably be the case, if the reference signal has a constant value  $r'_h$  over the time interval from the point of time  $t = 35$  ms until the end of the crash, with an as low as possible absolute value of the constant:

$$r''_h(t) = \begin{cases} r'_h & 40 \text{ ms} \leq t < 97.5 \text{ ms} \\ (r'_h/2) \cdot [1 + \cos(\frac{2\pi}{10}(t - 97.5))] & \text{for } 97.5 \text{ ms} \leq t < 102.5 \text{ ms} \\ 0 & 102.5 \text{ ms} \leq t \end{cases} \quad (3.9)$$

To prevent numerical problems during simulations with the closed loop system with the model  $\mathcal{M}$ , the reference signal is smoothed in the time interval from  $t = 35$  ms until  $t = 40$  ms by the first half period of a cosine with period of 10 ms and an amplitude of  $(r'_h - \ddot{h}_p(35 \text{ ms}))/2$ . Furthermore, the reference signal is smoothed in the time interval from  $t = 97.5$  ms until  $t = 102.5$  ms.

To check whether the bounds on the motion of the head are violated, the velocity and displacement of the head and the steering wheel are estimated by integration of  $r'_h(t)$  and  $\ddot{x}_{\text{veh}}(t)$  with the initial conditions  $r'_h(t') = \dot{x}_{\text{veh}}(t_0) = v_0$  and  $r_h(t_0) = x_{\text{veh}}(t_0) = 0$ .

Using trial-and-error, it is tried to find the value  $r'_h$  for which the bounds on the head motion are not violated. Starting with a value  $r'_h = -200 \text{ m/s}^2$ , this value is decreased until a reference signal is found, for which the bound on the head displacement is not violated and the chest velocity at the end of the crash is equal to the vehicle velocity. This is the case for  $r'_h = -290 \text{ m/s}^2$ .

In Figure 3.14(a), the reference signal  $r'_h(t)$  for the head acceleration and the vehicle acceleration  $\ddot{x}_{\text{veh}}(t)$  are shown. In Figure 3.14(b) and 3.14(c), the corresponding velocities and displacements are shown. The displacement  $x_{\text{veh}}(t) + \ell_0$  is to be interpreted as the displacement of the steering wheel, and the displacement  $x_{\text{veh}}(t)$  is to be interpreted as the displacement of the head rest. The smallest distance between the front of the head and the steering wheel is 2.5 cm at  $t = t_e$ .

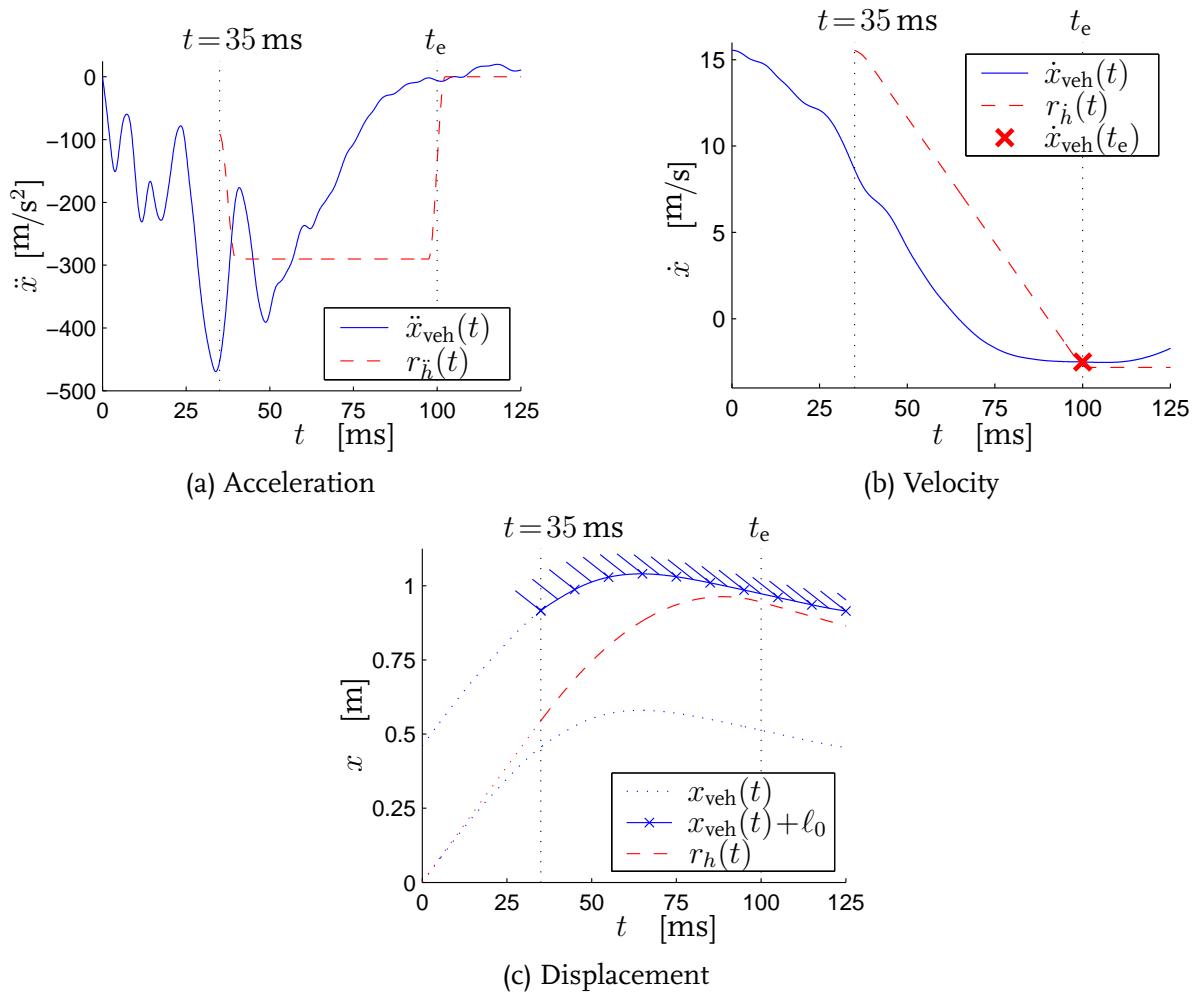


**Figure 3.14** Reference signal  $r_{\ddot{h}}(t)$  and the vehicle acceleration  $\ddot{x}_{veh}(t)$ , as well as the corresponding velocities and displacements

The shown reference signal suggests a reduction of the maximum absolute head acceleration to approximately 48% of its original value. Such a reduction will only be achieved if the reference signal is accurately followed and contacts of the head with the steering wheel are prevented. That can only be investigated by a simulation of the closed loop system with the complex nonlinear model, which is done in the following section.

## Evaluation

The evaluation of the controller of Equation 3.8 and the reference signal  $r_{\ddot{h}}(t)$  is based on a simulation with the closed loop system, see Figure 3.1. In Figure 3.7(a-c), some relevant results of the closed loop simulation are shown. In Figure 3.7(d), the vehicle and dummy at  $t = t_e$  are shown. In Figure 3.7(d), it can be easily seen that the pelvis almost slides underneath the lap belt. This phenomenon is called “submarining” [4] and it typically occurs due to severe braking, severe impact conditions or in the case that the belt is not properly aligned over the dummy. Here, it is caused by the airbag, being far too stiff. In the time interval from  $t = 35$  ms until  $t = 42$  ms, gas is injected in order to follow the reference signal. From that moment until the point of time  $t = 80$  ms, a negative mass

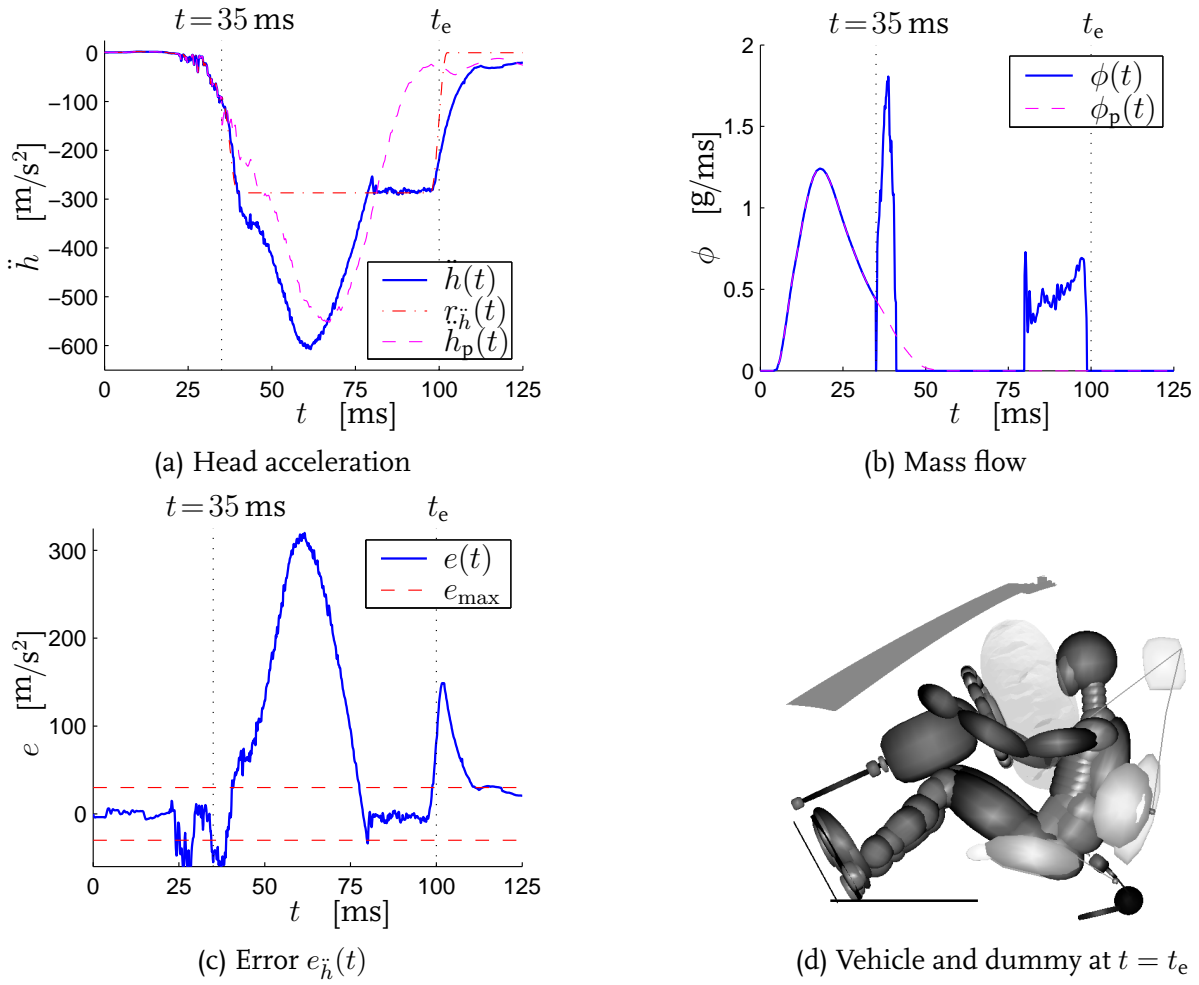


**Figure 3.15** Relevant results of the closed loop simulation for evaluation purposes

flow is required to follow the reference signal. However, a negative mass flow is seen as  $\phi = 0$  and the vent size is not manipulated, meaning that the airbag remains (too) stiff.

Apart from that, the results in the time interval from  $t = 80$  ms until  $t = t_e$  indicate that in this time interval, the closed loop system with the model  $\mathcal{M}$  is stable, the error rejection in the closed loop system is sufficient and show that the maximum allowable error is not violated. Based on these results, it may be concluded that the head acceleration can be controlled by the mass flow, but to actually reduce the risk of head injuries, other inflators or the manipulation of the vent size is required, at least for the considered combination of the crash and dummy. These results are not discussed in more detail.

### 3.4.2 Manipulating the vent size

In this section, the control of the head acceleration  $\ddot{h}$  by manipulation of the vent size  $A$  is presented in two consecutive steps, concerning the design of the controller and evaluation. The control design criteria and the reference signal  $r_{\ddot{h}}(t)$  of Section 3.4.1 are adopted.

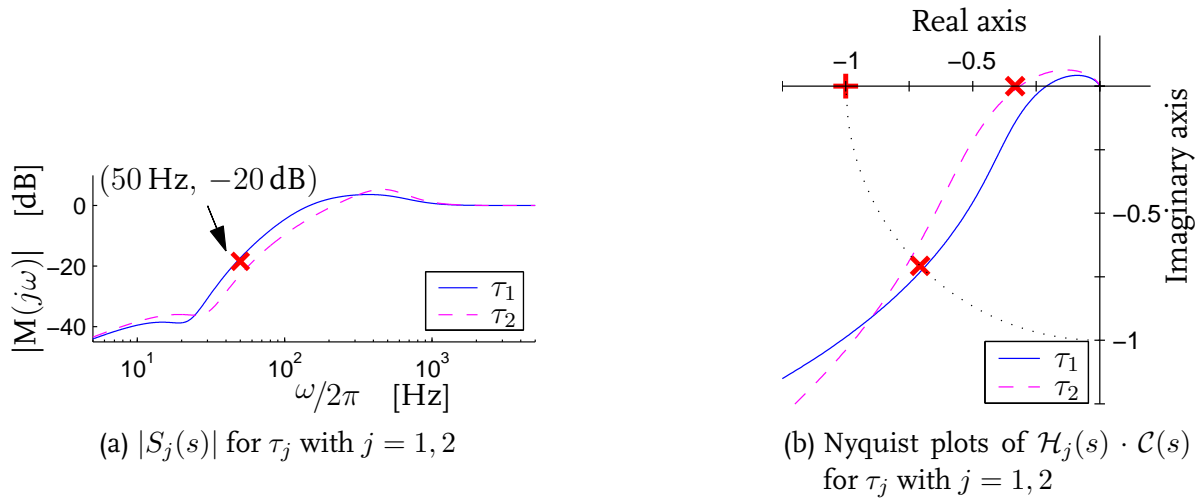


**Figure 3.16** Moduli of the sensitivity transfer functions and Nyquist plots of the open loop transfer functions

### Control design

In Section 2.5, it has been observed that relevant dynamic behavior of the dummy, interacting with the airbag, does not significantly change as a function of the operating point, at least for the considered points of application  $\tau_1 = 50$  ms and  $\tau_2 = 60$  ms. Therefore, the aim is one constant feedback controller. The Bode diagrams of the considered LTI control design models, see Figure 2.14, indicate that a derivative controller part is not necessary to achieve the desired phase margin, but that an integral controller part is required to achieve enough error rejection. Hence, the controller consists of a proportional plus an integral part, combined with a second order low-pass filter:

$$\mathcal{C}(s) = P \cdot \left(1 + \frac{2\pi f_I}{s}\right) \cdot \left(\frac{(2\pi f_{LP})^2}{s^2 + 2\zeta_{LP}(2\pi f_{LP})s + (2\pi f_{LP})^2}\right) \quad (3.10)$$

The low-pass filter effectively suppresses (computational) noise for  $f_{LP} = 750$  Hz and  $\zeta_{LP} = 0.7$ .

A controller that satisfies the control design criteria is found for  $P = 1.5$  and  $f_I = 50$  Hz. Then, a bandwidth of 200 Hz for  $\tau_1$  and 290 Hz for  $\tau_2$  is obtained. The moduli of the sensitivity transfer functions  $S_j(s)$  with  $j = 1, 2$  and the relevant parts of the Nyquist plots of  $\mathcal{H}_j(s) \cdot \mathcal{C}(s)$  with  $j = 1, 2$  are shown in Figure 3.16. Gain margins of 4.7 and 3.1 and phase margins of  $45^\circ$  and  $42^\circ$  are achieved for  $\tau_1$  and  $\tau_2$ , respectively.

### Evaluation

To evaluate the controller  $\mathcal{C}(s)$ , a simulation is performed with the closed loop system, see Figure 3.1. Some relevant results of the simulation are shown in Figure 3.17(a-c). At the end of the crash, the dummy head nearly touches the steering wheel, as shown in Figure 3.17(d). The difference between the expected distance of 2.5 cm and the observed distance, being almost 0, may be explained by the estimation of the head displacement by double integration of  $r_{\dot{h}}(t)$ , whereas the dummy head does rotate.



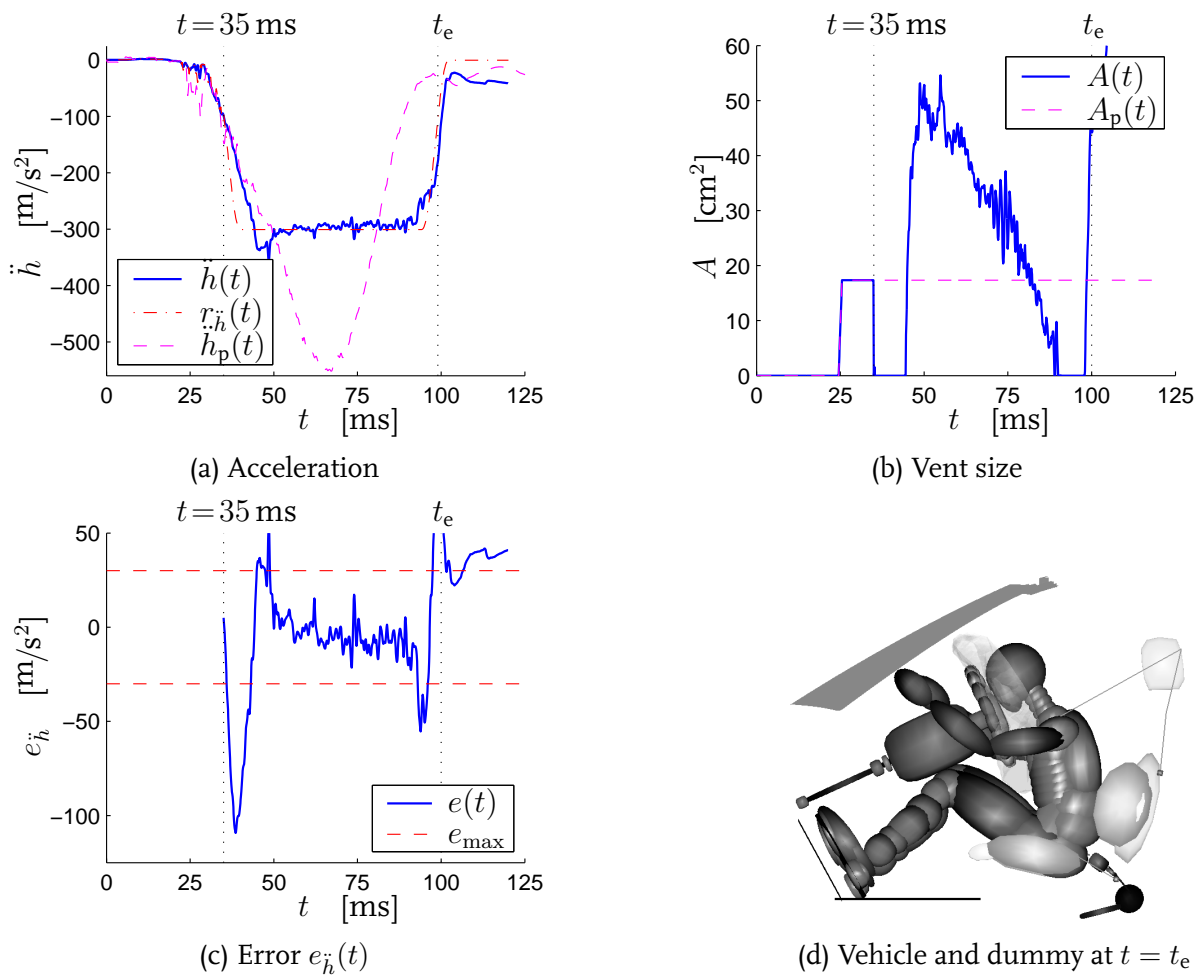


**Figure 3.17** Relevant results of the closed loop simulation for evaluation purposes

The closed loop results indicate that the closed loop system is stable. From the point of time that the controller is enabled, i.e. from  $t = 35$  ms, until  $t = 46$  ms, a negative vent size would be required to follow the reference signal. At  $t = 45$  ms, the integral controller part is reset to prevent anti-windup [134] and from that point of time, the reference signal is followed sufficiently fast. The error is less than the maximum allowable error  $e_{\max}$ , indicating that the error rejection in the closed loop system is sufficient. The error at  $t = 48$  ms is less than 5% of the maximum absolute reference signal, indicating that the reference signals is followed sufficiently fast.

A reduction of the maximum head acceleration to approximately 58% of its original value is obtained. The risk of injuries, represented by the maximum chest acceleration and the maximum chest deflection has reduced to approximately 83% and 94% of their original value, respectively.

### 3.5 Actuator saturation

Reference signals in the previous sections, represent the lowest possible risk of injuries, based on one measure only. However, forces applied to the dummy to follow the refer-

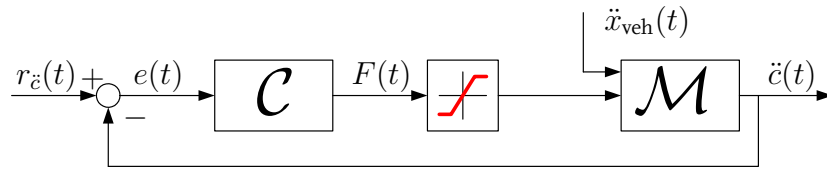


**Figure 3.18** Closed loop system with bounds imposed on the belt force

ence signal may lead to undesired injuries, which are not accounted for by the chosen measure. For example for the belt, a force of 15 kN, see Figure 3.7(b), probably leads to a broken clavicle or rib. Apart from that, the reference signals do not account for actuator saturation. For real world active restraint systems, this may require highly complex and high bandwidth actuators. In this section, these aspects are accounted for, exemplified by the case to control the chest acceleration by manipulation of the belt force, using the controller of Equations 3.5 and 3.6.

Load limiters are designed with the objective to limit the force applied to the dummy by the belt. These limits vary from 2 kN to 7 kN [81, 101, 103], depending on dummy mass or crash test characteristics. Here, a bound of  $F_{\max} = 6$  kN is adopted. Bounds on the time derivative of the belt force  $|\dot{F}(t)|$  are rarely discussed in literature. Therefore, the time history  $F_p(t)$  of the belt force for the passive belt system is analyzed. The maximum of the absolute rate per millisecond in the belt force, i.e.  $\max |\dot{F}_p(t)|$ , is approximately 1.5 kN/ms. Hence, a bound of  $|\dot{F}_{\max}| = 1.5$  kN/ms seems reasonable.

To a priori determine an appropriate reference signal is far from trivial. The model  $\mathcal{M}$  can not be used, since it is far too complex, whereas the LTI models are far too simple. Instead, the above mentioned bounds are imposed on the manipulated belt force  $F(t)$  and its time derivative  $\dot{F}(t)$ , illustrated in Figure 3.18. Next, an appropriate reference signal is determined iteratively.

Although bounds are imposed on the belt force, it still is plausible that the lowest risk of injuries is achieved, if the reference signal has a constant value  $r'_c$  as a function of time, at least in the time interval that the belt force is not saturated. To determine an appropriate value of  $r'_c$ , a constant reference signal is constructed with  $r'_c = -200$  m/s<sup>2</sup>. A simulation with the closed loop system with the model  $\mathcal{M}$  is performed to analyze whether the dummy contacts the steering wheel. This is the case. Next, the value  $r'_c$  is decreased until closed loop results show that the smallest distance between the dummy and the steering wheel is approximately 5 cm. After a few simulations,  $r'_c = -240$  m/s<sup>2</sup> shows to be appropriate. It is emphasized that this approach is not suitable for a real world implementation.

In Figure 3.19(a-c), some relevant results of the simulation are shown, and in Figure 3.19(d) the dummy and the vehicle at  $t = t_e$  are shown.

The closed loop results indicate that the closed loop system is stable. At the point of time that the error  $e_c$  is equal to zero for the first time, the integral controller part is reset to prevent anti-windup [134]. From that point of time on, i.e. for  $t > 40$  ms, the error is less

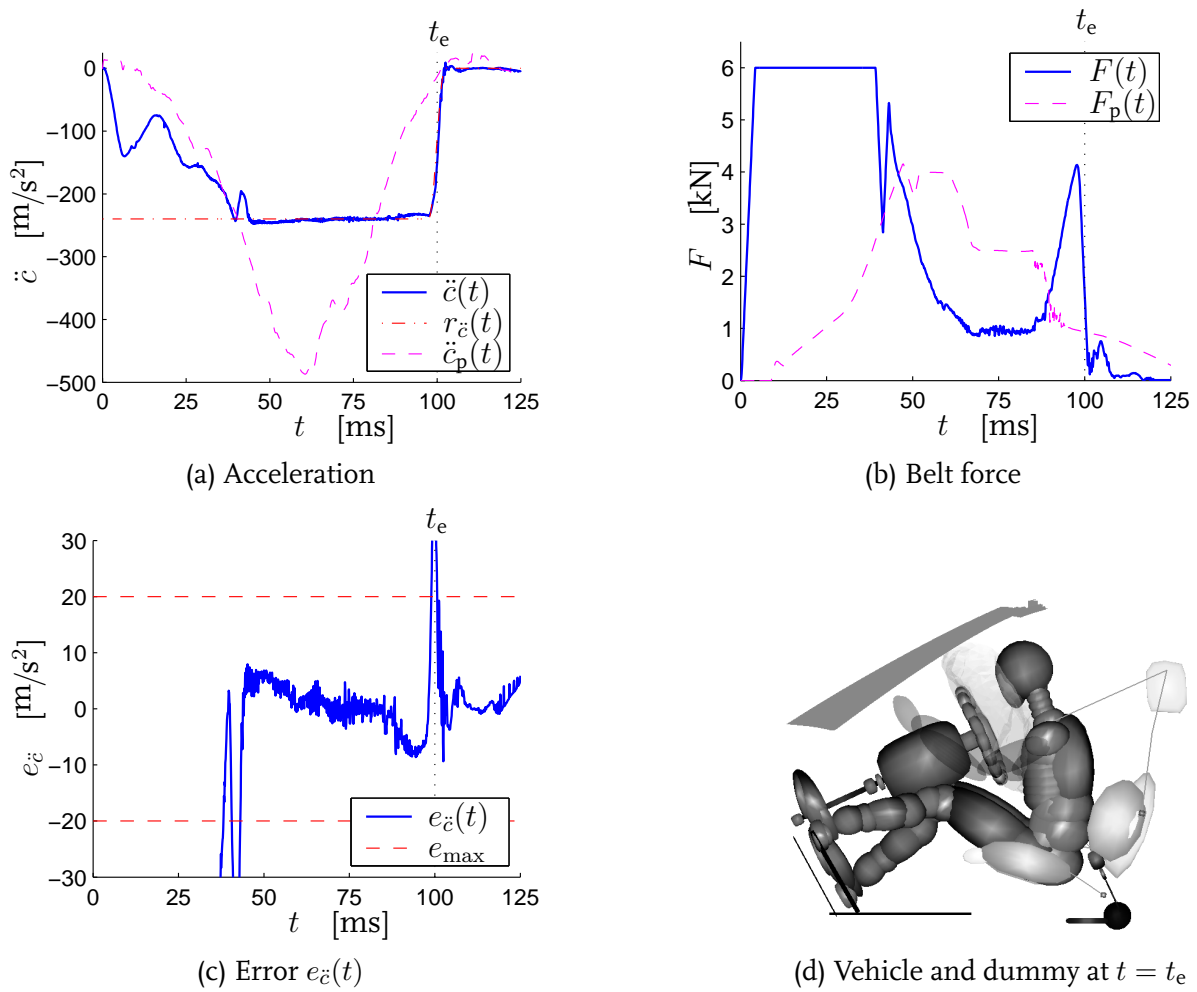


**Figure 3.19** Relevant results of the final simulation with the closed loop system with bounds imposed on the belt force

than the maximum allowable error  $e_{\max}$ , indicating that the reference signals is followed sufficiently fast and the error rejection is sufficient.

A reduction of the maximum chest acceleration to approximately 50 % of its original value is obtained. Furthermore, the risk of injuries, represented by the maximum head acceleration and the maximum chest deflection has reduced to approximately 56 % and 65 % of their original value, respectively.

A comparison of these closed loop results with those of Section 3.3 show some interesting differences. First, the reduction of the maximum chest acceleration here is only 19 % less than that of Section 3.3, whereas the maximum belt force has more than halved. This may be explained by the dummy, not being pushed into the back of the seat, but being smoothly coupled to the vehicle, which generally is beneficial for the risk of injuries [50]. In addition, the friction force in the contact of the belt with the D-ring, shown in Figure 3.20(a), here is approximately 1 kN lower. The second difference is that here the belt force increases significantly in the last phase of the crash, whereas it only slightly increase for the case of Section 3.3. Again, the friction in the contact of the belt with the D-ring plays an important role. To follow the reference signal in this phase of the crash,

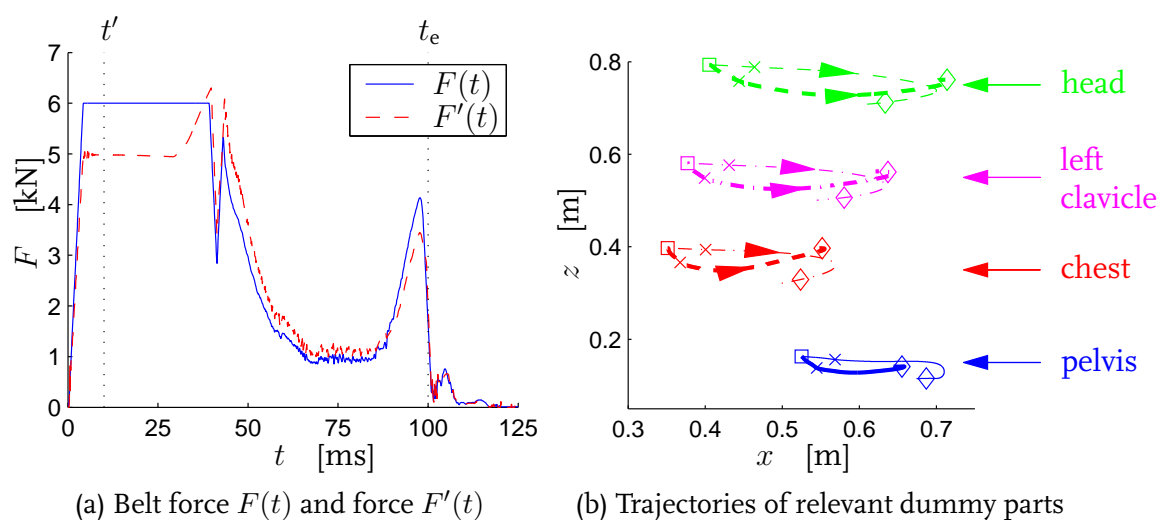


**Figure 3.20** Forces in the belt and trajectories of relevant dummy parts

the belt has to be retracted resulting in the reversal of the direction of the friction, whereas the belt is yield for the case in Section 3.3. The third difference is that here the maximum chest deflection here is reduced to 65 % of its original value, whereas it is reduced to 90 % of its original value in the case of Section 3.3. This may be explained by the lower level of the belt force.

In Figure 3.20(b), trajectories of the centers of gravity of the dummy head, left clavicle, chest and pelvis, relative to the vehicle, in the  $(x, z)$ -plane of the vehicle are shown. Initial positions are indicated with “□”, positions at  $t = 35$  ms with “×”, and positions at the end of the crash  $t = t_e$  with “◇”. Furthermore, thin lines denote the trajectories for the case that the restraint system is passive, and thick lines the trajectories for the case that the chest acceleration is controlled. The motion of the dummy resembles that of the dummy motion for the case that the restraint system is passive. However, the dummy moves more downward, and starts to move backward, relative to the vehicle, at a later point of time.

## 3.6 Discussion

In the previous sections, a fairly simple and general applicable, control design strategy has been presented. The strategy has been applied to design controllers for the most important control objectives of active restraint system components.

Most importantly, feedback control is very effective for our purposes. It has a linearizing effect on the behavior of the closed loop system, reduces the influence of disturbances, uncertainties and model mismatches on the closed loop behavior, and can enforce the desired closed loop behavior, using relatively simple low order controllers.

The measure for risk of chest injuries has been reduced to approximately 40 % of its original value by manipulation of the belt force. The manipulation of the vent size to control the head acceleration reduces the risk of injuries to the head to 60 % of its original

value. Besides that, the results in the previous sections suggest that the control of one occupant variable does not only reduce the controlled measure for the risk of injuries, but is also beneficial to other measures for the risk of injuries.

The dynamic behavior of the dummy, interacting with the belt, has been approximated by LTI models at both open loop and closed loop operating points of the complex nonlinear model. Comparison of the obtained LTI models revealed that differences between the models for quite different operating points are small, and can be appropriately handled by the designed feedback controllers. Furthermore, controllers that are designed using LTI control design models for open loop operating points, can enforce the desired behavior of the closed loop system. These observations indicate that for the considered class of relatively simple, low order controllers, LTI models for open loop operating points of the complex nonlinear model are sufficiently accurate. Nevertheless, considering the achieved bandwidth, it is noted that the length of the used time interval for approximation purposes in Chapter 2 is rather long, which may have lead to less accurate estimation of the high-frequent dynamic behavior. Furthermore, for highly complex and high bandwidth controllers, these LTI models may be not accurate enough.

Feedback controllers for various control objectives, being the control of the chest and of the head acceleration by manipulation of the belt force, the mass flow or the vent size, can be successfully designed with the proposed design strategy. Actually, the determination of appropriate reference signals poses a larger problem. Although the proposed approach is simply and fairly straightforward, it is only effective to reduce the risk of injuries, accounting for one controlled variable only. To account for injuries that can not be explicitly formulated in terms of the controlled variable, like the maximum belt force, an iterative approach is required. This approach is unsuitable for real world implementations. Nevertheless, the use of reference signals for the considered control problems is very effective. In Chapter 5, the first result of a study into the application of Model Predictive Control, without the need of a priori define reference signals, will be presented.

Results in Section 3.3 show that contact of the dummy with the airbag does not have a significant influence on control of the chest acceleration by the belt force. Results in Section 3.4 show that contact of the dummy with the belt does not have a significant influence on control of the head acceleration by the vent size. Furthermore, they show that manipulation of the vent size is sufficient to control the head acceleration, at least for the considered combination of the crash, dummy, belt and airbag system. These observations suggest that the control of the chest acceleration by the belt force and the head acceleration by the vent size may be effective to reduce the overall risk of injuries. This will be investigated in the following chapter.

# Control design for the restraint system

*The control objective is to reduce the risk of injuries to the head and to the chest as much as possible by manipulation of the belt and the airbag simultaneously. Interactions between control of the head acceleration and the chest acceleration are analyzed and it is made plausible that the control design problem can be split into two tracking problems, similar to those in the previous chapter. Reference signals are used that roughly account for neck injuries as well.*

## 4.1 Introduction

The control objective is to simultaneously control the chest and head acceleration by manipulation of the belt and the airbag. Closed loop results in Chapter 3 show that feedback controllers, designed using LTI control design models, can enforce the desired closed loop behavior of the complex nonlinear model. Besides that, they show that the airbag can be satisfactorily manipulated by the vent size only. Therefore, feedback control, using LTI control design models, seems to be attractive for the case with multiple inputs and multiple outputs (MIMO), where the chest acceleration  $\ddot{c}$  and the head acceleration  $\ddot{h}$  are controlled by the belt force  $F$  and the vent size  $A$ . In this chapter, a strategy to arrive at a MIMO controller for the restraint system, such that the controlled chest acceleration and the controlled head acceleration follow an a priori defined reference signals, is presented.

In Figure 4.1, the closed loop system with the MIMO controller  $\mathcal{C}$  and the complex nonlinear model  $\mathcal{M}$  is shown. Here, the vector quantity  $\underline{r}(t)$  contains the reference signals  $r_{\ddot{c}}(t)$  and  $r_{\ddot{h}}(t)$ ,  $\underline{e}(t)$  the error signals  $e_{\ddot{c}}(t) = r_{\ddot{c}}(t) - \ddot{c}(t)$  and  $e_{\ddot{h}}(t) = r_{\ddot{h}}(t) - \ddot{h}(t)$ ,  $\underline{u}(t)$  the

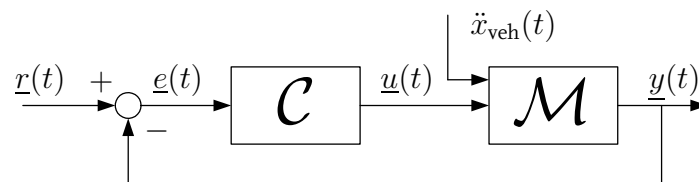


**Figure 4.1** Closed loop system with MIMO controller  $\mathcal{C}$  and model  $\mathcal{M}$

manipulated variables  $F(t)$  and  $A(t)$ , and  $\underline{y}(t)$  the controlled variables  $\ddot{c}(t)$  and  $\ddot{h}(t)$ .

In general, the MIMO controller configuration can be of the “multivariable” or the “decentralized” type. For a multivariable control configuration, all elements of the controller transfer matrix  $\mathcal{C}$  can be non-zero, whereas for a decentralized control configuration the off-diagonal elements are zero. In general, the closed loop performance using a decentralized control configuration will not be as high as that, using the multivariable configuration [146]. Nevertheless, a decentralized control configuration has advantages over the multivariable control configuration [139]. First, if an actuator or sensor fails, a limited degree of robustness and performance may be guaranteed for the other control loops. Second, control design and implementation is less complex and expensive.

For the problem at hand, there are two additional reasons why a decentralized control configuration may be suitable. First, almost all kinetic energy of the head is absorbed by the airbag [56]. Second, it is commonly believed that the belt is the most important component for the chest and that the airbag is the most important component for the head [75]. This may indicate that the control problem to reduce the risk of injuries to the head and to the chest can be formulated as two independent control design problems. If that is the case, the belt force controls the chest acceleration and the vent size controls the head acceleration. In Section 4.2, it will be made plausible that for the problem at hand, the advantages of the decentralized configuration more than counterbalance the disadvantages.

The reference signals are extremely important. In Chapter 3, reference signals have been constructed with the objective to reduce one measure for the risk of injuries as much as possible. Control of the chest acceleration and the head acceleration simultaneously may allow the reduction of other injuries as well. For example, the severity of neck injuries like whiplash [73] may be reduced in that manner. An approach to construct reference signals for the head and chest acceleration, pragmatically accounting for the risk of neck injuries, is presented.

In Section 4.2, interaction from the inputs of interest to the outputs of interest is analyzed using LTI control design models. In Section 4.3, a design strategy for the controllers of the belt and the airbag is proposed, controllers are designed and evaluated. Finally, the strategy and the results are discussed in Section 4.4.

## 4.2 Interaction analysis

In the previous chapters, it has been observed that the LTI control design models describe the dynamic behavior, relevant for design of feedback controllers, reasonably accurate. Therefore, it seems reasonable to use the LTI control design models for interaction analysis. The transfer matrix  $\mathcal{H}(s)$ , containing the transfer functions of a perturbation in the inputs  $\delta F$  and  $\delta A$  to the response in the outputs  $\delta\ddot{c}$  and  $\delta\ddot{h}$ , is defined as:

$$\begin{bmatrix} \delta\ddot{c}(s) \\ \delta\ddot{h}(s) \end{bmatrix} = \mathcal{H}(s) \cdot \begin{bmatrix} \delta F(s) \\ \delta A(s) \end{bmatrix} = \begin{bmatrix} \mathcal{H}_{11}(s) & \mathcal{H}_{12}(s) \\ \mathcal{H}_{21}(s) & \mathcal{H}_{22}(s) \end{bmatrix} \cdot \begin{bmatrix} \delta F(s) \\ \delta A(s) \end{bmatrix} \quad (4.1)$$

Several methods to analyze interactions exist [162], using for example the Niederlinski Index [119] or the (Dynamic) Relative Gain Array [25, 169]. Here, the concept of the Dynamic Relative Gain Array (*DRGA*) is used, mainly because of its simplicity and straightforwardness. The relative gain of an element of the transfer matrix  $\mathcal{H}(s)$  is defined as the ratio between its static gain in the case that all control loops are open, and its static gain in the case that the other control loops are closed with their outputs being perfectly controlled. The dynamic relative gain array of a  $2 \times 2$  MIMO system is defined as:

$$DRGA = \mathcal{H} \otimes \mathcal{H}^{-T} = \frac{1}{1 - \gamma} \begin{bmatrix} 1 & -\gamma \\ -\gamma & 1 \end{bmatrix} \quad \text{with} \quad \gamma = \frac{\mathcal{H}_{12} \cdot \mathcal{H}_{21}}{\mathcal{H}_{11} \cdot \mathcal{H}_{22}} \quad (4.2)$$

where the dependency on  $s = j\omega$  is omitted for brevity. The symbol “ $\otimes$ ” denotes the element-by-element multiplication, often called the Hadamard or Schur product. A (dynamic) relative gain  $|DRGA_{ij}|$  close to 1 over the frequency range of interest indicates that if input  $j$  controls output  $i$ , the disturbance to output  $i$  due to the control of the other output is weak. Otherwise, this disturbance is strong. To pair the inputs and outputs for a  $2 \times 2$  MIMO system, analysis of one of the elements of  $DRGA_{ij}(j\omega)$  is sufficient.

LTI control design models for the elements  $\mathcal{H}_{11}(s)$  and  $\mathcal{H}_{22}(s)$  have already been realized in Section 2.4 and Section 2.5, respectively. In the sequel, LTI control design models for the remaining elements  $\mathcal{H}_{12}(s)$  and  $\mathcal{H}_{21}(s)$  are determined, followed by the presentation of the complete transfer matrix  $\mathcal{H}(s)$  and the pairing of the inputs and outputs of interest.

### Modelling the transfer from the belt force to the head acceleration

To obtain LTI models for the transfer from a perturbation  $\delta F$  in the belt force to the disturbance  $\delta \ddot{h}$  in the head acceleration, results of simulations for modelling the transfer function from  $\delta F$  to  $\delta \ddot{c}$  see Section 2.4, are used. Interaction analysis makes sense only for the points of application  $\tau$ , at which the dummy head is in contact with the airbag. Therefore, only the points of application  $\tau_3 = 40$  ms and  $\tau_4 = 64$  ms are considered. In Figure 4.2, the normalized responses to positive and negative steps in the belt force,

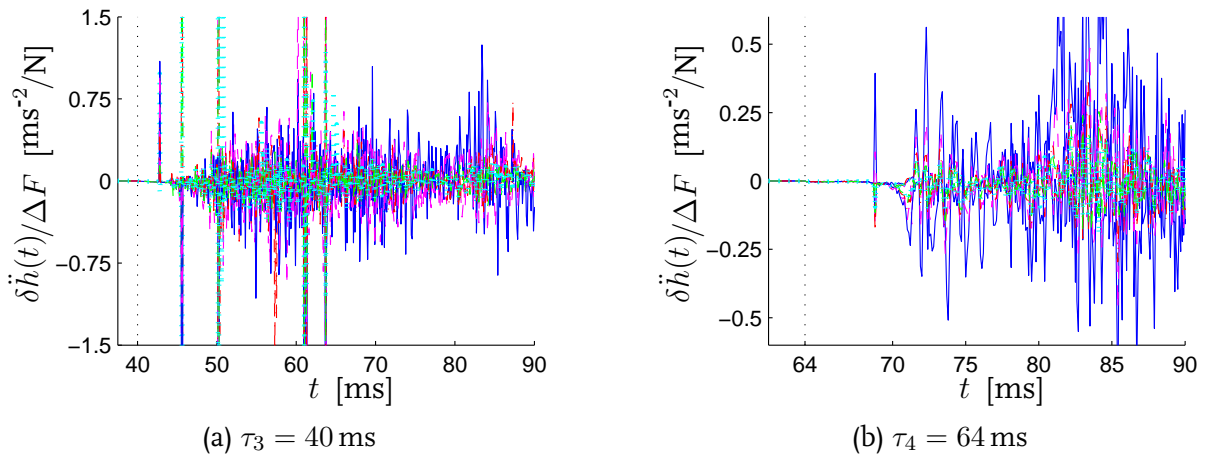


**Figure 4.2** Normalized responses in the head acceleration to steps in the belt force, added at  $\tau_3$  and  $\tau_4$



added at  $\tau_3$  and  $\tau_4$ , are shown. It may be concluded that these responses mainly consist of (computational) noise, meaning that the transfer  $\mathcal{H}_{12}(s)$  can be neglected, at least if the dummy is in contact with the airbag.

### Modelling the transfer from the vent size to the chest acceleration

To obtain LTI models for the transfer from a perturbation  $\delta A$  in the vent size to the disturbance  $\delta\ddot{c}$  in the chest acceleration, results of simulations in Section 2.5 for modelling the transfer function from  $\delta A$  to  $\delta\ddot{h}$  are used. Two points of application are considered, being  $\tau_1 = 50$  ms and  $\tau_2 = 60$  ms. The normalized responses in the head acceleration seem to justify the linearization of the investigated transfer. Furthermore, they indicate that the dynamic behavior changes slightly as a function of the operating point. Using approximate realization, an LTI model of second order is realized for each point of application  $\tau$ . In Figure 4.3, the averaged normalized responses  $\overline{\delta\ddot{c}_1}(t)$  and  $\overline{\delta\ddot{c}_2}(t)$  are shown, together with the unit step responses  $y_{\mathcal{H}_1}(t)$  and  $y_{\mathcal{H}_2}(t)$  of the realized LTI models. The quality measure is 0.14 for  $\tau_1$  and 0.10 for  $\tau_2$ . The low quality of the LTI models can be explained by the strong influence of (computational) noise, as can be easily observed in Figure 4.3. Since the shape and characteristics, like peak time and rise time, of the responses in Figure 4.3(a) and Figure 4.3(b) are similar, it is expected that the relevant dynamic behavior is reasonably captured by the LTI models, at least for small perturbations.

### The complete transfer matrix

For all elements of the transfer matrix  $\mathcal{H}(s)$ , except for  $\mathcal{H}_{21}(s)$ , LTI control design models are available, but the points of application  $\tau$  for these models do not coincide. Results in Chapter 2 and Chapter 3 show that the dynamic behavior, relevant for control design purposes, differs slightly at quite different operating points, at least if the dummy is in contact with the airbag. Therefore, it seems justified to neglect the differences between the points of application. Figures 4.4 and 4.5 show the modulus and phase of the ele-

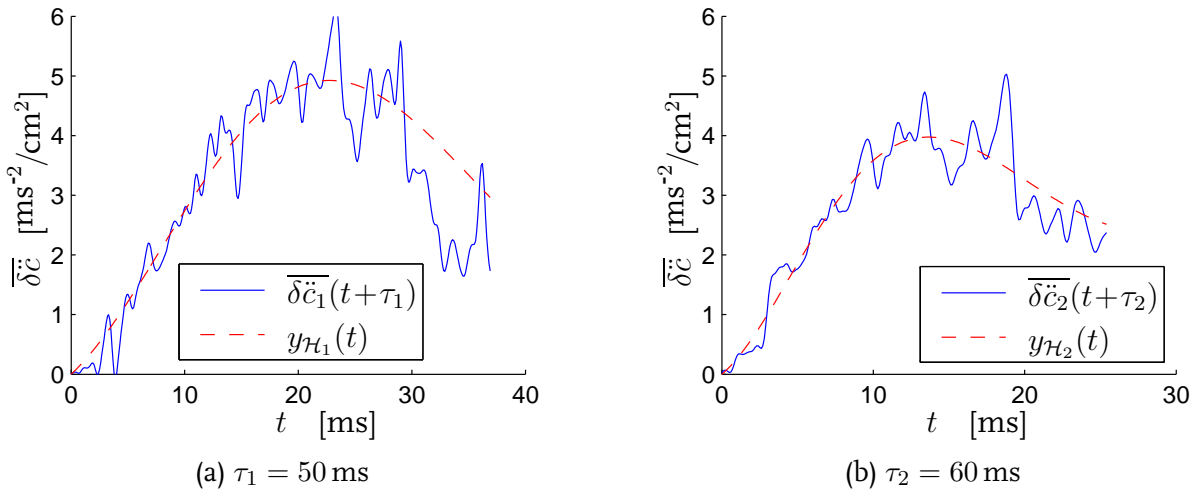


**Figure 4.3** Unit step response of the LTI models and the corresponding averaged normalized responses for  $\tau_1$  and  $\tau_2$

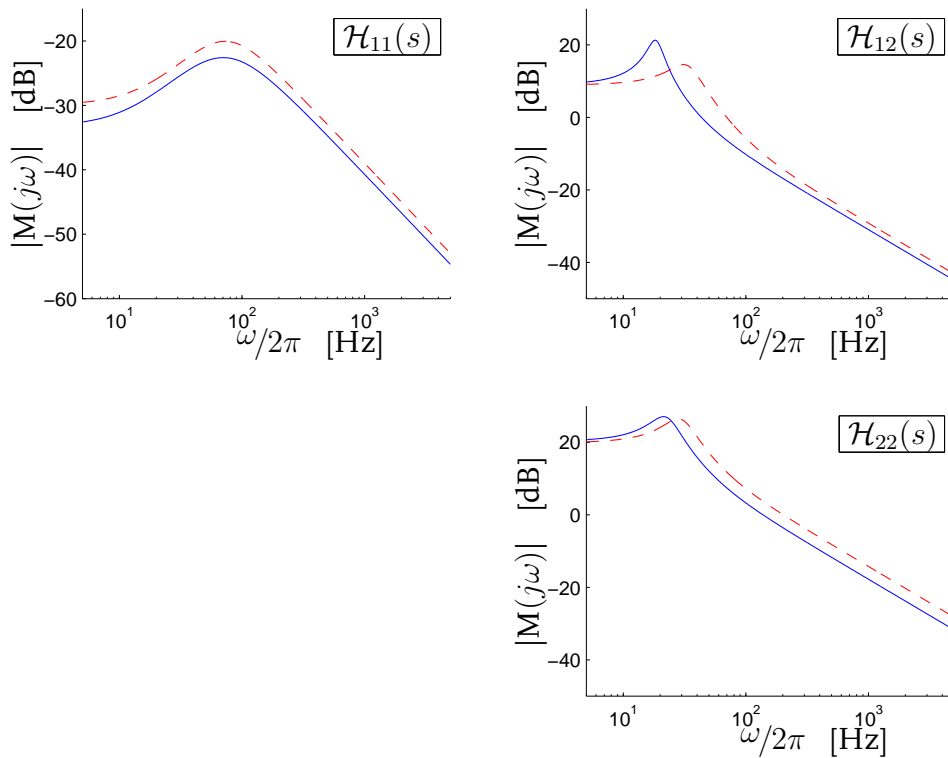


**Figure 4.4** Modulus of the transfer matrix  $\mathcal{H}(s)$

ments of the transfer matrix  $\mathcal{H}(s)$ . For  $\mathcal{H}_{11}(s)$ , the solid and the dashed lines correspond to the points of application  $\tau_3 = 40$  ms and  $\tau_4 = 64$  ms, respectively, whereas for  $\mathcal{H}_{12}(s)$  and  $\mathcal{H}_{22}(s)$ , they correspond to the points  $\tau_1 = 50$  ms and  $\tau_2 = 60$  ms, respectively.

For  $\mathcal{H}_{12}(s)$  and  $\mathcal{H}_{22}(s)$ , the damping factor and the damped eigenfrequency slightly increase as a function of the operating point, whereas for  $\mathcal{H}_{11}(s)$ , only the modulus over the whole frequency range of interest slightly increases as a function of the operating point. This has already been observed in Sections 2.4 and 2.5.

### Pairing of the inputs with the outputs

Using the transfer matrix  $\mathcal{H}(s)$ , the interactions can be analyzed in order to appropriately pair the inputs  $\delta F$  and  $\delta A$  and the outputs  $\delta \ddot{c}$  and  $\delta \ddot{h}$ . For the problem at hand, this analysis is redundant. The (Dynamic) Relative Gain Array here is a diagonal matrix, since the transfer  $\mathcal{H}_{21}(s)$  from  $\delta F$  to  $\delta \ddot{h}$  can be neglected. Hence, the chest acceleration  $\ddot{c}$  is to be controlled by the belt force  $F$ , and the head acceleration  $\ddot{h}$  is to be controlled by the vent size  $A$ , as illustrated in Figure 4.6. Here,  $C_{11}$  and  $C_{22}$  are the controllers to manipulate the belt force and the vent size, respectively.

This conclusion is the confirmation of earlier assumptions [56, 75] that the airbag is the most important component to reduce the risk of injuries to the head, whereas the belt is the most important component to reduce the risk of injuries to the chest.

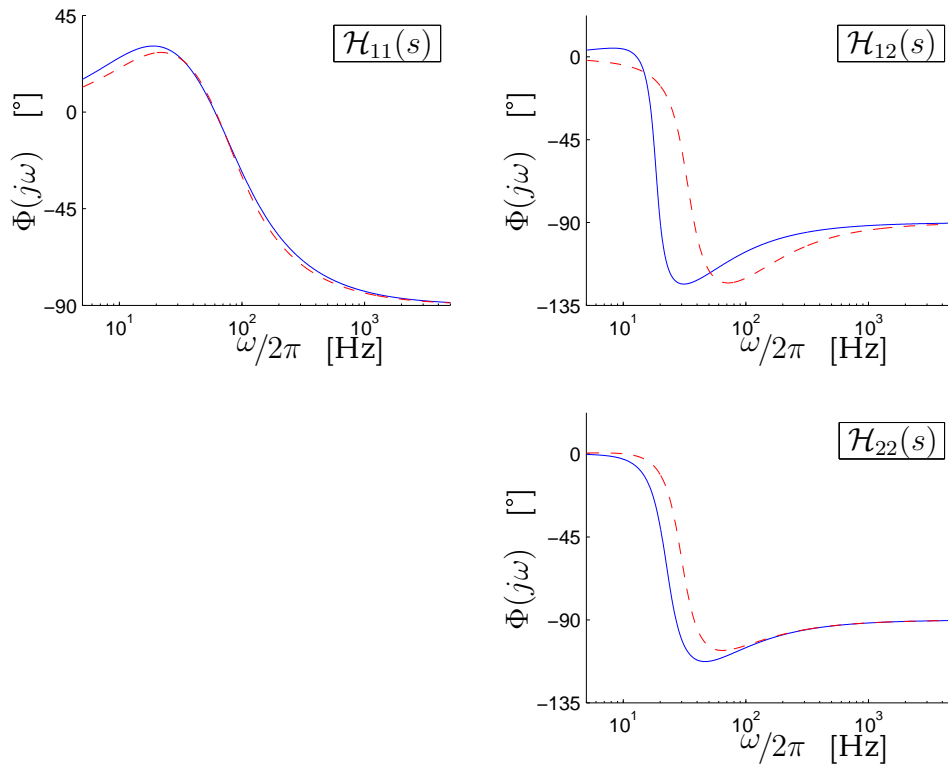


Figure 4.5 Phase of the transfer matrix  $\mathcal{H}(s)$

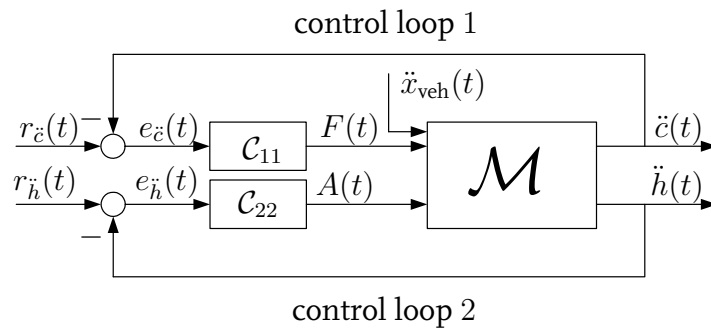


Figure 4.6 Closed loop system with the model  $\mathcal{M}$

### 4.3 Control of the chest and the head acceleration

In this section, the design of the controllers is elucidated, followed by the construction of appropriate reference signals. After that, the controllers are implemented and evaluated in the closed loop system with the model  $\mathcal{M}$ .

#### Control design

For the design of the controllers  $\mathcal{C}_{11}$  and  $\mathcal{C}_{22}$ , the closed loop system with the LTI control design models as illustrated in Figure 4.7, is used. Here, the transfer function  $\mathcal{H}_{21}(s)$  has been omitted. Furthermore,  $d_{12}(s)$  is the disturbance signal to the chest acceleration, due

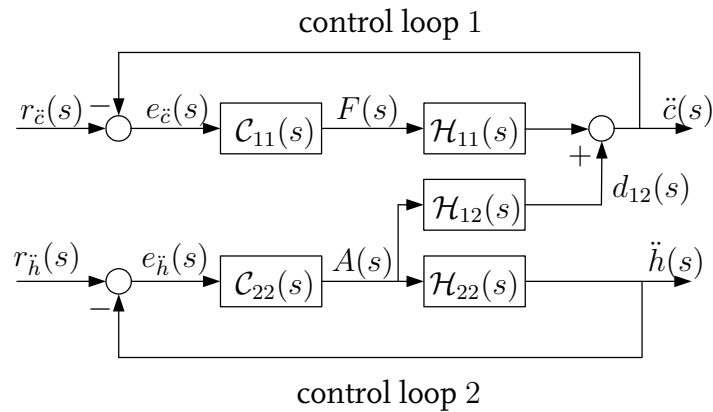


**Figure 4.7** Closed loop system for design purposes

to the control of the head acceleration by the vent size:

$$d_{12}(s) = \frac{C_{22}(s)\mathcal{H}_{12}(s)}{1 + C_{22}(s)\mathcal{H}_{22}(s)} \cdot r_{\ddot{h}}(s) \quad (4.3)$$

Several design strategies exist for controllers in a decentralized control configuration, e.g. [10, 32, 43, 104, 164]. For our purposes, Sequential Loop Closure [32, 86, 87, 88] is attractive, since it allows the use of the control design strategy of Section 3.2. First, the controller is designed for the control loop with the fastest (open loop) dynamic behavior, neglecting interactions. After closing that control loop, the design procedure is repeated for the remaining control loops, accounting for the interactions with the control loops that are already closed.

For the problem at hand, the controller of Equations 3.5 and 3.6 is adopted as the controller  $C_{11}$  for the chest acceleration, meaning that the control design criteria for this control loop are satisfied. Similarly, the controller  $C_{22}$  of Equation 3.8 is adopted as the controller for the head acceleration, meaning that the control design criteria for this loop are also satisfied. Still, it has to be investigated whether the disturbance  $d_{12}(s)$  deteriorates the performance of the control loop with the chest acceleration. Figure 4.8 shows the modulus of  $d_{12}(s)$ . Comparing this modulus to that of the element  $\mathcal{H}_{11}(s)$ , it seems reasonable to assume that the control of the chest acceleration is not deteriorated due to the interaction. Hence, the control design problem can be split in two independent control design problems and the controllers from Chapter 3 are adopted without any change.

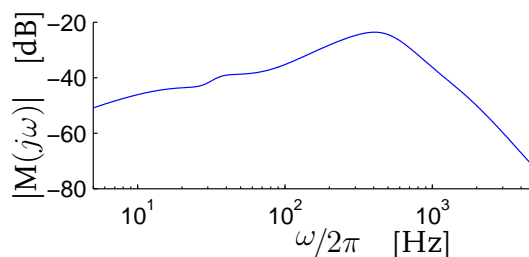


**Figure 4.8** Modulus of  $d_{12}(s)$

### Reference signals

The reference signals  $r_{\dot{c}}(t)$  and  $r_{\dot{h}}(t)$  have to reflect the lowest possible value of the maximum absolute chest and head acceleration, respectively. Furthermore, they have to prevent undesired contact of the dummy with the vehicle interior and have to ensure that the velocity of the chest and head at the end of the crash is lower than the vehicle velocity. In addition, the reference signal for the chest acceleration has to prevent that the dummy thorax is pushed through the seat. Finally, neck injuries occur due to the motion of the head, relative to the chest, meaning that the reference signals have to reduce the risk of injuries to the neck, if possible.

Several measures for the risk of neck injuries exist [58]. Amongst them, two measures are based on the motion of the head, relative to the first thoracic vertebrae. The use of the chest motion instead of the motion of the first thoracic vertebrae, makes these measures suitable for our purposes. The first measure is the time  $\Delta t$  between the sign change of the head velocity and that of the first thoracic vertebrae [110]. The maximum allowable  $\Delta t$  is 10 ms [110]. The second measure is the Frontal Neck Injury Criterion (*FNIC*) [21]:

$$FNIC = \max_{t \in (t_0, 150 \text{ ms})} (\ddot{x}_{\text{rel}}(t) \cdot \alpha + \dot{x}_{\text{rel}}(t) \cdot |\dot{x}_{\text{rel}}(t)|) \quad (4.4)$$

where  $\ddot{x}_{\text{rel}}(t)$  is the forward acceleration of the head, measured at its center of gravity, relative to the first thoracic vertebra,  $\dot{x}_{\text{rel}}(t)$  the relative velocity of these points, and  $\alpha = 0.2 \text{ m}$ . A tolerance level of  $25 \text{ m}^2/\text{s}^2$  [21] for the mid-size dummy is proposed but not yet generally accepted.

To determine reference signals that reflect the lowest possible value of the maximum chest and head acceleration and comply with the mentioned bounds and desires, is far from trivial. Here, a pragmatic approach is followed.

It is a plausible assumption that appropriate reference signals are constant as a function of time, with an as low as possible absolute value of the constant. To prevent that the dummy thorax is pushed through the seat, the absolute chest acceleration over the time interval from the start of the crash until a yet to-be-determined point of time  $t = t'$ , has to be lower than the absolute vehicle acceleration. Furthermore, until the head is in contact with the airbag, the absolute chest acceleration may not be too high, due to the risk of injuries to the neck. In agreement with Chapter 3, the crash is considered to be ended at  $t = t_e = 100 \text{ ms}$ . Considering these aspects, a reasonable shape of the reference signal for the chest acceleration is:

$$r_{\dot{c}}(t) = \begin{cases} r'_{\dot{c}}/2 \cdot [1 - \cos(\frac{2\pi}{2t'}t)] & 0 \leq t < t' \\ r'_{\dot{c}} & t' \leq t < 97.5 \text{ ms} \\ r'_{\dot{c}}/2 \cdot [1 + \cos(\frac{2\pi}{10}(t - 97.5))] & 97.5 \text{ ms} \leq t < 102.5 \text{ ms} \\ 0 & 102.5 \text{ ms} \leq t \end{cases} \quad \text{for} \quad (4.5)$$

with  $t'$  a yet to-be-determined point of time and  $r'_{\dot{c}}$  a yet to-be-determined constant value of the chest acceleration. For the acceleration of the head, the shape of the reference

signal of Section 3.4 seems reasonable, so:

$$r_{\ddot{h}}(t) = \begin{cases} r'_h/2 \cdot [1 - \cos(\frac{2\pi}{10}t)] & t'' \leq t < t'' + 5 \text{ ms} \\ r'_h & t'' + 5 \text{ ms} \leq t < 97.5 \text{ ms} \\ r'_h/2 \cdot [1 + \cos(\frac{2\pi}{10}(t - 97.5))] & 97.5 \text{ ms} \leq t < 102.5 \text{ ms} \\ 0 & 102.5 \text{ ms} \leq t \end{cases} \quad \text{for} \quad (4.6)$$

with  $t''$  a yet to-be-determined point of time and  $r'_h$  a yet to-be-determined constant value of the head acceleration. The reference signals are smoothed to prevent numerical problems during simulations with the complex nonlinear model. The point of time  $t = t''$ , at which the controller for the airbag is enabled, is chosen as early as possible, i.e. at the point of time when the dummy head contacts the airbag, so  $t'' = 35$  ms. To determine an appropriate value for  $t = t'$ , the vehicle deceleration is analyzed, shown in Figure 4.9(a) as the solid line. To prevent that the dummy thorax is pushed through the seat, a point of time  $t = t'$  shortly after  $t = 25$  ms seems reasonable. Here, it is arbitrarily chosen for  $t' = 35$  ms.

Next, the constant values  $r'_c$  and  $r'_h$  are to be determined. First, constant values are determined for which the maximum chest and head acceleration are as low as possible. If necessary and possible, these values are then adapted to reduce the risk of injuries to the neck. To check whether the bounds on the motion of the head and the chest are violated, the velocity and displacement of the chest, the head and of the steering wheel are roughly estimated by integration of  $r'_c(t)$ ,  $r'_h(t)$  and  $\ddot{x}_{\text{veh}}(t)$  with the initial conditions  $r_c(t_0) = r_h(t'') = v_0$  and  $r_c(t_0) = r_h(t'') = 0$ . Using trial-and-error, the values  $r'_c$  and  $r'_h$  are adapted until they are as low as possible and the bounds on the velocity and displacement are not violated. The obtained values  $r'_c = -210 \text{ m/s}^2$  and  $r'_h = -290 \text{ m/s}^2$  yield an estimated value of  $FNIC$  greater than  $55 \text{ m}^2/\text{s}^2$ . Therefore, the risk of neck injuries is reduced by decreasing the value  $r'_c$  until the time difference  $\Delta t$  is 10 ms. This is the case for  $r'_c = -260 \text{ m/s}^2$ , yielding  $FNIC \approx 30 \text{ m}^2/\text{s}^2$ .

In Figure 4.9(a), the reference signals  $r'_c(t)$  and  $r'_h(t)$  for the chest acceleration and the head acceleration are shown, respectively. Furthermore, the vehicle acceleration  $\ddot{x}_{\text{veh}}(t)$  is shown. In Figure 4.9(b), the corresponding velocities are shown, whereas Figures 4.9(c) and 4.9(d) show the displacements of the chest and the head, respectively. In Figure 4.9(c), the displacement  $x_{\text{veh}}(t) + \ell_c$  has to be interpreted as the displacement of the steering wheel, with  $x_{\text{veh}}(t)$  the displacement of the back of the seat. In Figure 4.9(d), the displacement  $x_{\text{veh}}(t) + \ell_h$  has to be interpreted as the displacement of the head rest.

The reference signals suggest a reduction of approximately 50% of the maximum absolute chest and head acceleration, compared to their original value. These reductions will be achieved if the reference signals are accurately followed and contacts with the steering wheel are indeed prevented. That can only be investigated by a simulation of the closed loop system with the complex nonlinear model, which is done in the following section.

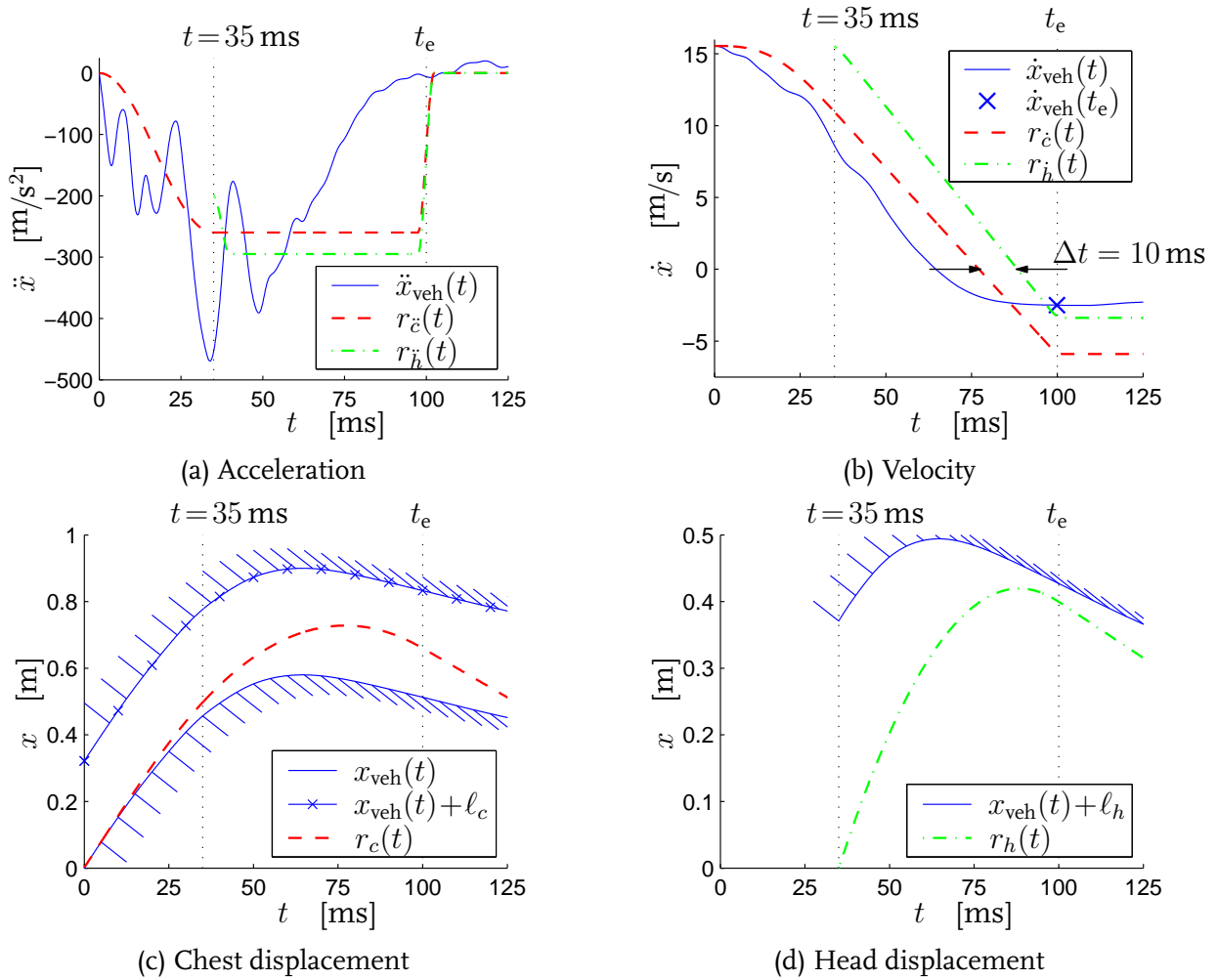


**Figure 4.9** Vehicle acceleration and reference signals for the chest and the head acceleration, as well as the corresponding velocities and displacements

## Evaluation

The evaluation of the controllers is based on a simulation using the closed loop system with the model  $\mathcal{M}$ , see Figure 4.1. In Figure 4.10(a-f), some relevant results are shown, together with the results for the case that the restraint system is passive. In Figure 4.10(g), the vehicle and the dummy at the end of the crash show that the chest and the head do not contact the steering wheel. In fact, the distance from the head to the steering wheel is far more than 3 cm, as would be expected from the estimated displacement of the head in Figure 4.9(c). This may be explained by the estimation of the head displacement by double integration of  $r_{\dot{h}}(t)$ , whereas the dummy head does rotate.

The closed loop results suggest that the closed loop system is stable and that model mismatches, uncertainties and (computational) noise are properly dealt with. The chest and the head acceleration follow the reference signals fast enough. The maximum allowable errors  $|e_{\ddot{c},\max}| = 0.1 \cdot \max |r_{\ddot{c}}(t)|$  and  $|e_{\ddot{h},\max}| = 0.1 \cdot \max |r_{\ddot{h}}(t)|$  are not violated. The maximum chest and head acceleration are reduced to 57% and 50% of their original value, and the Frontal Neck Injury Criterion has been reduced to 70% of its original value. Furthermore, the maximum chest deflection has been reduced to 90% of its original value.

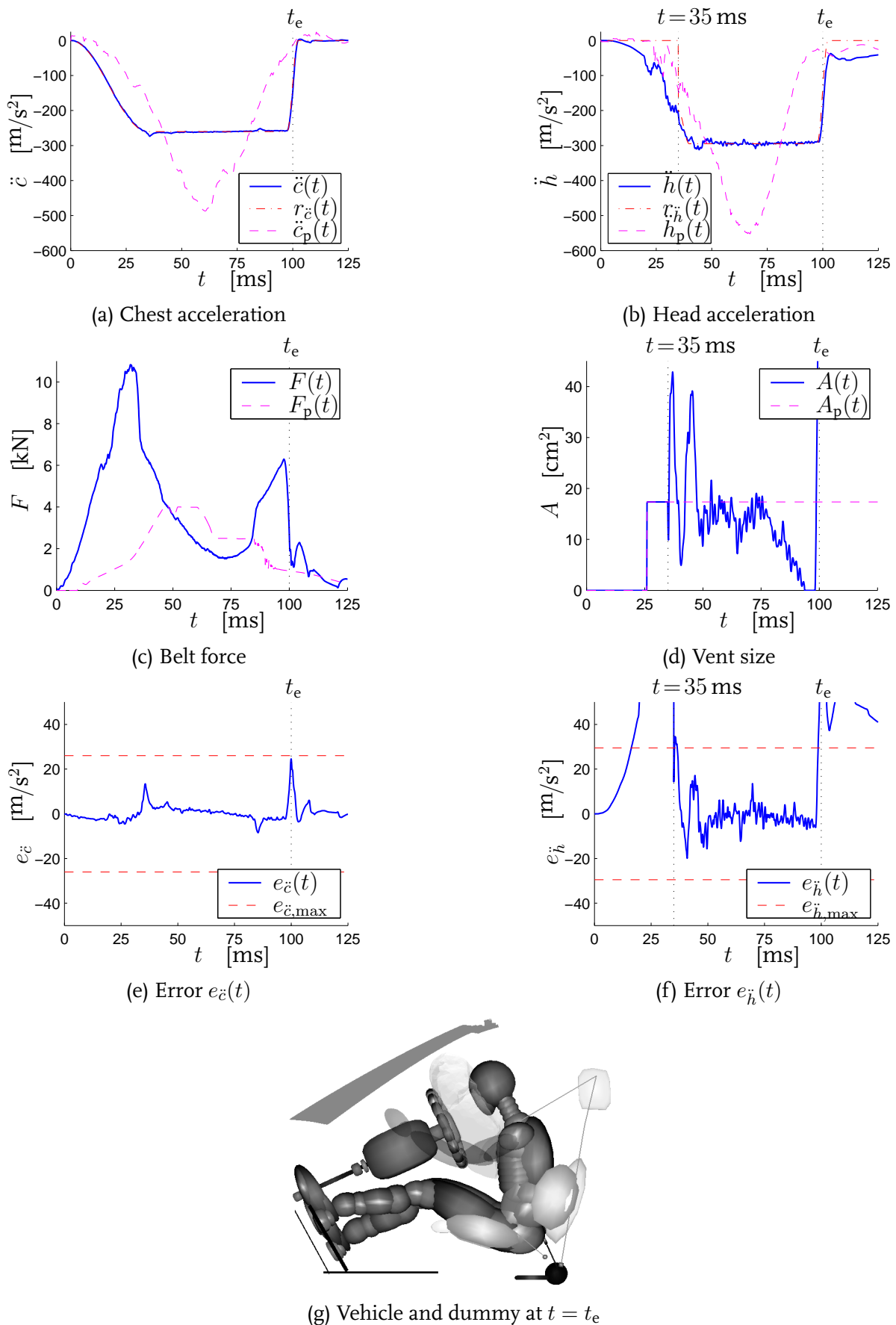


Figure 4.10 Results of the closed loop simulation for evaluation purposes



## 4.4 Discussion

In the previous sections, control design for the restraint system has been discussed. It has been made plausible that the control design problem can be split into two decoupled design problems, where the chest acceleration is controlled by the belt force and the head acceleration by the vent size.

The determination of appropriate reference signals remains a difficult problem. The proposed approach, accounting for injuries to the chest, the head and the neck, shows to be appropriate. A reduction of the risk of injuries to the chest, the head and to the neck to 57 %, 50 % and 70 % of the original values for the passive restraint system has been achieved, respectively. Nevertheless, it is very pragmatic and it is questionable whether the obtained reference signals actually represent the lowest achievable risk of injuries to the chest, the head and the neck.

The results in this chapter confirm, in line with the result in Chapter 3, that the manipulation of the vent size is sufficient to control the head acceleration, at least for the considered combination of the vehicle, restraint system and crash.

## CHAPTER FIVE

# Explorations

*In this chapter, the application of the modelling and control design strategy of the previous chapters is explored. Another measure for the risk of injury and another dummy are investigated. Furthermore, the development of adaptive restraint systems and the application of Model Predictive Control is glanced at.*

### 5.1 Introduction

In the previous chapters, the modelling and control design strategy have been elucidated and applied for the control of the maximum chest acceleration and the maximum head acceleration of one dummy. In this chapter, the suitability of the strategies as a design expedient in the case of other control objectives is explored. First, control of the chest deflection is presented in Section 5.2. Second, control of the chest acceleration and the head acceleration in the case of a small female crash dummy is elucidated in Section 5.3. After that, results of closed loop simulations are discussed in Section 5.4 from the point of view of a designer of passive or adaptive restraint system components. Finally, a first investigation towards the application of a control strategy which does not require an a priori known reference signal is presented in Section 5.5.

### 5.2 Control of the chest deflection by the belt

In this section, the modelling strategy of Section 2.3 and the control design strategy of Section 3.2 are applied for the case in which the chosen injury measure is the chest deflection  $s$ , defined as the compression of the sternum relative to the spine, [115]. The chest deflection is considered the best predictor of chest injuries [79], but difficult to control [80]. The belt force  $F$  is manipulated to reduce the maximum chest deflection as much as possible. The airbag system is not controlled, i.e. it behaves as if it is passive. It will be shown that the modelling strategy and the control design strategy can be applied without considerable modifications.

In the sequel, first LTI control design models are derived for the transfer from a per-

turbation  $\delta F$  in the belt force to the response  $\delta s$  in the chest deflection. After that, a controller for the belt is designed, implemented and evaluated in the closed loop system with the complex nonlinear model. Finally, control of the chest acceleration and the chest deflection is discussed.

### 5.2.1 Modelling for control design

To obtain LTI control design models for the transfer from  $\delta F$  to  $\delta s$ , the results of simulations from Section 2.4, are used. Here, only the most important results are presented.

Analysis of the normalized responses in the chest deflection suggests that it is justified to linearize the investigated transfer, at least for small perturbations. In Figure 5.1(a), the averaged normalized responses  $\overline{\delta s}_j(t)$  for  $\tau_1 = 20$  ms,  $\tau_2 = 25$  ms,  $\tau_3 = 40$  ms and  $\tau_4 = 64$  ms are given. They are shifted in time over  $\tau_j$ . The dynamic behavior clearly depends on the operating point. Therefore, an LTI control design model is derived for each of the points of application  $\tau_j$  with  $j = 1, 2, 3, 4$ . In Figure 5.1(b), the first five singular values of the matrices  $T_j$ , constructed from the shown part of the averaged normalized responses in Figure 5.1(a), are shown. Based on these results, the third and higher singular values are neglected, meaning that the LTI control design models will be of order two. From the normalized responses, it seems to be justified to neglect direct feed-through, meaning that the feed through matrices are omitted, when realizing the LTI control design models.

The LTI models, realized using Equation 2.6, are satisfactorily accurate, since the quality measure  $\kappa$  is less than 0.02 for each of the models. In Figure 5.2, the Bode diagrams are shown. Relatively large differences can be observed between the Bode diagrams for the operating points  $\tau_1$  and  $\tau_2$ , i.e. when the dummy is not in contact with the airbag, and the Bode diagrams for the operating points  $\tau_3$  and  $\tau_4$ , i.e. when the dummy is in

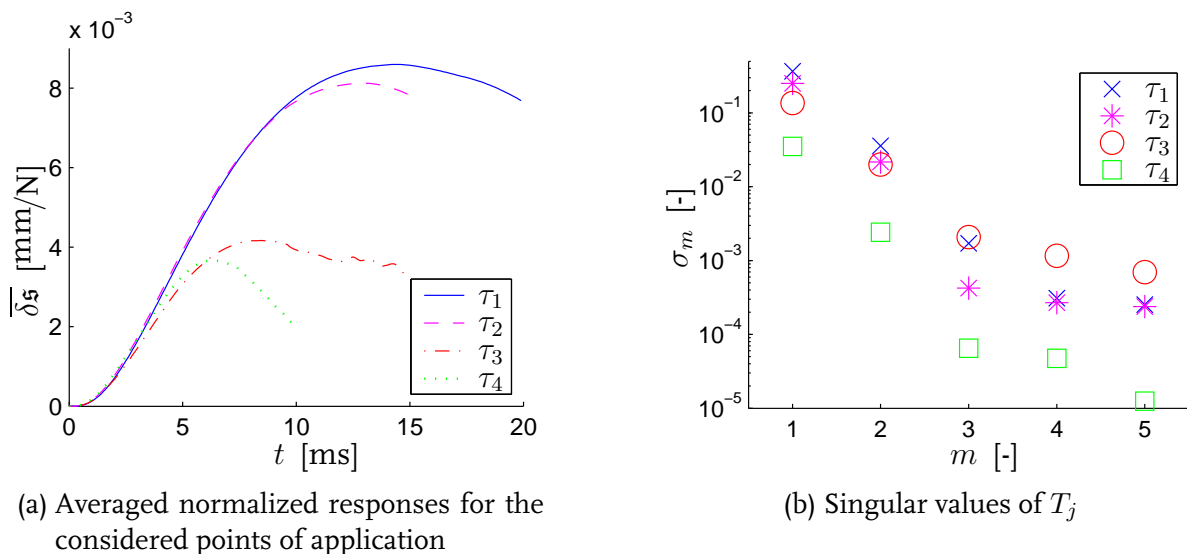


**Figure 5.1** Averaged normalized responses and singular values

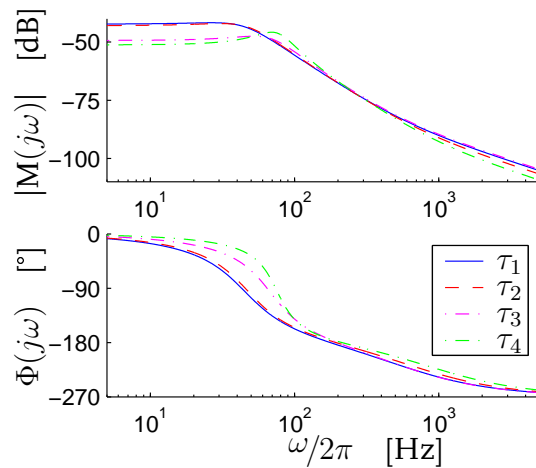


**Figure 5.2** Bode diagrams of the realized LTI models for the considered operating points

contact with the airbag. The damped eigenfrequency and the damping factor increase as a function of the operating point. A similar behavior was observed for the transfer from a perturbation in the belt force to the response in the chest acceleration. However, the static gain decreases as a function of the operating point, in contrast to an increasing static gain for the transfers to the chest acceleration. This difference may be explained by the progressive stiffness of the dummy thorax as a function of compression.

### 5.2.2 Control design

The control design criteria, formulated in Section 3.2, are the desired gain margin  $GM > 3$ , the desired phase margin  $PM > 45^\circ$ , and the bound on the modulus of the sensitivity transfer function  $|S(j\omega)| \leq -20$  dB for  $\omega/2\pi \leq f'$ . Furthermore, to achieve a sufficiently fast tracking of the reference signal, a bandwidth of at least 70 Hz is required, see Equation 3.2. To achieve sufficient error rejection, it is required that the sensitivity transfer function does not violate the bound  $|S(2\pi jf)| \leq -20$  dB for  $f \leq f'$  with  $f'$  a (yet) to-be-determined frequency. Due to the lack of knowledge about the frequency content of signals in the closed loop system, it is tried to find an appropriate frequency  $f'$  using the spectral density of the chest deflection  $s_p(t)$ , i.e. the chest deflection for the case that the restraint system is passive. From the cumulative spectral density in Figure 5.3, it can be concluded that more than 95 % of the total power in the signal is covered by frequencies below 30 Hz. Hence,  $f' = 30$  Hz seems appropriate.

Since the Bode diagrams of the LTI control design models do not drastically differ, especially for frequencies of 40 Hz and higher, it is aimed for one constant controller  $\mathcal{C}$ . The Bode diagrams also indicate that a (weak) derivative controller part is needed to achieve the desired phase margin and an integral part is needed to achieve the desired error rejection. A low-pass filter is not necessary:

$$C(s) = P \cdot \left(1 + \frac{2\pi f_I}{s}\right) \cdot \left(\frac{\frac{1}{2\pi f_{D_1}}s + 1}{\frac{1}{2\pi f_{D_2}}s + 1}\right) \quad (5.1)$$

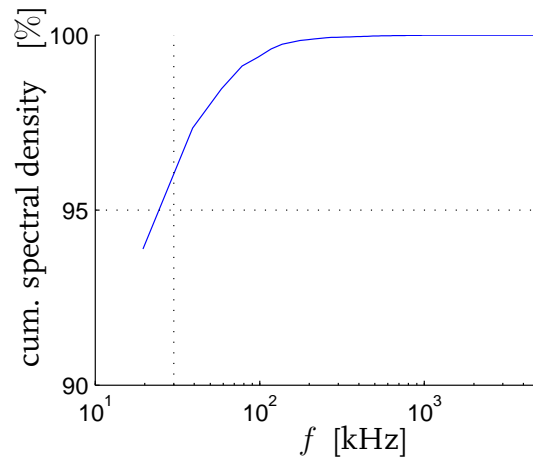


**Figure 5.3** Cumulative spectral density of the chest deflection  $s_p(t)$

Aiming at a bandwidth of 175 Hz, the controller parameters  $P$ ,  $f_I$ ,  $f_{D_1}$  and  $f_{D_2}$  are adapted until a controller is found, that satisfies the design criteria. This is the case for  $P = 668$ ,  $f_I = 50$  Hz,  $f_{D_1} = 70$  Hz and  $f_{D_2} = 1.5$  kHz. The bandwidth  $f_{BW}$  then is 175 Hz, 177 Hz, 188 Hz and 191 Hz for  $\tau_j$  with  $j = 1, 2, 3, 4$ . The moduli of the sensitivity functions  $S_j(s)$  and the relevant parts of the Nyquist plots of the open loop transfer functions  $\mathcal{H}_j(s) \cdot \mathcal{C}(s)$  for  $\tau_j$  with  $j = 1, 2, 3, 4$  are shown in Figure 5.4. Gain margins of 3.7, 4.4, 3.5 and 5.9 and phase margins of  $46^\circ$ ,  $49^\circ$ ,  $50^\circ$  and  $52^\circ$  are obtained for  $\tau_j$  with  $j = 1, 2, 3, 4$ , respectively.

### 5.2.3 Evaluation

The reference signal  $r_s(t)$  should represent the lowest possible value of the maximum chest deflection and prevent undesired contacts of the chest with the steering wheel. It is reasonable to assume that the maximum chest deflection will be as low as possible if the reference signal has a constant value  $r'_s$ , which is as low as possible. Obviously, the thorax may not be pushed through the seat and may not contact the steering wheel. Considering

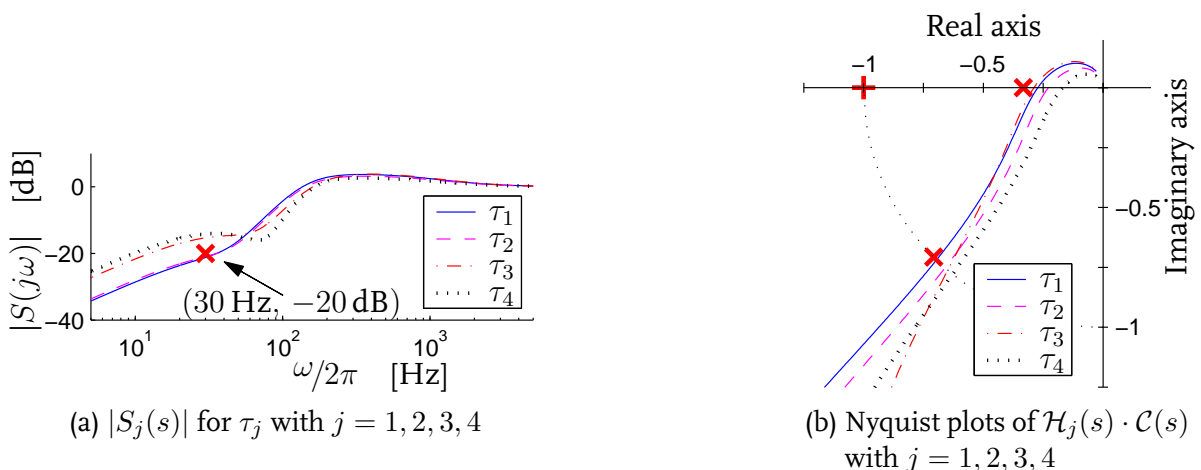


**Figure 5.4** Moduli of the sensitivity transfer functions and Nyquist plots

these aspects, a reasonable shape of the reference signal is:

$$r_s'(t) = \begin{cases} r_s'/2 \cdot [1 - \cos(\frac{2\pi}{2 \cdot t'} t)] & 0 \leq t < t' \\ r_s' & t' \leq t < 97.5 \text{ ms} \\ r_s'/2 \cdot [1 + \cos(\frac{2\pi}{10}(t - 97.5))] & 97.5 \text{ ms} \leq t < 102.5 \text{ ms} \\ 0 & 102.5 \text{ ms} \leq t \end{cases} \quad \text{for} \quad (5.2)$$

with  $r_s'$  a yet to-be-determined constant chest deflection, and  $t'$  a yet to-be-determined point of time. The reference signal is smoothed to prevent numerical problems during simulations. In agreement with the choices in previous chapters, the crash is considered to be ended at  $t = t_e = 100$  ms. To determine appropriate values for the point of time  $t = t'$  and the constant value  $r_s'$  is not trivial. Analogue to the choice of the point of time at which the reference signal for the chest acceleration becomes constant, the point of time  $t = t' = 11$  ms is chosen.

To determine an appropriate value for  $r_s'$ , first  $r_s' = 30$  mm is chosen, reflecting approximately 60 % of the maximum chest deflection if the restraint system is passive. For the case with the passive restraint system, a maximum chest deflection of 49 mm is obtained, see the dashed line in Figure 5.5(a). A simulation with the closed loop system with the complex nonlinear model is performed. The motion of the dummy is analyzed to determine whether the chest contacts the steering wheel. This is not the case. In fact, the smallest distance between the dummy thorax and the steering wheel is more than 10 cm, meaning that  $r_s'$  can be lowered. Next,  $r_s'$  is decreased until closed loop results show that the smallest distance between the thorax and the steering wheel is approximately 5 cm. After a few simulations,  $r_s' = 26$  mm shows to be appropriate.

In Figure 5.5(a-c), some relevant results of the final closed loop simulation are shown, together with the relevant results for the case that the restraint system is passive. The fairly smooth time histories of the chest deflection and the required belt force suggest that the closed loop system with the complex nonlinear model is stable. At  $t = 10$  ms, the error  $e_s(t) = r_s(t) - s(t)$  is approximately 1 mm, indicating that the reference signal is followed sufficiently fast. The maximum chest deflection has reduced to approximately 57 % of its original value, whereas the maximum chest and head acceleration have reduced to approximately 59 % and 72 % of their original value.

The manipulated belt force significantly drops at  $t \approx 32$  ms. This behavior of the belt system has already been observed for the case that the chest acceleration is controlled by the belt force, and the underlying cause of this drop is the same. Due to the reversal of the direction of friction in the contact of the belt with the D-ring, see Figure 5.6(a), the manipulated belt force  $F(t)$  drops. Besides that, the contact of the dummy with the airbag at  $t \approx 35$  ms results in additional forces applied to the dummy.

In Figure 3.8(b), trajectories of the centers of gravity of the dummy head, left clavicle, chest, sternum and pelvis, relative to the vehicle, in the  $(x, z)$ -plane of the vehicle are shown. Initial positions are indicated with “□”, and positions at the end of the crash  $t = t_e$  with “◇”. Furthermore, thin lines denote the trajectories for the case that the restraint system is passive, and thick lines the trajectories for the case that the chest deflection is controlled. It can be clearly observed that the sternum is pushed into the

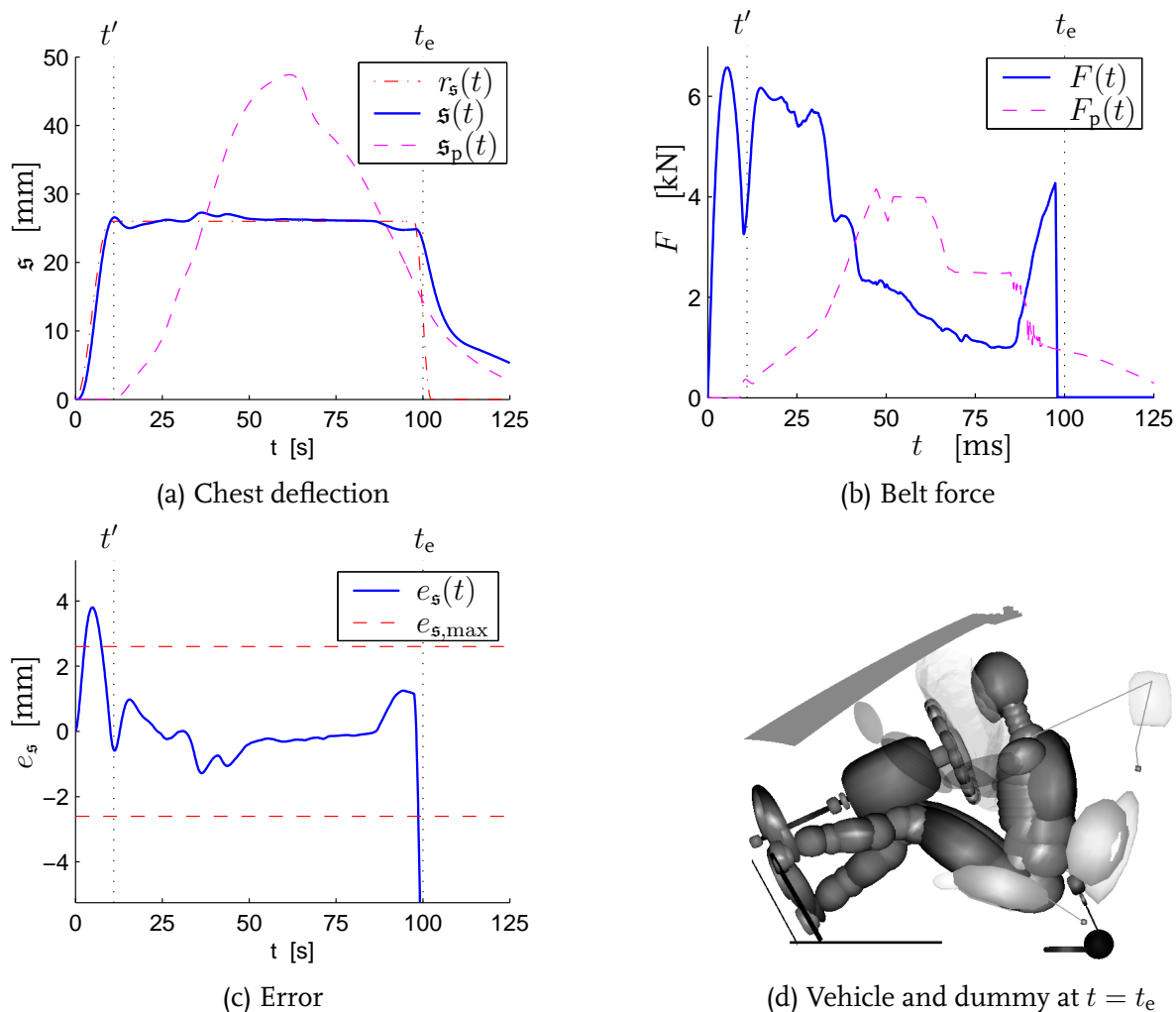


Figure 5.5 Results from the final closed loop simulation for evaluation purposes

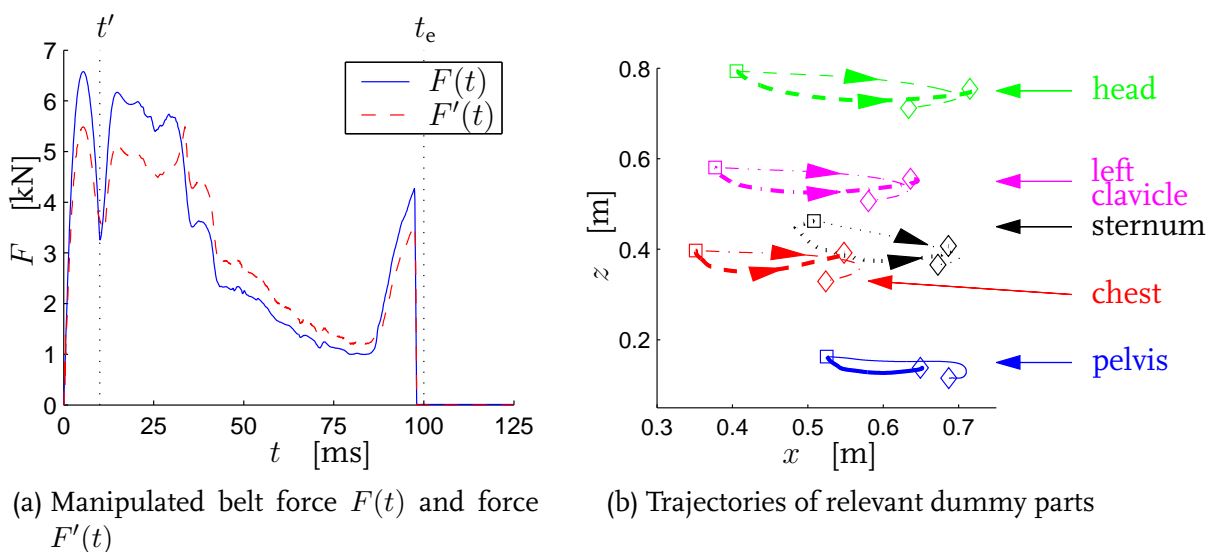


Figure 5.6 Forces in the belt and trajectories of relevant dummy parts

chest in the first phase of the crash. From that point of time, it moves parallel with the chest forward.

A comparison of these closed loop results with the results for the case that the chest acceleration is controlled by the belt force (Section 3.3), reveals interesting differences. The required belt force to control the chest deflection is similar in shape, compared to the required belt force to control the chest acceleration. However, in the time interval from the start of the crash until  $t \approx 40$  ms, the required belt force to control the chest deflection is significantly lower. Furthermore, this force increases over the time interval from  $t = 85$  ms until  $t = t_e$ , whereas that is not the case for the required belt force to control the chest acceleration.

A comparison of these results with the results for the case that the chest acceleration is controlled by the belt force, being imposed to bounds, see Section 3.5, reveals interesting similarities. The required belt force to control the chest deflection is more or less the same as the “clipped” belt force to control the chest acceleration, as can be seen in Figure 5.7. The level of the required belt force is the same, as well as the drop of the required belt force at  $t \approx 35$  ms and the increase for  $t \geq 85$  ms. In addition, the reduction of the measures for the risk of the injuries only differs slightly.

These observations suggest that control of the chest deflection is to be preferred. However, real world measurements of the chest deflection of an occupant are rather complicated.

#### 5.2.4 Control of the complete restraint system

For some purposes, the manipulation of the belt and the airbag may focus on the reduction of measures for the risk of injuries to the chest only. In such a case, one might want to use one restraint system component, e.g. the belt, to control the chest acceleration, and the other component, e.g. the airbag, for the chest deflection. Using first principles

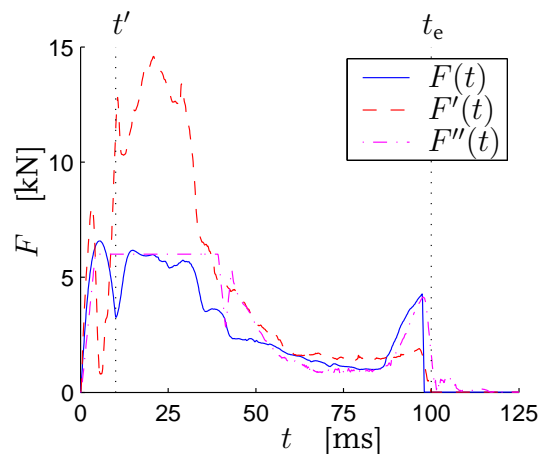


**Figure 5.7** Required belt force  $F(t)$  to control the chest deflection, the belt force  $F'(t)$  to control the chest acceleration, and the clipped belt force  $F''(t)$  to control the chest acceleration



of physics and the interaction analysis tools of Chapter 4, it will be made plausible that this leads to an ill-conditioned control problem.

A simple bio-mechanical analysis of the dummy thorax interacting with the restraint system already shows that the considered control problem is difficult. Under frontal impact conditions, the human thorax can be modelled by two rigid bodies, connected by a non-linear spring and damper [92, 111]. One body represents the mass of the ribs and a part of the thorax, and the other body the remaining part of the thoracic mass. The spring and damper represent the stiffness and viscous damping of the thorax. Other forces acting on these bodies are the forces exerted by the belt and the airbag. The forward acceleration of the thoracic body is the chest acceleration, whereas the relative displacement of the bodies is the chest deflection. Using this model, it is easily seen that the belt and the airbag simultaneously influence both the chest deflection and the chest acceleration. This interaction has to be taken into account in the design of controllers in the decentralized control configuration. As will be made plausible in the sequel, this is extremely difficult.

The same decentralized control configuration as in Chapter 4 is chosen. The transfer matrix  $\mathcal{H}(s)$  relates the perturbations  $\delta F$  and  $\delta A$  in the inputs to responses  $\delta\ddot{c}$  and  $\delta\mathbf{s}$  in the outputs:

$$\begin{bmatrix} \delta\ddot{c}(s) \\ \delta\mathbf{s}(s) \end{bmatrix} = \mathcal{H}(s) \cdot \begin{bmatrix} \delta F(s) \\ \delta A(s) \end{bmatrix} = \begin{bmatrix} \mathcal{H}_{11}(s) & \mathcal{H}_{12}(s) \\ \mathcal{H}_{21}(s) & \mathcal{H}_{22}(s) \end{bmatrix} \begin{bmatrix} \delta F(s) \\ \delta A(s) \end{bmatrix} \quad (5.3)$$

The transfer functions  $\mathcal{H}_{11}(s)$  and  $\mathcal{H}_{12}(s)$  have been obtained already in Section 2.4 and Section 5.2.1, respectively. To obtain the transfer functions  $\mathcal{H}_{21}(s)$  and  $\mathcal{H}_{22}(s)$ , the modelling strategy from Section 2.3 is applied. Using the results of the simulations from Section 2.5, satisfactorily accurate LTI models of second order are realized.

In Section 4.2, the concept of the Dynamic Relative Gain Array (*DRGA*) was introduced to investigate the interactions. For convenience, the definition of *DRGA* is given again, where the Laplace transform variable  $s = j\omega$  is omitted for brevity:

$$DRGA = \mathcal{H} \otimes \mathcal{H}^{-T} = \frac{1}{1 - \gamma} \begin{bmatrix} 1 & -\gamma \\ -\gamma & 1 \end{bmatrix} \quad \text{with} \quad \gamma = \frac{\mathcal{H}_{12} \cdot \mathcal{H}_{21}}{\mathcal{H}_{11} \cdot \mathcal{H}_{22}} \quad (5.4)$$

In Figure 5.8(a), the modulus  $|\gamma(j\omega)|$  is shown, whereas Figure 5.8(b) shows the modulus of  $|DRGA_{11}(j\omega)| = |1/(1 - \gamma(j\omega))|$ . It is seen that  $|\gamma(j\omega)|$  for frequencies less than 200 Hz is approximately 0 dB, meaning that a change in one of the manipulated inputs has a significant effects on both controlled outputs. For frequencies less than 200 Hz,  $|DRGA_{11}(j\omega)|$  is much greater than 0 dB, meaning that the outputs  $\delta\ddot{c}$  and  $\delta\mathbf{s}$  are difficult to control independently, due to strong interactions, whereas the performance of the closed loop system is sensitive to uncertainties, even when sophisticated control strategies are used [145]. In fact, this means that the to-be-controlled system is ill-conditioned.

Besides the earlier statement, these results confirm the conclusion from Chapter 4 that the belt system is the important component to reduce the risk of injuries to the dummy chest, whereas the airbag system is the important component to reduce the risk of injuries to the dummy head.

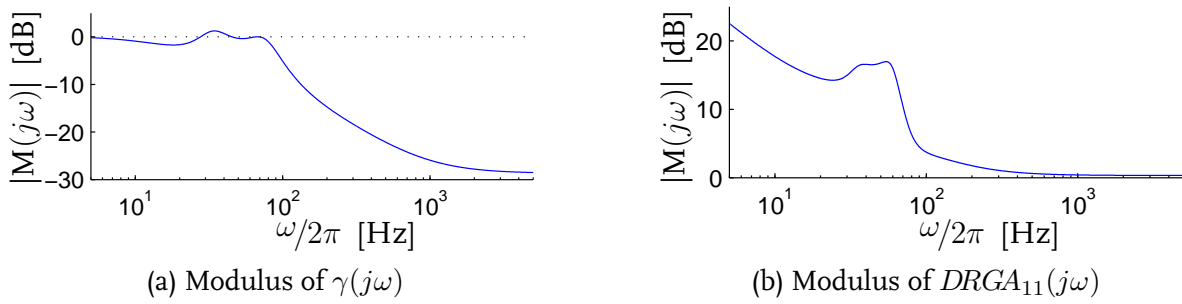


Figure 5.8 Moduli of  $\gamma(j\omega)$  and  $DRGA_{11}(j\omega)$

### 5.3 A small female dummy

In this section, the modelling strategy from Section 2.3 and the control design strategy from Section 4.3 are applied for the case that a small female crash dummy is the “driver”. The so-called HYBRID III 5th percentile crash dummy has a standing height of 1.52 m and a mass of 48 kg. Apart from two additional rigid bodies for the breasts, important differences between the numerical model of this dummy and the earlier used mid-size dummy are mass and geometry of the rigid bodies and characteristics of the springs and the dampers. The complex nonlinear models  $\mathcal{M}$  and  $\mathcal{M}_p$  are modified by replacing the mid-size dummy with the small dummy and adjusting the seat.

First, a simulation with the complex nonlinear model  $\mathcal{M}_p$  with the small dummy is performed. A detailed comparison of the obtained results with those for the mid-size dummy is beyond the scope of this section, but two relevant differences are mentioned. First, the small dummy contacts the airbag at  $t \approx 20$  ms due to the smaller distance to the steering wheel, whereas the mid-size dummy contacts the airbag at  $t \approx 35$  ms. Second, the dummy thorax rotates less around the pelvis, in comparison with the mid-size dummy. The measures of the risk of injuries do not differ, except for the maximum head acceleration, which is 10 % lower for the small dummy.

In this section, the objective is to control the chest acceleration and the head acceleration by the manipulation of the belt and the airbag. It is plausible that the basic assumptions and conclusions concerning the manipulation of the restraint system with the same control objective for the mid-size dummy in Chapter 4, also hold for the problem at hand. Hence, a decentralized control configuration is chosen, with the chest acceleration  $\ddot{c}$  controlled by the belt force  $F$  and the head acceleration  $\ddot{h}$  controlled by the vent size  $A$ . Furthermore, the design of a controller for the airbag and a controller for the belt is considered as a decoupled control design problem.

In the sequel, first LTI control design models are derived. After that, controllers are designed and reference signals are constructed. Finally, the controllers are implemented and evaluated in the closed loop system with the complex nonlinear model.

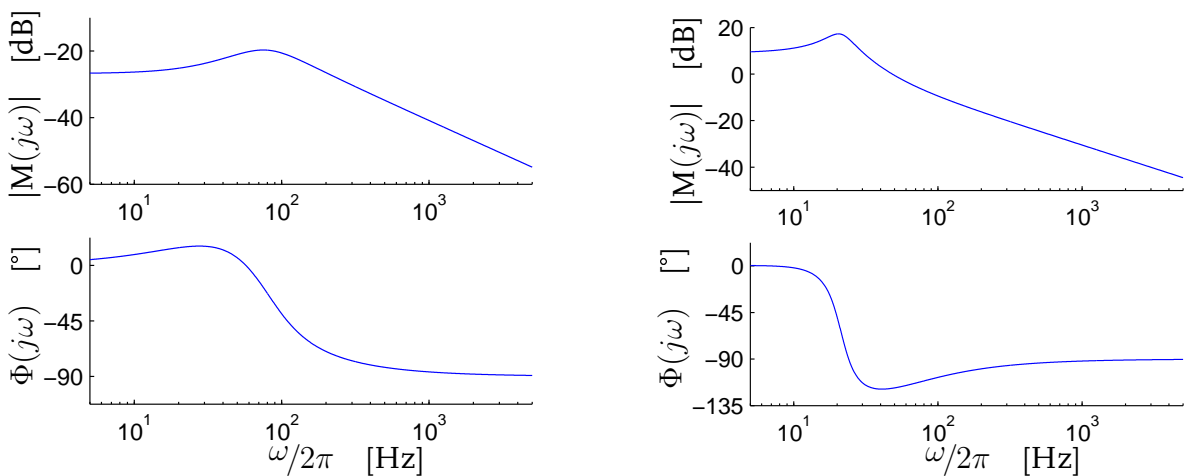
### 5.3.1 Modelling for control design

To realize LTI control design models for transfer from a perturbation  $\delta F$  in the belt force to the response  $\delta\ddot{c}$  in the chest acceleration and from a perturbation  $\delta A$  in the vent size to the response  $\delta\ddot{h}$  in the head acceleration, the operating points of Section 2.4 and of Section 2.5 can not be adopted here, since the interaction of the dummy with the restraint system components is different. For example, the slack in the belt system is removed at  $t \approx 18$  ms by the pre-tensioner, whereas the small dummy contacts the airbag at  $t \approx 20$  ms. Hence, the transfer from  $\delta F$  to  $\delta\ddot{c}$  can only be properly approximated at operating points at which the dummy is restrained by the belt and the airbag.

Results in Chapter 2 show that, for operating points at which the mid-size dummy is in contact with the airbag, the model parameters of the obtained LTI control design models only change slightly as a function of the operating point. Hence, approximation of the considered transfers at one operating point seems reasonable. Here, the operating point  $\tau = 40$  ms is chosen, since the airbag is then fully deployed. The results from Chapter 2 also show that the considered transfers can be reasonable approximated by LTI models, at least for small perturbations. Hence, one step size  $\Delta F$  and one step size  $\delta A$  are used. Here, it is chosen for sizes  $\Delta F = 50$  N and  $\Delta A = 1.7$  cm<sup>2</sup>, since these sizes will yield a (relatively) large signal-to-noise ratio of the responses.

Again, approximate realization is applied to arrive at second order LTI models. Figure 5.9(a) shows the Bode diagram of the transfer function from  $\delta F$  to  $\delta\ddot{c}$ , and Figure 5.9(b) shows the Bode diagram of the transfer function from  $\delta A$  to  $\delta\ddot{h}$ .

The Bode diagram of the transfer function from  $\delta F$  to  $\delta\ddot{c}$  for the small dummy does not differ considerably from the Bode diagrams of the same transfer function for the mid-size dummy for the points of application  $\tau_3 = 40$  ms and  $\tau_4 = 64$  ms. Apparently, differences between the dummies and the interaction of the dummies with the restraint system counterbalance each other, at least for small perturbations. The comparison of



(a) Bode diagram for the transfer function from  $\delta F$  to  $\delta\ddot{c}$

(b) Bode diagram for the transfer function from  $\delta A$  to  $\delta\ddot{h}$

**Figure 5.9** Bode diagram of the considered transfers at the operating point  $\tau = 40$  ms.

the Bode diagram from  $\delta A$  to  $\delta \ddot{h}$ , reveals a considerable difference. The modulus of the Bode diagram for the small dummy is approximately 10 dB lower over the full frequency range. Due to the differences in the interaction of the dummies with the restraint system it is difficult to explain the observed difference.

### 5.3.2 Control design

The control design criteria of Section 3.3 and 3.4 are adopted here. Obviously, the use of the controllers for the same control problem for the mid-size dummy is preferred. However, the Bode diagrams for the relevant transfers differ, meaning that the controllers have to be adapted.

For manipulation of the belt, the controller for the mid-size dummy, i.e. Equation 3.5 with  $P = 42$ , can be used as a starting point, since the Bode diagrams for the considered transfer are very similar. An appropriate controller for the belt is obtained by decreasing only the controller gain to  $P = 39$ .

For the airbag, the controller for the mid-size dummy has to be considerably changed, since the modulus of the Bode diagram of the transfer function from  $\delta A$  to  $\delta \ddot{h}$  for the small dummy, is significantly lower than that for the mid-size dummy. A drastic decrease of the controller gain makes the closed loop system more sensitive to (computational) noise in the head acceleration. At the expense of closed loop performance, the desired bandwidth is drastically reduced to 50 Hz to reduce the sensitivity, whereas a derivative controller part has to be added to achieve the desired phase margin. Aiming at a bandwidth of 50 Hz, the controller parameters are adapted until a controller is found such that at least the desired gain margin and the desired phase margin are satisfied. The moduli of the sensitivity function  $S(s)$  and the relevant part of the Nyquist plot of the open loop transfer function are shown in Figure 5.10. A gain margin of 9 and a phase margin of  $45^\circ$  are obtained. The bandwidth is 50 Hz.

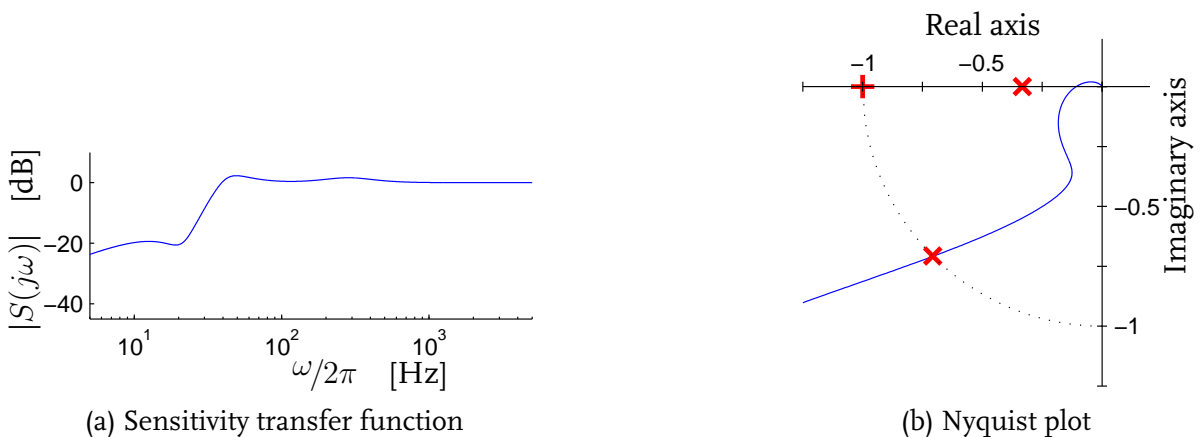


**Figure 5.10** Modulus of the sensitivity transfer function and Nyquist plot

### Reference signals

The shape of the reference signals of Chapter 4 are the starting point for the reference signal for the chest and the reference signal for the head acceleration for the small dummy:

$$r_{\ddot{c}}(t) = \begin{cases} r'_{\ddot{c}}/2 \cdot [1 - \cos(\frac{2\pi}{2 \cdot t'}t)] & 0 \leq t < t' \\ r'_{\ddot{c}} & t' \leq t < 97.5 \text{ ms} \\ r'_{\ddot{c}}/2 \cdot [1 + \cos(\frac{2\pi}{10}(t-97.5))] & 97.5 \text{ ms} \leq t < 102.5 \text{ ms} \\ 0 & 102.5 \text{ ms} \leq t \end{cases} \quad \text{for} \quad (5.5)$$

$$r_{\ddot{h}}(t) = \begin{cases} r'_{\ddot{h}}/2 \cdot [1 - \cos(\frac{2\pi}{10}t)] & t'' \leq t < t''+5 \text{ ms} \\ r'_{\ddot{h}} & t''+5 \text{ ms} \leq t < 97.5 \text{ ms} \\ r'_{\ddot{h}}/2 \cdot [1 + \cos(\frac{2\pi}{10}(t-97.5))] & 97.5 \text{ ms} \leq t < 102.5 \text{ ms} \\ 0 & 102.5 \text{ ms} \leq t \end{cases} \quad \text{for} \quad (5.6)$$

with  $t'$  and  $t''$  yet to-be-determined points of time and  $r'_{\ddot{c}}$  and  $r'_{\ddot{h}}$  yet to-be-determined constant values. The point of time  $t_e$  at which the crash is considered to be ended, is chosen again as  $t = t_e = 100$  ms. For the point of time  $t = t''$ , the point of time at which the dummy contacts the airbag is chosen, i.e.  $t = t'' = 25$  ms. To determine an appropriate value for  $t = t'$ , the vehicle deceleration is analyzed, shown in Figure 5.11(a) as the solid line. To prevent that the dummy is pushed through the seat, i.e. to prevent that the dummy chest decelerates stronger than the vehicle, a point of time  $t'$  at or shortly after  $t = 25$  ms seems reasonable. Here, it is chosen for  $t' = 25$  ms in order to reduce the maximum chest acceleration as much as possible.

Next, the constant values  $r'_{\ddot{c}}$  and  $r'_{\ddot{h}}$  are to be determined. Most importantly, contact of the head and chest with the steering wheel has to be prevented and the chest and head velocity at  $t = t_e$  have to be lower than the vehicle velocity. Since the vehicle acceleration is known, the velocity and displacement of the chest, the head, and of the vehicle can be roughly estimated by integration of  $r_{\ddot{c}}(t)$ ,  $r_{\ddot{h}}(t)$  and  $\ddot{x}_{\text{veh}}(t)$  with initial conditions  $r_{\ddot{c}}(t_0) = r_{\ddot{h}}(t'') = v_0$  and  $r_c(t_0) = r_h(t_0) = 0$ . Using trial-and-error, the values  $r'_{\ddot{c}}$  and  $r'_{\ddot{h}}$  are adapted until they are as low as possible and the bounds on the velocity and displacement are not violated. Unfortunately, the smallest distance of the chest and the head to the steering wheel is approximately 3 cm, meaning that neck injuries can not be prevented any further.

In Figure 5.11(a), the reference signals for the chest and head acceleration as well as the vehicle acceleration  $\ddot{x}_{\text{veh}}(t)$  are shown. Figure 5.11(b) shows the velocities and Figure 5.11(c) and 5.11(d) show the displacements of the chest and the head, respectively. In Figure 5.11(c),  $x_{\text{veh}}(t) + \ell_c$  has to be interpreted as the displacement of the steering wheel and  $x_{\text{veh}}(T)$  has to be interpreted as the displacement of the back of the seat. In Figure 5.11(d),  $\ell_h$  denote the initial distance between the steering wheel and the front of the chest and between the steering wheel and the front of the head, respectively.

The reference signals suggest a reduction of more than 50 % of the maximum absolute chest and head acceleration, compared to their original value. These reductions will be achieved if the reference signals are accurately followed and contacts with the steering wheel are indeed prevented. That can only be investigated by a simulation of the closed loop system with the complex nonlinear model, which is done in the following section.

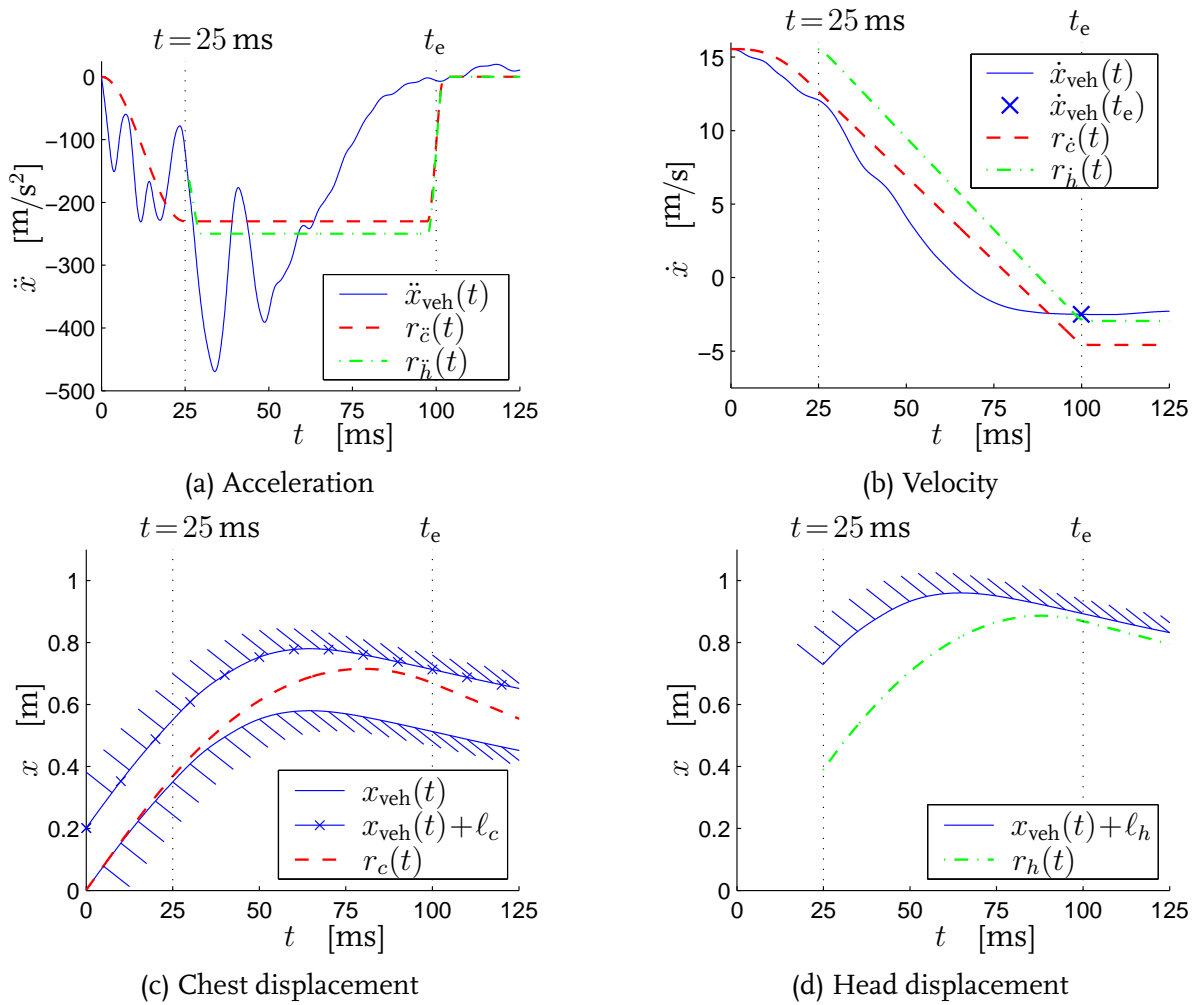


**Figure 5.11** Reference signals for the chest acceleration and the head acceleration, as well as the corresponding velocities and displacements

### 5.3.3 Evaluation

The evaluation is based on a simulation with the closed loop with the complex nonlinear  $\mathcal{M}$  with the small dummy. In Figure 5.12(a-f), relevant results of the simulation are shown. In these figures, also the results for the passive restraint system, are shown. The dummy does not contact the steering wheel, as can be seen in Figure 5.12(g).

The results in Figure 5.12(a-f) show that the closed loop with the complex nonlinear model with the small dummy is stable. Only for  $t = 25$  ms until  $t = 40$  ms, the vent size strongly oscillates due to (computational) noise, although the bandwidth of the controller for the airbag only is 50 Hz. Nevertheless, the specifications on the closed loop behavior are satisfied. The reference signals are followed fast enough and over the time interval that the controllers are enabled, the maximum allowable error is hardly violated. A reduction of the maximum chest and head acceleration to approximately 48 % and 51 % of their original value is obtained, whereas the maximum chest deflection has reduced to 67 % of its original value (not shown).

A comparison of these closed loop results with those for the same control problem with

the mid-size dummy, see Figure 4.10, shows some interesting differences and similarities. The required belt forces to control the chest acceleration are quite similar in shape. However, for the mid-size dummy, the required belt force is significantly higher; from a 6 kN difference at  $t \approx 30$  ms to a 1 kN difference at  $t \approx 75$  ms. The required size of the vent to control the head acceleration is larger for the small dummy than for the mid-size dummy. Both observations may be explained by, amongst others, differences in the mass of the relevant body parts.

A comparison of these controllers with those for the same control problem with the mid-size dummy, shows interesting differences. The controllers to control the chest acceleration differ only in gain, suggesting that the controller gain depends on dummy mass. The controllers to control the head acceleration differ in gain and in structure, due to the sensitivity of the closed loop system to (computational) noise for the case with the small dummy. This observations suggest that for real world active restraint systems, an adaptation of the controller structure and the controller parameters is required, whereas for the design of modes of operation different controllers are to be designed.

## 5.4 Adaptive restraint systems

In the previous sections and chapters, the focus was the manipulation of restraint system components. In this section, the focus is on the interpretation of closed loop results in the light of development of real world adaptive restraint system components. The closed loop simulations, with the chest and the head acceleration as the controlled variables, are considered. More specifically, results of Section 4.3, concerning a mid-size male dummy, and of Section 5.3, concerning a small female dummy, are investigated.

Figure 5.13(a) shows the vent size  $A$  as a function of time. The time histories have been filtered in a causal and anti-causal manner using a second order, digital Butterworth filter, with a cut-off frequency of 200 Hz to show only the essential characteristics of the required vent size. Figure 5.13(b) shows the belt force  $F$  as a function of the belt outlet  $x$ , being the length of belt, pulled out the load limiter, see Section 2.2. The points of maximum force and minimum belt outlet, represent the point of time at which the dummy contacts the airbag and the friction in the contact of the belt with the D-ring changes sign.

In the case that feedback is not applied, it is clear that adaptive components are necessary to achieve such reductions, since the results for the small dummy and the mid-size dummy differ significantly. Nevertheless, the vent size  $A(t)$  for both cases show similarities. The vent has to be quickly opened after the dummy contacts the airbag, and from  $t \approx 50$  ms, it has to be partially closed. The deformation characteristics of the load limiter for both cases show strong similarities. For both cases, the belt is retracted with an almost linear relation between force and belt outlet, followed by a steep decrease of the belt force and yielding of the belt. The amplitude of the deformation characteristics of the load limiters can be almost adapted linearly for the specific dummy.

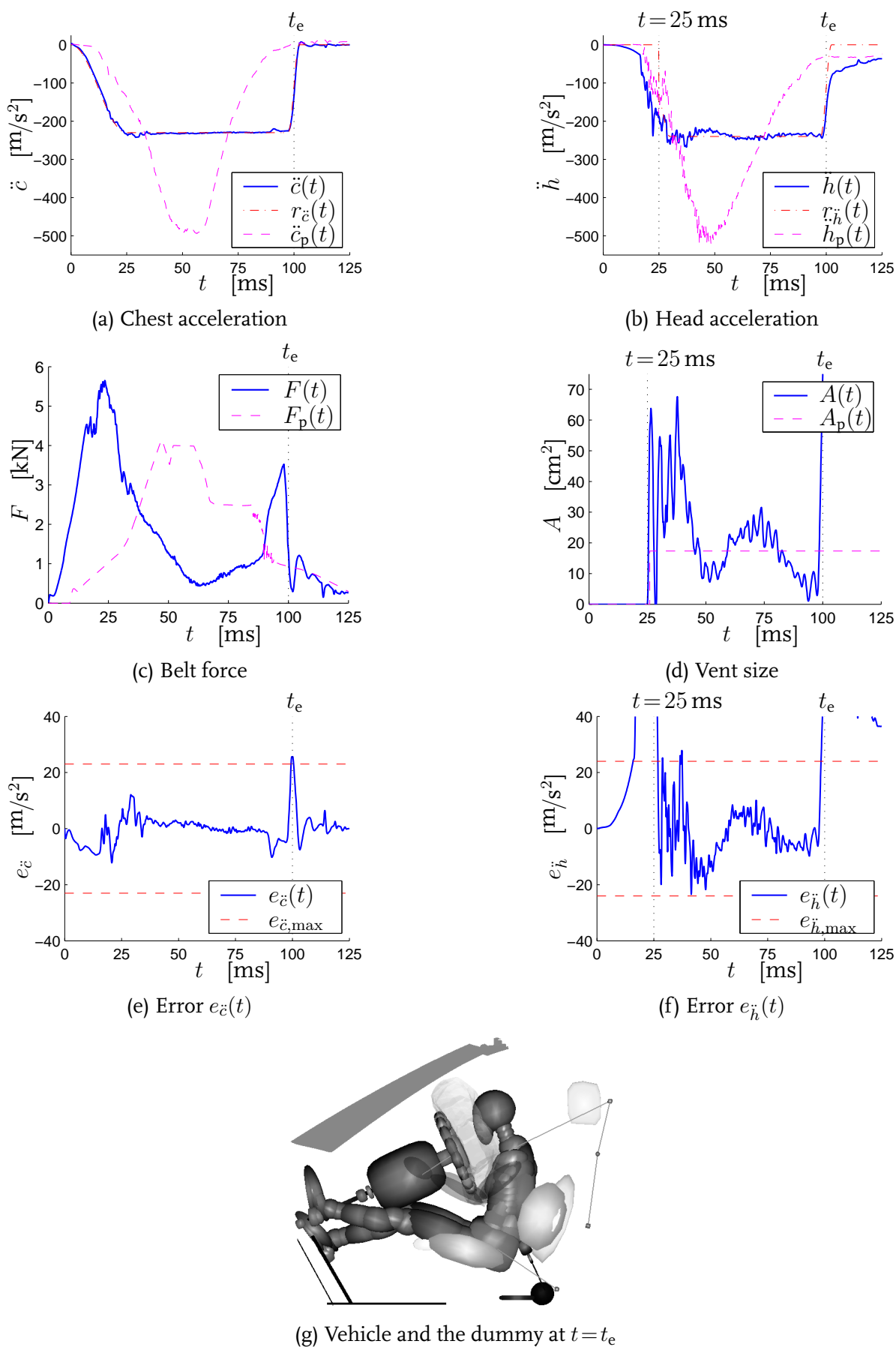
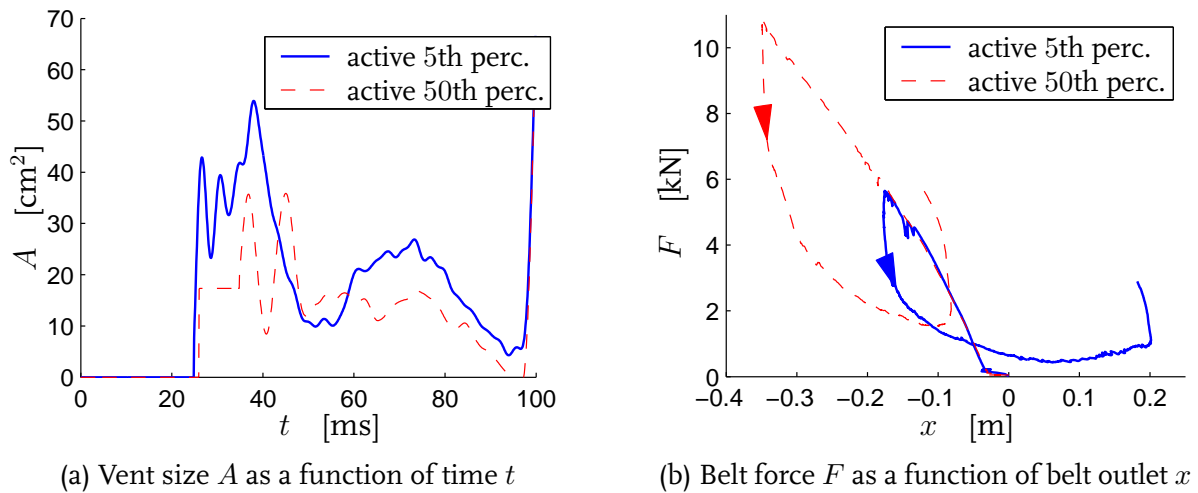


Figure 5.12 Results of the closed loop simulation for evaluation purposes.





**Figure 5.13** Closed loop results, relevant for adaptive restraint systems

## 5.5 A first investigation towards a new control strategy

In the previous sections and chapters, the control objective is to follow a reference signal. In this section, a first investigation towards a new control strategy is presented. This strategy does not require the a priori definition of a reference signal. In addition, violation of bounds on the inputs and the outputs can be anticipated. The new control strategy is a version of Model Predictive Control (MPC) [93, 107, 129]. The quintessence of MPC comes down to the formulation of the control objective in terms of an optimization problem, solved at regular time intervals during the crash. The objective of the optimization is to determine a sequence of optimal, future inputs, by the minimization of a cost function  $J$ , subject to bounds on future inputs and outputs. Only the first part of this sequence is actually implemented during a short time interval, after which the procedure is repeated with new data.

Optimization is performed in discrete-time and typically consists of two successive steps. First, the relevant outputs are predicted with an internal prediction model, given a rough estimate of the sequence of future inputs. Second, these estimates are used as the starting point of the optimization of the future inputs, using an internal optimization model.

The internal prediction and optimization model preferably are as accurate as possible and easy-to-compute, but not necessarily the same [158]. In fact, MPC can be applied using a nonlinear prediction model in combination with a linear optimization model. In that case, a starting point of the optimization of the future inputs is determined, according to the prediction model, accounting for nonlinear phenomena in the dynamic behavior of the to-be-controlled system. The linear optimization model is then used to optimize the sequence of inputs, relative to this starting point. Examples of the application of MPC with different prediction and optimization models are given in [125, 126, 136]. For our purposes, such an approach is attractive, since the (global) dynamic behavior

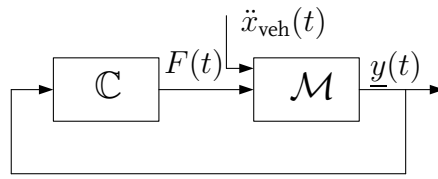


**Figure 5.14** Closed loop system with the model  $\mathcal{M}$  and the MPC control algorithm  $\mathbb{C}$

of the dummy interacting with the restraint system components is nonlinear, but the (local) dynamic behavior may be considered linear for small perturbations. Besides that, nonlinear optimization is time-consuming and thus unattractive. Hence, the idea is to investigate whether that approach is successful for the problem at hand.

The focus is on the reduction of the maximum chest acceleration by the manipulation of the belt force. The bounds on the dummy displacement and velocity, discussed in Section 3.3, as well as the bounds on the belt force, discussed in Section 3.5, are adopted. In this first investigation, the case in which the dummy is restrained by the belt only, is considered. The airbag is not taken into account, so the complex nonlinear model is modified by removing the finite element model of the airbag. In Figure 5.14, the closed loop system with the complex nonlinear model  $\mathcal{M}$  without the airbag and the MPC control algorithm  $\mathbb{C}$  is depicted. In this figure,  $F(t)$  is the belt force, and  $\underline{y}(t)$  is the vector containing relevant outputs of the complex nonlinear model.

In the sequel, first the nonlinear model for prediction purposes and the linear model for optimization purposes are introduced. After that, the MPC control algorithm  $\mathbb{C}$  is presented. Finally, the control algorithm is implemented and evaluated in the closed loop system with the complex nonlinear model without the airbag.

### 5.5.1 Modelling

Obviously, the complex nonlinear model  $\mathcal{M}$  without the airbag is the most accurate prediction model, but not suitable since it is far too time-consuming. Instead, an easy-to-compute model is desired. To arrive at such a model, the theoretical modelling approach using first principles of physics is followed.

Some relevant phenomena in the dynamic behavior of the dummy, interacting with the belt, were observed in previous sections and chapters. First, the friction of the belt with the D-ring significantly influences the force applied on the dummy thorax. Second, the knees do not contact the knee bolsters. Furthermore, it is known [39, 94] that the rotation of the dummy thorax with respect to the pelvis and the rotation of the head with respect to the neck are larger, if the airbag is removed.

A simple, two-dimensional, lumped-mass model that describes these phenomena is shown in Figure 5.15. It consists of four rigid bodies. The safety cage is represented by body  $b_1$  with a translational degree of freedom in the global  $x$ -direction. The D-ring is rigidly connected to the safety cage. Body  $b_2$  represents the belt force actuator and can

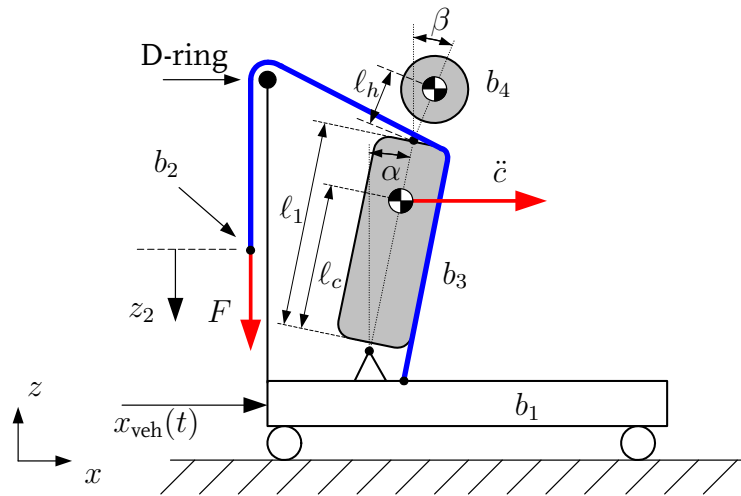


**Figure 5.15** Simple, two-dimensional model for prediction purposes

translate only in the local  $z$ -direction with respect to body  $b_1$ . The dummy thorax, represented by body  $b_3$ , can only rotate with respect to body  $b_1$  around the local  $y$ -axis. The dummy head is represented by body  $b_4$ . It is connected to body  $b_3$ , such that its only relative degree of freedom is the rotation  $\beta$  around the local  $y$ -axis. The belt is modelled as a series structure of three massless, one-dimensional elements of a spring parallel with a damper. One end of the structure is connected to the actuator, i.e. body  $b_2$ . From that point, the structure goes through the D-ring, over the top of body  $b_3$ , to body  $b_1$ , where the other end is attached. Contact with body  $b_2$  and the D-ring is defined for the nodal points of the belt model. A force  $F$ , representing the belt force, can be applied body to  $b_2$ .

The numerical model of the HYBRID III 50th percentile dummy is used to choose appropriate masses  $m_3$  and  $m_4$  of the bodies  $b_3$  and  $b_4$ , locations of the centers of gravity  $\ell_c$  and  $\ell_h$ , as well as the height  $\ell_1$  of body  $b_3$ , yielding  $m_3 = 40$  kg,  $m_4 = 4.5$  kg,  $\ell_c = 0.30$  m,  $\ell_h = 0.22$  m and  $\ell_1 = 0.5$  m. The forward, horizontal acceleration of the center of gravity of body  $b_3$  is taken as the measure for the chest acceleration  $\ddot{c}$ . Characteristics of the belt elements, friction and stiffness parameters are taken from the complex nonlinear model  $\mathcal{M}$ . The displacement of the safety cage  $x_{\text{veh}}(t)$  is prescribed to body  $b_1$  in the forward  $x$ -direction.

To evaluate the model quality, the predicted chest acceleration is compared with the chest acceleration, according to the complex nonlinear model  $\mathcal{M}$  without the airbag. For that purpose, the simulation of Section 3.5 is repeated using the complex nonlinear model without the airbag. In this simulation, a low order feedback controller controls the chest acceleration by manipulation of the belt force, being imposed to the bounds  $F_{\text{max}} = 6$  kN and  $|\dot{F}_{\text{max}}| = 1.5$  kN/ms. In Figure 5.16, the required belt force  $F(t)$  and the chest acceleration  $\ddot{c}(t)$  according to the complex nonlinear model, are shown by solid lines.

The initial conditions for the prediction model are chosen such that at  $t = t_0 = 0$ , the rotation of bodies  $b_3$  and  $b_4$  resemble that of the dummy thorax and the head, according to the complex nonlinear model  $\mathcal{M}$ .

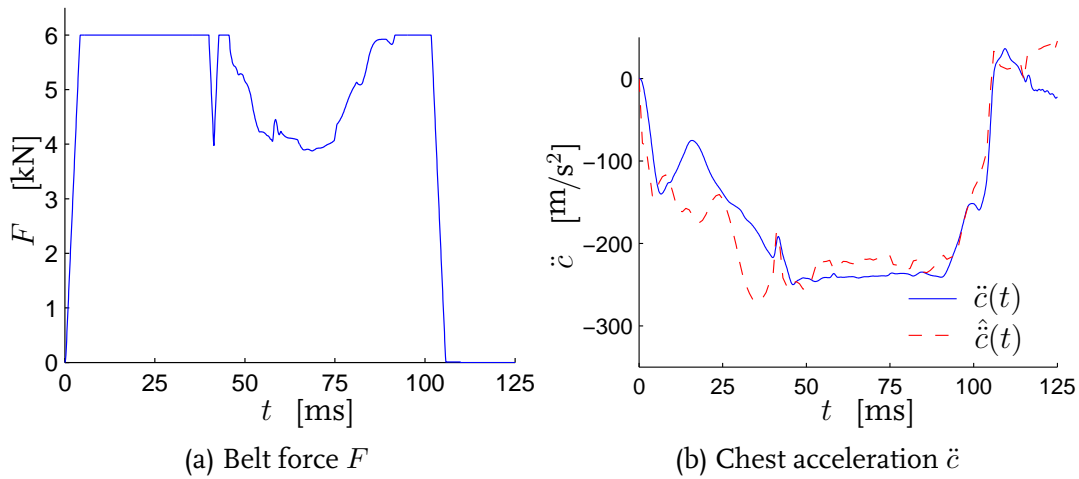


**Figure 5.16** Results for the evaluation of the prediction model

Adopting the belt force in Figure 5.16(a) as the to-be-applied force to body  $b_2$ , the chest acceleration according to the prediction model is determined. The predicted chest acceleration  $\hat{c}(t)$  is shown in Figure 5.16(b) by the dashed line. For  $t = 0$  until  $t \approx 35$  ms, the prediction of the chest acceleration is moderately accurate. This may be explained by non-modelled phenomena like compression of the dummy thorax. For  $t > 35$  ms, the chest acceleration is predicted fairly accurate. Therefore, it is assumed that the most important phenomena of the dynamic behavior of the dummy, interacting with the belt are accounted for.

In the previous chapters, it has been made plausible that the relevant dynamic behavior of the belt interacting with the dummy may be approximated by LTI models, at least for small perturbations. Hence, the LTI control design models from a small perturbation in the belt force to the response in the chest acceleration are used for optimization purposes. More specifically, the LTI control design model for the (open loop) operating point  $\tau = 25$  ms of the complex nonlinear model is used.

### 5.5.2 Design of the control algorithm

At regular time intervals, the MPC control algorithm  $\mathbb{C}$  performs two successive steps to arrive at the optimal sequence of the future belt force. First, the relevant outputs, like the chest acceleration, velocity and displacement, are predicted, according to the simple nonlinear prediction model with a rough estimate of the future belt force as its input. Second, the chest acceleration is minimized by optimizing the sequence of the future belt force, relative to the starting point, obtained from the simple nonlinear prediction model. The LTI control design model is used for the optimization.

For prediction purposes, a constant belt force is chosen as the mentioned rough estimate  $\{F\}_k^{k+N}$ , with  $N$  the length of the prediction horizon in discrete-time samples. More specifically, the belt force is assumed to remain constant for  $t \geq k$ , i.e.  $\{F\}_k^{k+N} = F_k$ . Initial conditions for the prediction model are determined from measurements of the

complex nonlinear model at time  $t = k$ . Using the estimate of the future belt force, the chest acceleration, velocity and displacement is predicted, according to the simple nonlinear prediction model. The predicted sequences are used as the starting point for optimization at  $t = k$ .

Cost functions, suitable for different optimization goals are discussed in [57, 107, 129]. Here, it is chosen for the standard cost function, which boils down to:

$$J_k(\Delta\ddot{c}, \Delta F) = \sum_{j=0}^N (\hat{c}(k+j|k) + \Delta\ddot{c}(k+j|k))^2 + \lambda \sum_{j=1}^{N_c} (\hat{F}(k+j|k) + \Delta F(k+j|k))^2, \quad (5.7)$$

with  $\ddot{c}_k = \hat{c}_k + \Delta\ddot{c}_k$  and  $F_k = \hat{F}_k + \Delta F_k$ ,  $N_c$  the length of the control horizon in discrete-time samples and  $\lambda$  a weighting parameter. The first and second right term of this equation represents the control performance and the control effort, respectively.

The objective of the optimization problem is then formulated as:

$$F_{\text{opt}} = \arg \min_{\Delta F} J_k(\Delta\ddot{c}, \Delta F), \quad (5.8)$$

subject to the bounds on the belt force and the motion of the dummy, formulated in discrete-time samples as:

$$\begin{aligned} F(k+j|k) &\leq 6 \text{ kN} \\ F(k+j|k) - F(k+j-1|k) &\leq 1.5 \text{ kN} \\ c(k+j|k) &\geq x_{\text{veh}}(k) \\ c(k+j|k) &\leq x_{\text{veh}}(k) + \ell_0 \\ \dot{c}(k+j=100|k) &\leq \dot{x}_{\text{veh}}(k+j=100|k) \end{aligned} \quad (5.9)$$

In line with previous choices for the point of time  $t_e$  at which the crash is considered to be ended,  $t_e = 100$  ms is chosen. Furthermore, a sample time of 1 ms is chosen.

Typically, the weighting parameter, the length of the prediction horizon  $N$  and the control horizon  $N_c$  are based on the behavior of the to-be-controlled system [18, 148, 171]. For the problem at hand, violations of bounds are expected in the last phase of the crash, but they have to be anticipated as early as possible. Therefore, the length of the prediction and control horizon are to be as long as possible. The length  $N$  of the prediction horizon is  $N = 100 - k$  at  $t = k$ . For stability of the closed loop system and to achieve a smooth sequence of the optimized belt force, the control horizon has to be shorter than the prediction horizon [18]. The longest possible control horizon  $N_c$  is  $N_c = N - 1 = 100 - k - 1$  at  $t = k$ . For  $N_c < k \leq N$ , the belt force is kept constant, i.e.  $\{F\}_{k+N_c}^{k+N} = F_{k+N_c}$ . The weighting parameter  $\lambda$  is chosen as small as possible, since the level of the belt force is not of major importance. Considering the order of magnitude of the belt force and the chest acceleration, it chosen here for  $\lambda = 1 \cdot 10^{-4}$ , meaning that the control effort is approximately 1 % of the total cost.

### 5.5.3 Evaluation

The evaluation of the MPC control algorithm  $\mathbb{C}$  is based on a simulation with the closed loop system including the complex nonlinear model without the airbag. In Figure 5.17,

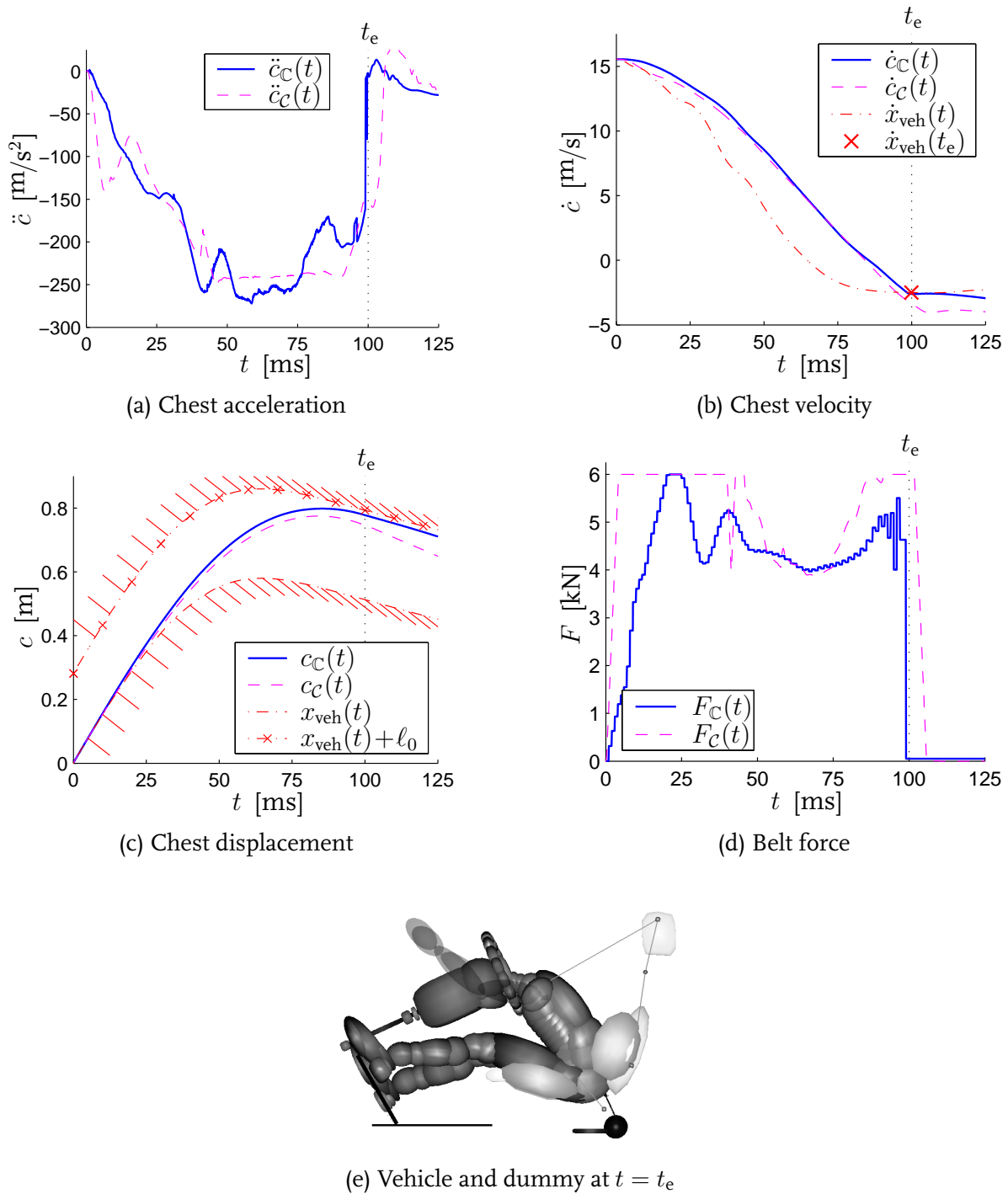


**Figure 5.17** Relevant results for evaluation purposes of the MPC control algorithm  $\mathbb{C}$

some relevant results of this simulation are shown. These results are indicated with lower index “C”. The lower index “C” refers to the results of the simulation of Section 5.5.1.

The results in Figure 5.17 suggest that the closed loop with the MPC control algorithm  $\mathbb{C}$  is stable. The results in Figure 5.17(b-c) indicate that the bounds on the chest velocity and displacement are not violated. However, the dummy chest does contact the steering wheel, as can be observed in Figure 5.17(e). This discrepancy may be explained by the measurement and prediction of the chest displacement in the horizontal plane, whereas

the dummy chest does rotate. Nevertheless, these results are hopeful and indicate that the application of MPC is promising for the case that more accurate prediction and/or optimization models are used.

# Conclusions and Recommendations

*The main ideas, strategies and observations presented in this thesis are discussed. In retrospect, the initial hypothesis concerning active restraint systems is evaluated. Finally, recommendations for future research are given.*

## 6.1 Introduction

In this thesis, the use of active restraint systems to reduce the risk of severe or fatal injuries to vehicle occupants, subjected to a frontal crash, is investigated. Frontal crashes cover the greater part of crashes, resulting in severe or fatal injuries to vehicle occupants. Numerical simulation of frontal crash tests is a powerful tool to evaluate the risk of injuries during the development of restraint systems. In this thesis, the maximum chest and head acceleration were chosen as the measures for the risk of injuries. The mass flow into the airbag and the size of the vent were chosen to manipulate the airbag system, whereas the belt force was chosen to manipulate the belt system.

In Section 1.5, the basic hypothesis was formulated as:

- **active restraint systems can reduce the risk of physical injuries.**

The research objectives for this thesis were formulated as:

- Develop a strategy to reveal the dynamic behavior of the dummy, interacting with the belt and the airbag, as far as this behavior is relevant for control design purposes.
- Develop a strategy to design controllers to manipulate the belt and the airbag.
- Assess the proposed strategies for cases of different dummies and measures for the risk of injury.

Development of sensors and actuators for active restraint system components was not a topic of this research. Idealized actuators to manipulate the belt and the airbag and idealized sensors to measure the occupant injuries were taken for granted. It was assumed that the vehicle acceleration over the full crash duration is known at the start of the crash.



In Section 6.2, the strategies and their application are discussed. Conclusions will be formulated in Section 6.3 and recommendations for future research will be given in Section 6.4.

## 6.2 Discussion

In this section, the relevant results presented in this thesis are discussed, focussing on the modelling strategy, the control design strategy and the design expedient, successively.

### 6.2.1 Modelling for control design

The dynamic behavior of the complex nonlinear model, as far as it is relevant for control design purposes, is modelled by LTI models, describing the local dynamic behavior at several operating points. To arrive at an LTI model, approximate realization is applied on the results from crash test simulations, in which a small, stepwise perturbation is added to an input of the restraint system components.

Approximate realization accurately determines an LTI model from the output response over a finite time interval. For nonlinear models with non-smooth phenomena, it is difficult to determine the length of this interval, because the dynamic properties of this model may change during this interval. Furthermore, the choice of appropriate operating points at which a perturbation is to be added is difficult. Considering these aspects, the obtained LTI control design models have to be used with care.

The dynamic behavior of the dummy, interacting with the belt has been approximated at both open loop operating points and at closed loop operating points of the complex nonlinear model. Comparison of the obtained LTI models revealed that differences between the models for quite different operating points are fairly small. Furthermore, controllers that are designed using the LTI control design models for open loop operating points, can enforce the desired behavior of the closed loop system with the complex nonlinear model. These observations indicate that for the considered class of relatively simple, low order controllers, LTI models for open loop operating points of the complex nonlinear model are sufficiently accurate. For highly complex and high bandwidth controllers, these LTI models may be not accurate enough. These observations also indicate that the dynamic behavior, relevant for control design purposes, is more or less smooth and linear.

The dynamic behavior of the dummy, interacting with the belt and the airbag has been approximated for the case of a mid-size male dummy and for the case of a small female dummy. Comparison of the obtained LTI models revealed that differences exist, indicating that the relevant dynamic behavior differs as a function of mass and/or size of the dummy. Furthermore, it is emphasized that only one combination of a (frontal) crash test and a vehicle has been considered.

### 6.2.2 Control design

Feedback tracking controllers for the active restraint system components are designed with the loopshaping technique, using the realized LTI control design models. A fairly straightforward, i.e. heuristic approach is applied to determine reference signals.

The closed loop results show that low-order controllers can enforce the desired behavior of the closed loop with the complex nonlinear model. The designed controllers consist of a proportional part combined with an integral part and, if necessary for stability purposes, a derivative part. In some cases, a low pass filter is added for signal processing purposes. A comparison of controllers for the same control objective but different dummies revealed that controller parameters has to be slightly adapted, and in one case, the controller structure has to be changed, too. This means that the controllers for active restraint system components will have to be (slightly) adapted as a function of mass, and/or size.

The proposed control design strategy has been applied to arrive at controllers for the most important injury measures, being the chest acceleration, the head acceleration and the chest deflection. Comparison of the results for control of the chest deflection and control of the chest acceleration has shown that control of the chest deflection is preferred.

The proposed approaches to determine reference signals are simple and fairly straightforward, but effective. Except for the case that the head acceleration was controlled by the mass flow, reference signals could be determined, yielding a reduction of the controlled measures of at least 40 % in comparison with the passive restraint system. This implies an equivalent reduction of the risk of injuries for the considered body parts. For the cases where the chest and the head acceleration were controlled simultaneously, appropriate reference signals were determined for the chest and the head acceleration. By taking into account the acceleration of the head, relative to the chest, also the risk of neck injuries was reduced as much as possible. Unfortunately, a reference signal for the chest deflection had to be determined iteratively, using the closed loop with the complex nonlinear model. Furthermore, the acceleration of the safety cage over the full duration of the crash has to be a priori known, imposing limits on the suitability of the proposed way to determine reference signals for real world applications.

Interaction analysis has shown that the design of a controller for the belt and of a controller for the airbag can be decoupled. However, the risk of injuries to the neck has to be taken into account. As was expected from [56, 75], the belt system is the important component for the thorax, whereas the airbag system is the important component for the head. The closed loop results for the cases in which the head acceleration and the chest acceleration were controlled, indicate that manipulation of the vent size is sufficient to control the head acceleration, at least for the considered combination of the vehicle, the restraint system and the crash.

### 6.2.3 Design expedient

The proposed modelling and control design strategy have been applied to different cases to show their suitability as a design expedient. These cases concern the control of the chest acceleration and the head acceleration of the mid-size male and small female dummy, as well as the control of the chest deflection of the mid-size male dummy.

The proposed modelling and control design strategies have shown to be generalizable to various cases. Besides that, the number of simulations to arrive at appropriate feedback controllers is drastically lower than that required for optimization purposes. However, some issues remain difficult, especially concerning the modelling strategy. These issues are already discussed. Concerning the control design strategy, only the determination of a reference signal is a difficult issue, especially if the chest and the head acceleration are to be controlled simultaneously. Besides that, the results of these approaches can not be straightforwardly generalized. This means that appropriate LTI control design models and appropriate controllers have to be determined for each of the considered cases. Nevertheless, the proposed strategies can be (and are being) used as a design expedient.

## 6.3 Conclusions

The main conclusions of this thesis can be formulated as:

- active restraint systems can drastically reduce the risk of severe or fatal injuries, compared to passive restraint systems,
- the developed strategies are suitable for use as a design expedient,
- data-based linearization is effective to reveal the dynamic behavior, as far as it is relevant for feedback control design purposes,
- dynamic behavior of the dummy, interacting with the belt and the airbag can be considered linear, at least for control design purposes,
- feedback control is extremely effective as the basis for active restraint systems,
- feedback controllers of low order can successfully manipulate the belt and the airbag,
- design of controllers for the belt and for the airbag can be treated as a decoupled control design problem, at least for the considered combination of vehicle, restraint system and crash,
- manipulation of the vent size is sufficient to manipulate the airbag, at least for the considered combination of vehicle, restraint system and crash,
- for different dummies, the controller structure differs, as well as the controller parameters.

## 6.4 Recommendations

One of the topics of this thesis is modelling for control design purposes. The realized LTI control design models give some insight into the local dynamic behavior of the complex nonlinear model. It is not yet fully understood why these models are so well suited for the design of feedback controllers, since the complex nonlinear model is thought to be highly nonlinear, non-smooth and time-invariant. For a better understanding, a manageable model that describes the relevant aspects of the dummy, the restraint system, the vehicle and their interactions with an acceptable accuracy would be very useful. Such a model of reduced complexity may also be beneficial for other control goals, as will be made clear in the following. If only the belt system is considered, manageable models may be obtained rather easily. However, when the airbag is considered also, this is not the case anymore.

To arrive at a manageable model, two approaches are distinguished, i.e. the theoretical approach, using first principles of physics to describe the real world system, and the experimental approach, using experimental results to determine a relationship between variables of the real world system. The theoretical approach is preferred, since it can result in a physical understanding of relevant phenomena in the investigated system. It is not clear yet, how state-of-the-art complex models can be simplified and reduced when only the relevant physical phenomena are to be taken into account. A possible approach may be the use of 2D models, e.g. [54, 76, 118, 128], as commonly used in the early times of crash simulation.

Feedforward controllers were not a topic of this thesis. For some cases, feedforward control techniques are attractive. To be able to properly apply feedforward techniques, manageable, sufficiently accurate models are required.

Reference signals were constructed, only roughly taking into account the relation of the controlled injury measure with other injury measures. If manageable, sufficiently accurate models are available, a new strategy to construct reference signals can be developed, taking into account the essential characteristics of the vehicle, the occupant and the crash. A first, rudimentary application of Model Predictive Control shows promising results. If manageable, sufficiently accurate models are available, the application of Model Predictive Control is very attractive, since one or more injuries can be controlled, violations of variables of the restraint system can be anticipated and a reference signal is not required. In addition, the application of an extremely attractive predictive control technique, based on the so-called reference governor philosophy [12, 13, 14, 55], will then be possible. Its main idea is to separate the stabilization problem from the constraint problem. At regular time intervals, bounds are enforced by manipulation of the reference signal by the reference governor. Conventional linear controllers, like the controllers presented in this thesis, can then be used to force the controlled output to follow the generated reference signal.

One of the important aspects of the developed modelling and control design strategies is that it should be possible to use them as a design expedient. It has been shown that the strategies can be applied successfully to different control problems. A next step would

be to use the proposed strategies to define the modes of operation of real world restraint systems components. Based on an investigation of the characteristics of occupants and crashes, representative combinations occupants and crashes can be determined. For each of these combinations, the modelling and control design strategy should be applied. Next, closed loop simulations are to be performed, in which the belt and/or the airbag are manipulated. Based on the results of these simulations, the most appropriate mode of operation for the restraint system components for each combination can be determined. Next, aspects like cost, comfort, mass, durability and size are to be accounted for to arrive at a (limited) set of realizable modes of operation.

State-of-the-art restraint systems are adaptive, in the sense that they have different modes of operation, chosen at the start of the crash. Nevertheless, these modes of operation are still passive modes. For example, the point of time at which the inflators of the airbag are triggered can be adapted, but if chosen, the mass flow generated by the inflators can not be changed. A next step would therefore be the development of real world restraint system components that can actually imitate the behavior of active restraint system components. For example, an airbag system can be developed with several small vents in the bag that can be opened or closed to let gas flow out of the airbag, and several small vents in the inflators to prevent gas to flow into the airbag.

Future real world active restraint systems probably will consist of several sophisticated sensors and actuators. Some of these devices concern the pre-crash situation, i.e. the time (just) before the crash takes place. Pre-crash sensors should predict sufficiently accurate some of the relevant crash characteristics, like impact velocity, impact angle and offset [108, 157]. Occupant characteristics like mass and seating position can be estimated when the occupant gets in, shortly thereafter, or continuously [53]. Based on this information on the crash and the occupant and the information of the compartment geometry and injury tolerance levels, a reference signal for the relevant occupant variables can be determined. Furthermore, the seat can be adjusted [141], the belt can be tightened by a pre-crash belt pre-tensioner [17] and the inflators of the airbag can be triggered.

Other sensing devices have to provide the information to manipulate the restraint system components during the crash. Obviously, measuring relevant occupant variables is not straightforward. The acceleration of the chest may be determined by measurements of the belt outlet [53], the belt force and information from ultrasonic, infrared or other sensing devices [16, 22, 24]. The acceleration of the head may be determined from measurements of relevant variables of the airbag, like pressure, and information from the earlier mentioned sensing devices.

Actuators to manipulation the restraint system components during the crash do rarely exist and will have to be developed. First, it should be investigated which location is the most appropriate to manipulate the belt force. For example, the manipulation of the belt force near the buckle may be more effective than near the load limiter. Second, actuators are to be developed. To manipulate the belt force, actuators in which a fluid is squeezed through a controlled restriction or in which the viscosity of the fluid [78] or the volume of the cylinder that contains the fluid [147] is controlled, are promising and should be developed further. For the airbag, the amount of gas flowing into the airbag and the amount

of gas flowing out of the airbag should be manipulated by the size of a vent within the inflator and one in the airbag. For that purpose, the patented ideas [69] and [167] are promising and further developments should be encouraged.

As mentioned in Chapter 1, costs of transport crashes are extremely high, over 170 billion Euros in 2001. Based on statistical analyses [117] of real world crashes and experimental data, an estimate of the economic cost of a single crash can be calculated from, amongst others, the adopted measures for the risk of injuries [46]. Using the results of Chapter 4, the estimated cost of the crash reduces from 46 042 Euros with the original restraint system to 7 824 Euros with the active restraint system. It may therefore be concluded that the field of active restraint systems is interesting, not only for (academic) research, but also for developments with a more industrial and commercial perspective.



# Bibliography

- [1] —, 2003. [Online]. <http://www.crashtest.com>
- [2] —, “European New Car Assessment Program,” 2003. [Online]. <http://www.euroncap.com>
- [3] —, “CARE,” 2004. [Online]. <http://www.europa.eu.int/comm/transport/care/statistics/>
- [4] D. Adomeit and A. Heger, “Motion sequence criteria and design proposals for restraint devices in order to avoid unfavorable biomechanic conditions and submarining,” SAE Technical Paper nr. 751146, Society of Automotive Engineers, Warrendale, PS, USA, 1975.
- [5] M. D. Aldman, “The early history of the lap and shoulder threepoint safety belt,” June 1998. [Online]. [http://www.autoliv.com/appl\\_alv/autoliv.nsf/pages/research\\_reports](http://www.autoliv.com/appl_alv/autoliv.nsf/pages/research_reports)
- [6] K. J. Åström and T. Hägglund, *PID Controllers: Theory, Design, and Tuning*, 2nd ed. Instrument Society of America, 1995, ISBN 1-55617-516-7.
- [7] F. Azimzadeh, O. Galán, and J. Romagnoli, “On-line optimal trajectory control for a fermentation process using multi-linear models,” *Computers and Chemical Engineering*, vol. 25, pp. 15 – 26, 2001.
- [8] F. A. Bandak, P. C. Chan, K. H. Ho, and Z. Lu, “An experimental air bag test system for the study of air bag deployment loads,” *International Journal of Crashworthiness*, vol. 7, no. 2, pp. 129 – 165, 2002.
- [9] R. Bandstra, U. Meissner, C. Y. Warner, S. Momoghan, R. Mendelsohn, and D. MacPherson, “Seat-belt injuries in medical and statistical perspectives,” in *Proceedings of the 16th International Technical Conference on Experimental Safety Vehicles*, Windsor, Canada, May 1998, paper nr. 98-S6-W-25.
- [10] J. Bao, J. F. Forbes, and P. J. McLellan, “Robust multiloop PID controller design: a successive semidefinite programming approach,” *Industrial and Engineering Chemistry Research*, vol. 38, no. 9, pp. 3407 – 3419, 1999.
- [11] N. E. Bedewi, D. Marzougui, and V. Motevalli, “Evaluation of parameters affecting simulation of airbag deployment and interaction with occupants,” *International Journal of Crashworthiness*, vol. 1, no. 4, pp. 339 – 354, 1996.
- [12] A. Bemporad, “Reference governor for constrained non-linear systems,” *IEEE Transactions on Automatic Control*, vol. 43, no. 3, pp. 415 – 419, 1998.
- [13] A. Bemporad, A. Casavola, and E. Mosca, “Nonlinear control of constrained linear systems via predictive reference management,” *IEEE Transactions on Automatic Control*, vol. 42, no. 3, pp. 340 – 349, 1997.
- [14] A. Bemporad and E. Mosca, “Fulfilling hard constraints in uncertain linear systems by reference managing,” *Automatica*, vol. 34, no. 4, pp. 451 – 416, 1998.
- [15] S. Birch, “Safety and its progress,” *Automotive Engineering*, vol. 101, no. 9, pp. 33 – 35, 1993.
- [16] S. Birch, “Smarter airbags from Jaguar,” *Automotive Engineering International*, vol. 108, no. 11, pp. 75 – 75, November 2000.
- [17] S. Birch, “Pre-Safe headlines S-class revisions,” *Automotive Engineering International*, vol. 111, no. 1, pp. 15 – 17, January 2003.
- [18] T. J. J. van den Boom and T. C. P. M. Backx, “Model predictive control,” Lecture Notes for the Dutch Institute of Systems and Control, Winterterm 2003 – 2004.
- [19] O. H. Bosgra, “Physical modelling for systems and control,” Lecture Notes for the Eindhoven University of Technology, Department of Mechanical Engineering, 2004.
- [20] O. H. Bosgra, H. Kwakernaak, and G. Meinsma, “Design methods for control systems,” Lecture Notes for the Dutch Institute of Systems and Control, Winterterm 2002 – 2003.



- [21] O. Boström and Y. Håland and K. Bohmann and A. Kullgren and M. Krafft, "New AIS1 long-term neck injury criteria candidates based on real frontal crash analysis," in *Proceedings of the 2000 International IRCOBI Conference on the Biomechanics of Impact*, Montpellier, France, September 2000, pp. 249 – 264.
- [22] S. Boverie, M. Devy, and F. Lerasle, "Comparison of structured light and stereovision sensors for new airbag generations," *Control Engineering Practice*, vol. 11, pp. 1413 – 1421, November 2003.
- [23] G. E. P. Box, W. G. Hunter, and J. S. Hunter, *Statistics for Experimenters: An Introduction to Design, Data Analysis and Model Building*. New York, New York, USA: John Wiley & Sons, Inc., 1978, ISBN 0-471-09315-7.
- [24] D. S. Breed, L. Summers, J. Carlson, and M. Koyzreff, "Development of an occupant position sensor system to improve frontal crash protection," in *Proceedings of the 17th International Technical Conference on Experimental Safety Vehicles*, Amsterdam, The Netherlands, June 2001, paper nr. 325.
- [25] E. H. Bristol, "On a new measure of interaction for multivariable process control," *IEEE Transactions on Automatic Control*, vol. 11, pp. 133 – 134, 1966.
- [26] S. J. Brown, S. Larry, and M. Tarczynski, "Inflator capable of modulating airbag inflation rate in a vehicle occupant restraint apparatus," World Patent, August 1998, WO 98/33684.
- [27] M. Bunse, A. Kuttenberger, and M. Theisen, "Precrash sensing by use of a radar-based surround sensing system," in *Proceedings of Airbag 2000*, Karlsruhe, Germany, May 2002, pp. 9–1 – 9–16.
- [28] D. G. Buzeman, D. C. Viano, and P. Lövsund, "Car occupant safety in frontal crashes: A parameter study of vehicle mass, impact speed, and inherent vehicle protection," *Accident Analysis and Prevention*, vol. 30, no. 6, pp. 713 – 722, June 1998.
- [29] D. G. Buzeman, D. C. Viano, and P. Lövsund, "Injury probability and risk in frontal crashes: Effects of sorting techniques on priorities of offset testing," *Accident Analysis and Prevention*, vol. 30, no. 5, pp. 583 – 595, May 1998.
- [30] M. G. McCarthy and B. P. Chinn and J. Hill, "The effect of occupant characteristics on injury risk and the development of active-adaptive restraint systems," in *Proceedings of the 17th International Technical Conference on Experimental Safety Vehicles*, Amsterdam, the Netherlands, June 2001, paper nr. 314.
- [31] C. Y. Chan, "A treatise on crash sensing for automotive air bag systems," *IEEE Transactions on Mechatronics*, vol. 7, no. 2, pp. 220 – 234, June 2002.
- [32] M. S. Chiu and Y. Arkun, "A methodology for sequential design of robust decentralized control systems," *Automatica*, vol. 28, no. 5, pp. 997 – 1001, 1992.
- [33] J.-Y. Choi, B. H. Cho, H. F. VanLandingham, H.-S. Mok, and J.-H. Song, "System identification of power converters based on a black-box approach," *IEEE Transactions on Circuits and Systems I: Fundamental Theory and Applications*, vol. 45, no. 11, pp. 1148 – 1158, November 1998.
- [34] G. Clute, "Potentials of adaptive load limitation," in *Proceedings of the 17th International Technical Conference on Experimental Safety Vehicles*, Amsterdam, the Netherlands, June 2001, paper nr. 134.
- [35] Committee on Trauma Research, "Injury in america. A continuing public health problem," National Research Council and the Institute of Medicine, Warrendale, PS, USA, 1985.
- [36] J. Cooper and J. S. H. M. Wismans, "personal communication," TNO Automotive Safety Solutions, Delft, the Netherlands, 2004.
- [37] C. Copperthite, M. Digiacomio, R. Bishop, C. Woods, S. Gold, and R. Husband, "Variable output driver side hybrid inflator," US Patent, December 1998, US 5.851.027.
- [38] A. Danne and P. Shah, "Stochastic analysis of frontal crash model," in *Proceedings of the NAFEMS Seminar: Use of Stochastics in FEM Analyses*, Wiesbaden, Germany, May 2003.
- [39] Y. C. Deng, "How air bags and seat belts work together in frontal crashes," in *Proceedings of the 39th Stapp Car Crash Conference*, San Diego, California, USA, November 1995, pp. 11 – 18.
- [40] C. A. Desoer and Y.-T. Wang, "Foundations of feedback theory for nonlinear dynamical systems," *IEEE Transactions on Circuits and Systems*, vol. 27, no. 2, pp. 104 – 123, February 1980.
- [41] G. van Ditzhuijzen and D. Staalman and A. Koorn, "Identification and model predictive control of a slab reheating furnace," in *Proceedings of the 2002 IEEE International Conference on Control Applications*, Glasgow, UK, October 2002, pp. 361 – 366.

- [42] M. Driels, *Linear Control Systems Engineering*, 1st ed., ser. McGraw-Hill Series in Mechanical Engineering. Singapore: McGraw-Hill, 1996, ISBN 0-07-113997-4.
- [43] C. G. Economou and M. Morari, "Internal model control: 6 multiloop design," *Industrial & Engineering Chemistry Process Design and Development*, vol. 25, no. 2, pp. 411 – 419, 1986.
- [44] T. F. Edgar, W. J. Campbell, and C. Bode, "Model-based control in microelectronics manufacturing," in *38th IEEE Conference on Decision and Control*, Phoenix, Arizona, USA, December 1999, pp. 4185 – 4191.
- [45] S. A. Eker and M. Nikolaou, "Linear control of nonlinear systems: The interplay between nonlinearity and feedback," *American Institute of Chemical Engineering Journal*, vol. 48, no. 9, pp. 1957 – 1980, 2002.
- [46] R. Eppinger, E. Sun, F. Bandak, M. Haffner, N. Khaewpong, M. Maltese, S. Kuppa, T. Nguyen, E. Takhounts, R. Tannous, and A. Zhang, "Development of improved injury criteria for the assessment of advanced automotive restraint systems - II," National Highway Traffic Safety Administration, Tech. Rep., November 1999.
- [47] ESI Group, *PAM-CRASH 2000 Notes Manual*, ESI Group, Rungis-Cedex France, March 2000.
- [48] —, "Assessment protocol and biomechanical limits," European New Car Assessment Programme, Tech. Rep., January 2003.
- [49] European Transport Safety Council, "Transport safety performance in the EU: A statistical overview," 2003, ISBN 90-76024-154.
- [50] J.-P. Faldy, "The coupling phenomenon in the case of a frontal car crash," in *Proceedings of the 39th Stapp Car Crash Conference*, San Diego, California, USA, November 1995, pp. 71 – 78.
- [51] G. F. Franklin, J. D. Powell, and A. Emami-Naeini, *Feedback Control of Dynamic Systems*, 3rd ed., ser. Addison-Wesley Series in Electrical and Computer Engineering. Amsterdam: Addison-Wesley Longman, Inc., November 1993, ISBN 0-201-52747-2.
- [52] M. Galer Flyte, "Frontal impact protection: Tailoring safety system performance by the prediction of driver size and seated position," in *Proceedings of the 16th International Technical Conference on the Enhanced Safety of Vehicles*, Windsor, Canada, May 1998, paper nr. 98-S1-O09.
- [53] M. Galer Flyte and A. J. Grafton, "The development of a "smart seat" occupant size and position sensing system for the enhancement of occupant protection," *International Journal of Crashworthiness*, vol. 2, no. 2, pp. 153 – 164, 1997.
- [54] U. N. Gandhi and S. J. Hu, "Data-based approach in modeling automobile crash," *International Journal of Impact Engineering*, vol. 16, no. 1, pp. 95 – 118, 1995.
- [55] E. G. Gilbert, I. Kolmanovsky, and K. T. Tan, "Discrete-time reference governors and the non linear control of systems with state and control constraints," *International Journal of Robust and Non Linear Control*, vol. 5, pp. 487 – 504, 1995.
- [56] T. Grandfils and K. Ikels, "Improvement of occupant restraint systems using enhanced hybrid III dummy models in MADYMO-3D," in *Proceedings of the 3rd European MADYMO Users Conference*, Stuttgart, Germany, September 2001.
- [57] M. J. Grimble and A. W. Ordys, "Predictive control for industrial applications," *Annual Review in Control*, vol. 25, pp. 13 – 24, 2001.
- [58] F. Heitplatz, R. Sferco, P. Fay, J. Reim, A. Kim, and P. Prasad, "An evaluation of existing and proposed injury criteria with various dummies to determine their ability to predict the levels of soft tissue neck injury seen in real world accidents," in *Proceedings of the 17th International Technical Conference on the Enhanced Safety of Vehicles*, Nagoya, Japan, May 2003, paper nr. 504.
- [59] J. B. van Helmont and A. J. J. van der Weiden and H. Anneveld, "Design of optimal controllers for a coal fired Benson boiler based on a modified approximate realization algorithm," in *Proceedings of Application of Multivariable System Techniques*. London, UK: Elsevier, 1990, pp. 313 – 320.
- [60] R. H. A. Hensen, "Controlled mechanical systems with friction," PhD Dissertation, Technische Universiteit Eindhoven, Eindhoven, The Netherlands, 2002.
- [61] R. J. Hesselting, M. Steinbuch, F. E. Veldpaus, and S. Aulinger, "Optimization oriented modelling of airbag and belt," in *Proceedings of ISATA 2000*, Dublin, Ireland, September 2000, pp. 299 – 304, ISBN 1-902856-10-4, Paper nr. 00SAF019.
- [62] R. J. Hesselting, M. Steinbuch, F. E. Veldpaus, and T. Klisch, "Control design for safety restraint systems," in *Proceedings of the 3rd International Conference on Control Theory and Applications*, Pretoria, South Africa, December 2001, pp. 440 – 444, ISBN 981-04-4794-9.

- [63] R. J. Hesselting, M. Steinbuch, F. E. Veldpaus, and T. Klisch, "Control design of a safety restraint system," in *Proceedings of the 4th Asian Control Conference*, Singapore, September 2002, pp. 244 – 249, ISBN 981-04-6440-1.
- [64] R. J. Hesselting, M. Steinbuch, F. E. Veldpaus, and T. Klisch, "Identification and control for future restraint systems," in *42nd IEEE Conference on Decision and Control*, Maui, Hawaii, USA, December 2003, pp. 2780 – 2785.
- [65] J. W. Hetrick, "Safety cushion assembly for automotive vehicles," U.S. Patent, 5 August 1952, 2.649.311.
- [66] B. L. Ho and R. E. Kalman, "Effective construction of linear state-variable models from input/output functions," in *Proceedings of the 3rd Annual Allerton Conference on Circuit and System Theory*, Monticello, Illinois, U.S.A., 1965, pp. 449 – 459.
- [67] P. M. J. van den Hof and R. J. P. Schrama, "Identification and control - closed loop issues," *Automatica*, vol. 31, no. 12, pp. 1751 – 1770, 1995.
- [68] J. H. Hong, M. S. Mun, and S. H. Song, "An optimum design methodology development using a statistical technique for vehicle occupant safety," *Proceedings of the Institution of Mechanical Engineers*, vol. 215, no. 4, pp. 795 – 801, 2001.
- [69] B. Hussey and K. B. Johnson, "Continuously variable controlled orifice inflator," European Patent, March 1997, EP 0.763.451.
- [70] R. L. Huston, "A review of the effectiveness of seat belt systems: Design and safety considerations," *International Journal of Crashworthiness*, vol. 6, no. 2, pp. 243 – 251, 2001.
- [71] A. L. Irwin and H. J. Mertz, "Biomechanical bases for the Crabi and Hybrid III Child Dummies," in *Proceedings of the 41st Stapp Car Crash Conference*, Lake Buena Vista, Florida, USA, November 1997.
- [72] T. Iyota and T. Ishikawa, "The effect of occupant protection by controlling airbag and seatbelt," in *Proceedings of the 18th International Technical Conference on the Enhanced Safety of Vehicles*, Nagoya, Japan, May 2003, paper nr. 198.
- [73] L. Jakobsson, H. Norin, and O. Bunketorp, "In-depth study of whiplash associated disorders in frontal impacts: Influencing factors and consequences," in *Proceedings of the 2002 International IRCOBI Conference on the Biomechanics of Impact*, Munich, Germany, September 2002, ISBN 2-9514210-3-6.
- [74] H. G. Johannessen and M. Mackay, "Why "intelligent" automotive occupant restraint systems?" in *Proceedings of the 39th Annual Meeting of the AAAM*, Chicago, USA, October 1995, pp. 519 – 525.
- [75] D. Kallieris and A. Rizzetti and R. Mattern and R. Morgan and R. Eppinger and L. Keenan, "On the synergism of the driver airbag and the 3-point belt in frontal collisions," in *Proceedings of the 39th Stapp Car Crash Conference*, San Diego, California, USA, November 1995, pp. 389 – 401.
- [76] M. Kamal, "Analysis and simulation of vehicle to barrier impact," SAE Technical Paper nr. 700414, Society of Automotive Engineers, Warrendale, PS, USA, 1970.
- [77] K. Kamiji and N. Kawamura, "Study of airbag interference with out of position occupant by the computer simulation," in *Proceedings of the 17th International Technical Conference on the Enhanced Safety of Vehicles*, Amsterdam, the Netherlands, June 2001, paper nr. 374.
- [78] J. P. Karlow, "Variable level seatbelt energy management device," US Patent, Februar 2000, US 6.019.392.
- [79] R. Kent, J. Bolton, J. Crandall, P. Prasad, G. Nusholtz, H. Mertz, and D. Kallieris, "Restrained Hybrid III dummy-based criteria for thoracic hard-tissue injury prediction," in *Proceedings of the 2001 International Research Conference on the Biomechanics of Impact*, Isle of Man, United Kingdom, October 2001.
- [80] T. Klisch, "personal communication," Bayerische Motoren Werke A.G., Munich, Germany, 1999-2004.
- [81] F. Kramer, *Passive Sicherheit von Kraftfahrzeugen*, 1st ed., ser. Programm Fahrzeugtechnik. Braunschweig, Germany: Vieweg, 1998, ISBN 3-528-06915-5.
- [82] E. Kreyszig, *Advanced Engineering Mathematics*, 8th ed. Singapore: John Wiley & Sons, Inc., 1999, ISBN 0-471-33328-X.
- [83] S. Y. Kung, "A new identification and model reduction algorithm via singular value decomposition," in *Proceedings of the 12th Asilomar Conference on Circuits, Systems and Computers*, California, USA, 1978, pp. 705 – 714.

- [84] H. Kwakernaak and R. Sivan, *Modern Signals and Systems*, 1st ed. New Jersey, USA: Prentice Hall, 1991, ISBN 0-13-809252-4.
- [85] D. J. Leith and W. E. Leithead, "Survey of gain scheduling analysis & design," *International Journal of Control*, vol. 73, no. 11, pp. 1001 – 1025, 2000.
- [86] W. E. Leithead and J. O'Reilly, "Performance issues in the individual channel design of 2-input 2-output systems: Part 1. structural issues," *International Journal of Control*, vol. 54, no. 1, pp. 47 – 82, 1991.
- [87] W. E. Leithead and J. O'Reilly, "Performance issues in the individual channel design of 2-input 2-output systems: Part 2. robustness issues," *International Journal of Control*, vol. 55, no. 1, pp. 3 – 47, 1992.
- [88] W. E. Leithead and J. O'Reilly, "Performance issues in the individual channel design of 2-input 2-output systems: Part 3. non-diagonal control and related issues," *International Journal of Control*, vol. 55, no. 2, pp. 265 – 312, 1992.
- [89] M. G.-D. Leveau, "Bretelles protectrices pour voitures automobiles et autres," French Patent, October 1903, 2.649.311.
- [90] A. Lindquist and G. Picci, "Geometric methods for state space identification," *Identification, Adaptation, Learning: The Science of Learning Models from Data*, vol. F-153, pp. 1 – 69, 1996.
- [91] L. Ljung, *System Identification - Theory for the User*, 2nd ed. Upper Saddle River, USA: PTR Prentice Hall, 1999, ISBN 0-13-656695-2.
- [92] T. E. Lobdell, C. K. Kroell, D. C. Schneider, W. E. Hering, and A. M. Nahum, "Impact response of the human thorax," in *Symposium on Human Impact Response*, Warren, Michigan, USA, October 1972, pp. 201 – 245.
- [93] J. M. Maciejowski, *Predictive Control: with Constraints*, 1st ed. Essex, England: Prentice Hall, 2002, ISBN 0-201-39823-0.
- [94] M. Mackay and A. M. Hassan and J. R. Hill, "Observational studies of car occupants' positions," in *Proceedings of the 16th International Technical Conference on the Enhanced Safety of Vehicles*, Windsor, Canada, May 1998, paper nr. 98-S6-W42.
- [95] M. Mackay and S. Parkin and A. Scott, "Intelligent restraint systems: What characteristics should they have?" in *Advances in Occupant Restraint Technologies: Joint AAAM-IRCOBI Special Session*, Lyon, France, September 1994, pp. 113 – 126.
- [96] S. M. Mahmud and A. I. Alrabady, "A new decision making algorithm for airbag control," *IEEE Transactions on Vehicular Technology*, vol. 44, no. 3, pp. 690 – 697, August 1995.
- [97] J. Marczyk, *Principles of Simulation-based Computer-Aided Engineering*, 1st ed. Barcelona, Spain: Artes Gráficas Torres, 1999.
- [98] The Mathworks Inc., *The Student Edition of MATLAB Version 5.3*, Upper Saddle River, NJ 07458, 1997.
- [99] W. Medla, U. Rick, M. Nitsche, H. Maul, and B. Steeger, "Interpretation and optimization of an adaptive restraint system with special consideration for "out of position" situations," in *Proceedings of Airbag 2000*, Karlsruhe, Germany, December 2000, pp. 9–1 – 9–19.
- [100] H. J. Mertz, A. L. Irwin, J. W. Melvin, R. L. Stalnaker, and M. S. Beebe, "Size weight and biomechanical impact response requirements for adult size small female and large male dummies," SAE Technical Paper nr. 890756, Society of Automotive Engineers, Warrendale, PS, USA, 1989.
- [101] H. J. Mertz, J. E. Williamson, and D. A. van der Lugt, "The effect of limiting shoulder belt load with air bag restraint," SAE Technical Paper nr. 950886, Society of Automotive Engineers, Warrendale, PS, USA, 1995.
- [102] S. Meurant and L. Richard, "Robust analysis of a safety model," in *Proceedings of the 3rd European MADYMO Users Conference*, Stuttgart, Germany, September 2001.
- [103] H. J. Miller, "Injury reduction with smart restraint systems," in *Proceedings of the 39th Annual Meeting of the AAAM*, Chicago, USA, October 1995, pp. 527 – 541.
- [104] T. J. Monica, C.-C. Yu, and W. L. Luyben, "Improved multiloop single-input/single-output (SISO) controllers for multivariable processes," *Ind. Engineering Chemical Res.*, vol. 27, no. 6, pp. 969 – 973, 1988.

- [105] D. C. Montgomery, *Design and Analysis of Experiments*, 5th ed. New York, New York, USA: John Wiley & Sons, Inc., 2001, ISBN 0-471-26591-8.
- [106] D. C. Montgomery and G. C. Runger, *Applied Statistics and Probability for Engineers*, 3rd ed. New York, New York, USA: John Wiley & Sons, Inc., 2003, ISBN 0-471-38181-0.
- [107] M. Morari and J. H. Lee, "Model predictive control: Past, present, and future," *Computers and Chemical Engineering*, vol. 23, pp. 667 – 682, 1999.
- [108] R. Moritz, "Pre-crash sensing: Functional evolution based on short range radar sensor platform," in *Proceedings of the International Body Engineering Conference and Exposition*, Detroit, Michigan, USA, October 2000, pp. 249 – 263.
- [109] MSC.Software Corporation, *MSC.ADAMS 2003 Manuals*, MSC.Software Corporation, Michigan, USA, 2003.
- [110] M. Muser, F. Walz, and H. Zellmer, "Biomechanical significance of the rebound phase in low speed rear end impacts," in *Proceedings of the 2000 International IRCOBI Conference on the Biomechanics of Impact*, Montpellier, France, September 2000, pp. 411 – 424.
- [111] R. F. Neathery and T. E. Lobdell, "Mechanical simulation of human thorax under impact," SAE Technical Paper nr. 730982, Society of Automotive Engineers, Warrendale, PS, USA, 1972.
- [112] NHTSA, "Federal Motor Vehicle Safety Standard no. 201.," U.S. Department of Transportation, Tech. Rep. 49 CFR 571.201, 1996.
- [113] NHTSA, "Federal Motor Vehicle Safety Standard no. 210: Seat belt assembly anchorages," U.S. Department of Transportation, Tech. Rep. 49 CFR 571.210, 1996.
- [114] NHTSA, "Federal Motor Vehicle Safety Standard no. 572.6: Anthropomorphic test devices; head," U.S. Department of Transportation, Tech. Rep. 49 CFR 571.571, 1996.
- [115] NHTSA, "Laboratory test procedure frontal impact testing," U.S. Department of Transportation, Tech. Rep. NHTSA-99-4962-37, 1999.
- [116] NHTSA, "Traffic safety facts 2000 - overview," U.S. Department of Transportation, Tech. Rep. DOT HS 809 329, 2000.
- [117] NHTSA, "The economic impact of motor vehicle crashes, 2000," U.S. Department of Transportation, Tech. Rep. DOT HS 809 446, 2002.
- [118] J. J. Nieboer, J. S. H. M. Wismans, and E. Fraterman, "Status of the MADYMO 2D airbag model," in *Proceedings of the 32nd Stapp Car Crash Conference*, Atlanta, USA, 1988.
- [119] A. Niederlinski, "A heuristic approach to the design of linear multivariable interacting control systems," *Automatica*, vol. 7, pp. 691 – 701, 1971.
- [120] M. Nikolaou and P. Misra, "Linear control of nonlinear processes: Recent developments and future directions," *Computers and Chemical Engineering*, vol. 27, pp. 1043 – 1059, 2003.
- [121] S. J. Norquay, A. Palazoglu, and J. Romagnoli, "Application of Wiener model predictive control (WMPC) to an industrial C2-splitter," *Journal of Process Control*, vol. 9, pp. 461 – 473, 1999.
- [122] G. S. Nusholtz, D. Wang, and E. B. Wylie, "An evaluation of airbag tank-test results," SAE Technical Paper nr. 980864, Society of Automotive Engineers, Warrendale, PS, USA, 1998.
- [123] M. Ostertag, E. Nock, and U. Kiencke, "Optimization for airbag release algorithms using evolutionary strategies," in *Proceedings of the 4th IEEE Conference on Control Applications*, Albany, NY, USA, September 1995, pp. 275 – 280.
- [124] P. van Overschee and B. de Moor, *Subspace Identification for Linear Systems: Theory, Implementation and Applications*, 1st ed. Boston, USA: Kluwer Academic Publishers, May 1996, ISBN 0-7923-9717-7.
- [125] L. Özkan, M. V. Kothare, and C. Georgakis, "Control of a solution copolymerization reactor using multi-model predictive control," *Chemical Engineering Science*, vol. 58, pp. 1207 – 1221, 2003.
- [126] H. Peng, T. Ozaki, Y. Toyoda, H. Shioya, K. Nakano, V. Haggan-Ozaki, and M. Mori, "RBF-ARX model-based nonlinear system modeling and predictive control with application to a NO<sub>x</sub> decomposition process," *Control Engineering Practice*, vol. 12, pp. 191 – 203, 2004.
- [127] B. Pipkorn and M. Eriksson, "A method to evaluate the validity of mathematical models," in *Proceedings of the 4th European MADYMO Users Meeting*, Brussels, Belgium, October 2003.
- [128] P. Prasad, "Comparative evaluation of the MVMA2D and the MADYMO 2D occupant simulation models with MADYMO-test comparisons," in *Proceedings of the 10th International Technical Conference on the Experimental Safety Vehicles*, Oxford, England, 1985, pp. 480 – 487.

- [129] S. J. Qin and T. A. Badgwell, "A survey of industrial model predictive control technology," *Control Engineering Practice*, vol. 11, pp. 733 – 764, 2003.
- [130] R. Reuter and R. Hoffmann, "Bewertung von Berechnungsergebnissen mittels stochastischer Simulation," in *Tagung der Berechnung und Simulation im Fahrzeugbau*, Würzburg, Germany, 2000, pp. 697 – 719, VDI Band 1559.
- [131] D. H. Robbins, "Development of anthropometrically based design specifications for an advanced adult anthropomorphic dummy family. Volume 2: Anthropomorphic specifications for mid-sized male dummy," The University of Michigan Transportation Research Institute, Ann Arbor, Michigan, USA, Tech. Rep. UMTRI-83-53-2, 1983.
- [132] R. Y. Rubinstein, *Simulation and the Monte Carlo Method*, 1st ed. USA: John Wiley & Sons, Inc., 1981, ISBN 0-471-08917-6.
- [133] W. J. Rugh and J. S. Shamma, "Survey paper: Research on gain scheduling," *Automatica*, vol. 36, pp. 1401 – 1425, 2000.
- [134] L. Rundqwist, "Anti-windup reset for PID controllers," in *Preprints 11th IFAC World Congress*, Tallinn, Estonia, 1990.
- [135] S. Schaub and A. C. Bosio, "Intelligente Rückhaltesysteme für den europäischen Markt," in *Tagung der innovativer Insassen- und Partnerschutz im PKW*. Berlin, Germany: VDI, 1998, pp. 145 – 153, ISBN 3-18-091354-1.
- [136] T. S. Schei and P. Stingstad, "Nonlinear model predictive control of a batch polymerization process," in *Proceedings of the American Control Conference*, Philadelphia, Pennsylvania, USA, June 1998, pp. 3381 – 3385.
- [137] C. van Schie, "Lineariseren van bewegingsvergelijking met betrekking tot multibody-systemen," Master's thesis, Technische Universiteit Eindhoven, Eindhoven, the Netherlands, October 1992, WFW 92.102.
- [138] C. van Schie, "personal communication," TNO MADYMO B.V., Delft, the Netherlands, 1999-2004.
- [139] H. Schmidt, "Model based design of decentralized control configurations," PhD Dissertation, Royal Institute of Technology, Stockholm, Sweden, 2002, ISBN 91-7283-290-8.
- [140] L. W. Schneider, D. H. Robbins, M. A. Pfueg, and R. G. Snyder, "Development of anthropometrically based design specifications for an advanced adult anthropomorphic dummy family. Volume 1: Anthropometry of motor vehicle occupants," The University of Michigan Transportation Research Institute, Ann Arbor, Michigan, USA, Tech. Rep. UMTRI-83-53, 1983.
- [141] R. Schöneburg and K.-H. Baumann and R. Justen, "Pre-safe: The next step in the enhancement of vehicle safety," in *Proceedings of the 18th International Technical Conference on Experimental Safety Vehicles*, Nagoya, Japan, May 2003, paper nr. 410.
- [142] B. de Schutter, "Minimal state-space realization in linear system theory: an overview," *Journal of Computational and Applied Mathematics*, vol. 121, no. 1 - 2, pp. 331 – 354, January 2000, special Issue on Numerical Analysis in the 20th Century: Vol I, Approximation Theory.
- [143] P. Shah, "Stability of the E46/4," BMW A.G., München, Germany, Tech. Rep. 260.4764, March 2002, *confidential*.
- [144] F. Shokoohi, "Airbag sensor fire time: Occupant performance criterion," SAE Technical Paper nr. 950873, Society of Automotive Engineers, Warrendale, PS, USA, 1995.
- [145] S. Skogestad and M. Morari, "Implications of large RGA elements on control performance," *Industrial and Engineering Chemistry Research*, vol. 26, no. 11, pp. 2323 – 2330, 1987.
- [146] K. J. Smith, R. W. Pratt, K. Newby, J. Cogrove, and P. Sellars, "A comparison of multivariable control and sequential loop closure control in a dynamic structural test system: Design and implementation," in *Proceedings of the American Control Conference*, Seattle, Washington, USA, June 1995, pp. 1474 – 1478.
- [147] A. Smithson, D. Blackadder, J. Taylor, A. Downie, J. Harte, A. Park, and E. Rees, "Load limiting device for a seat belt," US Patent, March 6 2001, US 6.196.589.
- [148] A. R. M. Soeterboek, *Predictive Control - A unified Approach*, 1st ed. Englewood Cliffs, Prentice Hall, 1992, ISBN 0-136783-03.
- [149] M. Steinbuch and M. L. Norg, "Advanced motion control: An industrial perspective," *European Journal of Control*, vol. 4, pp. 278 – 293, 1998.

- [150] D. E. Struble, "Airbag technology: What it is and how it came to be," SAE Technical Paper nr. 980648, Society of Automotive Engineers, Warrendale, PS, USA, 1998.
- [151] S. L. Stucki, W. t. Hollowell, and S. Fessahaie, "Determination of frontal offset test conditions based on crash data," in *Proceedings of the 16th International Technical Conference on Experimental Safety Vehicles*, Windsor, Canada, May 1998, paper nr. 98-S1-O-02.
- [152] A. F. Tencer, S. Mirza, and P. Huber, "The response of the MADYMO 50th percentile male human model, human volunteers and cadaveric specimens: A comparison in rear end impact," in *Proceedings of 9th International MADYMO User Conference*, Como, Italy, October 2002.
- [153] TNO Automotive, *MADYMO Version 5.4 Manuals*, TNO Road-Vehicles Research Institute, Delft, The Netherlands, November 1999.
- [154] TNO Automotive, *MADYMO Version 5.4 Manuals: 3D Dummy Databases*, TNO Road-Vehicles Research Institute, Delft, The Netherlands, November 1999.
- [155] TNO Automotive, *MADYMO Version 5.4 Manuals: Theory Manual*, TNO Road-Vehicles Research Institute, Delft, The Netherlands, November 1999.
- [156] TNO Automotive, *MADYMO Version 5.4 Manuals: User's Manual 3D*, TNO Road-Vehicles Research Institute, Delft, The Netherlands, November 1999.
- [157] S. Tokoro, K. Kuroda, T. Nagao, T. Kawasaki, and T. Yamamoto, "Pre-crash sensor for pre-crash safety," in *Proceedings of the 18th International Technical Conference on Experimental Safety Vehicles*, Nagoya, Japan, May 2003, paper nr. 545.
- [158] A. A. Tyagunov, "High-performance model predictive control for process industry," PhD Dissertation, Technische Universiteit Eindhoven, Eindhoven, The Netherlands, 2004.
- [159] P. Ullrich, "Simulationsmethoden und Modellierungstechniken für die Entwicklung von "Advanced Airbags", in *Proceedings of Airbag 2000*, Karlsruhe, Germany, December 2000, pp. 6–1 – 6–17.
- [160] M. S. Varat and S. E. Husher, "Vehicle impact response analysis through the use of accelerometer data," SAE Technical Paper nr. 2000-01-0850, Society of Automotive Engineers, Warrendale, PS, USA, 2000.
- [161] M. Viberg, "Subspace-based methods for the identification of linear time-invariant systems," *Automatica*, vol. 31, no. 12, pp. 1835 – 1851, 1995.
- [162] M. van de Wal and B. de Jager, "A review of methods for input/output selection," *Automatica*, vol. 37, pp. 487 – 510, 2001.
- [163] J. T. Wang and D. J. Nefske, "A new CAL3D airbag inflation model," SAE Technical Paper nr. 880654, Society of Automotive Engineers, Warrendale, PS, USA, 1988.
- [164] Q. C. Wang, T. H. Lee, and Y. Zhuang, "Multi-loop version of the modified ziegler-nichols method for two input two output process," *Industrial and Engineering Chemistry Research*, vol. 37, no. 12, pp. 4725 – 4733, 1998.
- [165] K. Watanabe, Y. Umezawa, and K. Abe, "Advanced passive safety system via prediction and sensor fusion," in *IEEE Vehicle Navigation and Information Systems Conference Proceedings*, Yokohama, Japan, August 1994, pp. 435 – 440.
- [166] C. L. Wendell, "Deflagration venting system for airbag systems," US Patent, May 1999, US 5.899.494.
- [167] G. Winkler and M. Frimberger, "Gassack mit einer in ihrem Öffnungsquerschnitt geregelten Abströmöffnung," German Patent, June 2002, DE 109.59.956.
- [168] J. S. H. M. Wismans, E. G. Janssen, M. Beusenberg, W. P. Koppens, and H. A. Lupker, "Injury Biomechanics," Lecture Notes for the Eindhoven University of Technology, Department of Mechanical Engineering, 1994.
- [169] M. F. Witcher and T. J. McAvoy, "Interacting control systems: Steady-state and dynamic measurement of interaction," *ISA Transactions*, vol. 16, no. 1, pp. 35 – 41, 2002.
- [170] H. Yajima, A. Nozaki, Q. Yu, and M. Shiratori, "Influence on injury criteria of occupant restraint system," in *Proceedings of SAE World Congress*, Detroit, Michigan, USA, March 2000, SAE Technical Paper nr. 2000-01-0623.
- [171] K. Yamuna Rani and H. Unbehauen, "Study of predictive controller tuning methods," *Automatica*, vol. 33, no. 12, pp. 2243 – 2248, December 1997, brief Paper.

- 
- [172] F. Zeidler and F. Knöchelmann, "The influence of frontal crash test speeds on the compatibility of passenger cars in real world accidents," *International Journal of Crashworthiness*, vol. 3, no. 1, pp. 7 – 15, 1998.
- [173] D. Zhang and J. Cooper, "Folding of 3D airbags used in restraint system simulation," in *Proceedings of the 5th MADYMO Users Meeting of the Americas*, Troy, Michigan, USA, October 2003.
- [174] H. Zhang, C. S. Parenteau, D. Katta, and S. V. Raman, "Applications of human body model in a vehicle environment," in *Proceedings of the 9th International MADYMO User Conference*, Como, Italy, 2002.





# Samenvatting

Belangrijk nadelen van gemotoriseerd verkeer zijn ongelukken met dodelijke afloop en ongevallen die ernstig lichamelijk letsel tot gevolg hebben. Om het aantal doden en het lichamelijk letsel te reduceren zijn de veiligheidsgordel en de airbag, oftewel het “restraint system”, geïntroduceerd. Het gedrag van het restraint system dient zich in het ideale geval aan te passen aan de karakteristieken van de botsing en de inzittende. Moderne restraint systems zijn “adaptief”. Dit betekent dat zij in beperkte mate hun eigenschappen, bijvoorbeeld de deformatiekenmerken van de gordelkrachtbegrenzer en het tijdstip waarop de airbag in werking treedt, kunnen aanpassen.

Het doel bij het bepalen van dergelijke eigenschappen is het behalen van een acceptabel letselrisico voor groepen van botsingen en inzittenden. Indicatoren voor dit letselrisico zijn onder andere de maximale versnelling en indrukking van de borstkas, en de maximale versnelling van het hoofd. Normaliter worden de meest geschikte eigenschappen bepaald door deze indicatoren te minimaliseren. Hiertoe wordt gebruikt gemaakt van complexe niet-lineaire modellen van het voertuig en de inzittende tijdens het botsing. Een dergelijke aanpak is echter tijdrovend en de verkregen eigenschappen zijn een compromis.

In dit proefschrift wordt een innovatieve visie op restraint systems uitgewerkt. Het toevoegen van sensoren en actuatoren maakt het mogelijk het gedrag van het restraint system te regelen. De airbag en/of de gordel worden tijdens de botsing gemanipuleerd zodat één of meerdere, voor het letselrisico relevante variabelen van de inzittende een tevoren vastgesteld referentiesignaal volgen. Dit referentiesignaal weerspiegelt het laagst haalbare letselrisico. Deze visie vormt een uitgangspunt voor de verbetering van huidige en de ontwikkeling van toekomstige restraint systems.

Bij het uitwerken van deze visie op “actieve” restraint systems is gebruik gemaakt van een numeriek model. Dit model beschrijft het gedrag van een dummy als de mannelijke “bestuurder” van gemiddelde grootte van een middenklasse auto tijdens de frontale US-NCAP bots proef. De airbag wordt gemanipuleerd door de grootte van de luchtopening in en de massa stroom naar de airbag te beïnvloeden. Het gedrag van de gordel wordt beïnvloed door het manipuleren van de trekkracht in de gordel bij de gordelkrachtbegrenzer. De te regelen variabelen van de inzittende zijn de versnelling en de indrukking van de borstkas, en de versnelling van het hoofd. Referentiesignalen voor deze variabelen worden op pragmatische wijze geconstrueerd.

Het beschikbare numerieke model is ongeschikt voor het ontwerp van regelaars, aange-

zien het niet-lineair en complex is. Daarom zijn lineaire tijdsonafhankelijke modellen afgeleid om het relevante gedrag van de airbag, de gordel, de dummy en de onderlinge interacties te benaderen. Deze eenvoudige modellen zijn verkregen met “approximate realization”. Hiertoe is gebruik gemaakt van responsies in de variabelen van de inzittende op stapsgewijze verstoringen in de gemanipuleerde variabelen van het restraint system. Middels “loopshaping” technieken zijn regelaars van een lage orde ontworpen die moeten resulteren in een stabiel gesloten-lus systeem met acceptabele performance. Tenslotte worden de ontworpen regelaars geëvalueerd door ze toe te passen op het complexe, niet-lineaire model.

Het letselrisico wordt significant gereduceerd door de toepassing van het “actieve” restraint system, in vergelijking met het oorspronkelijke restraint system. Het regelen van de borstkas versnelling door manipulatie van de gordelkracht verlaagt het letselrisico met 60 %. Bij het regelen van de versnelling van het hoofd door manipulatie van de grootte van de luchtopening wordt het letselrisico met 50 % verminderd. Het gelijktijdig regelen van de versnelling van de borstkas en het hoofdversnelling leidt tot een afname met minstens 50 % van het letselrisico.

De aanpak blijkt tevens succesvol voor het ontwerp van een regelaar die de indrukking van de borstkas regelt door manipulatie van de gordelkracht. Daarnaast is de aanpak succesvol om regelaars te ontwerpen die de borst- en hoofdversnelling van een kleine, vrouwelijke dummy als de “bestuurder” regelen.

De behaalde resultaten maken het plausibel dat het dynamisch gedrag van de airbag en/of de gordel, de dummy en de interacties als lineair beschouwd mag worden bij het ontwerpen van regelaars. Het is gebleken dat lage orde regelaars het gewenste gedrag van het gesloten-lus systeem met het complexe niet-lineaire model effectief kunnen afdwingen. Ook is gebleken dat interacties tussen de gelijktijdige regeling van de versnelling van het hoofd en van de borstkas te verwaarlozen is. De beide regelaars kunnen daarom onafhankelijk van elkaar ontworpen worden. De beschreven aanpak is effectief en efficiënt en de hiermee verkregen resultaten geven inzicht in de gewenste eigenschappen van het restraint system.

# Kurzfassung

Wichtige Nachteile des motorisierten Straßenverkehrs sind Unfälle sowie deren Folgen wie Verletzungen und Tötungen. Sicherheitsgurt und Airbag, Rückhaltesystem genannt, tragen dazu bei, die Häufigkeit und Schwere der Verletzungen effektiv zu reduzieren. Das Rückhaltesystem sollte sich je nach Unfalltyp und Insasse unterschiedlich verhalten. Moderne Rückhaltesysteme sind bereits "adaptiv", das heißt die Eigenschaften können in begrenztem Umfang an den Insassen und Unfalltyp angepasst werden. Beispiele für diese Eigenschaften sind unterschiedliche Deformationskennungen des Gurtkraftbegrenzers und die unterschiedlichen Zeitpunkte, zu denen der Airbag ausgelöst wird.

Der Entwurf solcher Eigenschaften zielt auf ein akzeptables Verletzungsrisiko für Klassen von Insassen und Unfällen. Maßstäbe für das Verletzungsrisiko sind unter anderem die maximale Brust- und Kopfbeschleunigung sowie die maximale Brusteingdrückung. Geeignete Eigenschaften werden in der Regel durch die Minimierung des Verletzungsrisikos bestimmt, wobei komplexe nicht-lineare Modelle zur Simulation des Insassen und des Fahrzeugs bei einem Crashtest verwendet werden. Die auf diese Weise bestimmten Eigenschaften stellen jedoch einen Kompromiss dar, deren Entwurf zeitintensiv ist.

In dieser Arbeit wird eine innovative Sicht auf Rückhaltesysteme ausgearbeitet. Sensoren und Aktuatoren werden dabei dem Rückhaltesystem hinzugefügt, wodurch eine Feedback Regelung realisiert werden kann. A priori wird für eine oder mehrere Variablen eine Referenzkurve definiert, die dem niedrigsten Verletzungsrisiko entspricht. Die Rückhaltesystem-Komponenten werden während des Crashes so beeinflusst, dass der Referenzkurve gefolgt wird. Diese Sicht auf Rückhaltesysteme kann als Grundlage für zukünftige Entwicklungen betrachtet und als effektives Werkzeug für den Entwurf von Eigenschaften der Rückhaltesystem-Komponente eingesetzt werden.

Das Konzept der "aktiven" Rückhaltesysteme wurde unter Anwendung des numerischen Modells eines Dummys als durchschnittlich grosser männlicher Fahrer eines mittelgroßen Fahrzeugs in einem US-NCAP Crashtest erarbeitet. Um den Airbag zu beeinflussen wurde die Größe der Ausströmöffnung und der Massenstrom des Gasgenerators gewählt. Zur Beeinflussung des Gurts wurde die Kraft im Gurtabschnitt in der Nähe des Gurtkraftbegrenzers gewählt. Die zu regelnden Variablen des Insassen sind die Brust- und Kopfbeschleunigung sowie die Brusteingdrückung. Die zugehörigen Referenzkurven werden pragmatisch bestimmt.

Regler zur Beeinflussung von Airbag oder Gurt können nicht mit Hilfe des verfü-

baren numerischen Modells entworfen werden, da dieses nicht-linear und zu komplex ist. Aus diesem Grund werden lineare zeit-unabhängige Modelle für den Reglerentwurf hergeleitet, um das relevante dynamische Verhalten der Rückhaltesystem-Komponenten, des Dummys und deren Interaktion anzunähern. Diese Modelle werden mit der "Approximate Realization" erstellt, unter Verwendung von Antworten der Insassenvariablen auf Sprünge in den beeinflussten Variablen des Rückhaltesystems. Feedback-Regler niedriger Ordnung werden unter Verwendung von Loopshaping-Methoden entworfen, um einen stabilen geschlossenen Regelkreis mit ausreichender Regelgüte zu erzielen. Am Ende werden die Regler in dem Regelkreis mit dem komplexen nicht-linearen Modell implementiert und evaluiert.

Im Vergleich mit dem ursprünglichen Rückhaltesystem kann die Regelung der Brustbeschleunigung durch Beeinflussung der Gurtkraft das Risiko von Brustverletzungen um 60 % verringern. Die Regelung der Kopfbeschleunigung durch Beeinflussung der Ausströmöffnung senkt das Risiko von Kopfverletzungen um 50 %. Die gleichzeitige Regelung der Brust- und Kopfbeschleunigung reduziert das Risiko von Kopf- und Brustverletzungen um mindestens 50 %.

Die Modellierungs- und Reglerentwurfsstrategie werden auch erfolgreich auf den Entwurf eines Reglers für die Brusteingdrückung mittels Beeinflussung der Gurtkraft angewendet. Darüber hinaus werden die Strategien erfolgreich für einen Regler der Brust- und Kopfbeschleunigung für den kleinen weiblichen Dummy auf dem Fahrersitz angewendet.

Es zeigt sich, dass das dynamische Verhalten des Rückhaltesystems das mit dem Dummy interagiert, als linear betrachtet werden kann, zumindest im Bezug auf den Reglerentwurf. Zudem wird die Effektivität von Feedback-Reglern niedriger Ordnung im Hinblick auf das gewünschte Verhalten des komplexen nicht-linearen Modells gezeigt. Des Weiteren stellt sich heraus, dass das Reglerentwurfssproblem für die gleichzeitige Regelung der Kopf- und Brustbeschleunigung mittels Beeinflussung der Ausströmöffnung und der Gurtkraft als ein entkoppeltes Reglerentwurfssproblem betrachtet werden kann. Die Modellierungs- und Reglerentwurfsstrategie erweisen sich als effektiv und effizient. Aus den erzielten Ergebnissen können Aussagen über geeignete Eigenschaften für adaptive Rückhaltesysteme getroffen werden.

# Dankwoord

Graag wil ik de personen bedanken die hebben bijgedragen aan dit proefschrift. Allereerst Jan Kok en Hennes Baldauf, die mij de kans hebben gegeven om als promovendus te beginnen, oftewel “die mir die Möglichkeit gegeben haben, die Doktorarbeit anzufangen”. Maarten Steinbuch, Frans Veldpaus en Thomas Klisch wil ik bedanken, niet alleen voor hun grote bijdrage aan de inhoud van dit proefschrift, maar ook voor de ondersteuning bij het overbruggen van het spanningsveld tussen de industrie en de universiteit. Daarnaast wil ik Maarten bedanken voor zijn enthousiasme, goede ideeën en de peptalk. Frans, jou wil ik bedanken voor je kritische blik, de nuttige discussies en je onvermoeibaarheid bij het hanteren van de “rode pen”. Thomas bin ich nicht nur wegen der fachlichen Diskussionen dankbar, sondern auch wegen dem Vertrauen, der Unterstützung und nicht zuletzt unserer Freundschaft. Paul van den Bosch, Okko Bosgra en Jac Wismans ben ik dankbaar voor het zetten van de puntjes op de “i”.

Een woord van dank gaat ook uit naar Cees van Schie voor zijn interesse in mijn project en het (in zijn vrije tijd) oplossen van problemen met de koppeling van MADYMO met MATLAB/SIMULINK. Ausserdem möchte ich Sven Link und Wolf Bartelheimer danken für die Interesse und Mithilfe.

De studenten Bart Consten, Hans Dekker, Arjen den Hamer, Bart Peeters Weem en Geert van der Zalm hebben niet alleen een waardevolle bijdrage geleverd, maar ook voor plezier en afleiding gezorgd. Dank daarvoor.

En dan zijn er de personen wiens bijdrage tussen de regels door te lezen is. Naast mijn ex-kamergenoten, wil ik Eric van den Bosch (Erich), Dave Brands (Plukmans), François Debiesme (Belg), Rogier Ellenbroek (Onderbroek), Rob Fey, Jan van Helvoirt (Keu-metkrullen), Tim Klaassen (Time) en Lia Neervoort-Sanders bedanken. Vanaf deze plek wil ik naast Jan, ook zijn ouders bedanken voor het (denk)werk voor de kaft.

Bas, Erik, Natasja, Frank, Patrick en Xander, bedankt voor de afwisseling en relativering. Amsterdammers zijn voor Limburgers een hele ervaring [60]. Maurice Heemels (Himmels) en Ronnie Hensen (Hensenius) zijn dat echter ook voor mij. Daarnaast hebben ze mij geleerd dat de beste inter-provinciale integratie in de kroeg plaatsvindt. Anja, ich bin dir nicht nur sehr dankbar für deine Gastfreundschaft und die Balkon-Gespräche, sondern auch für unsere Freundschaft. Jaimie, simpel maar waar, bedankt voor alles.

Tot slot zijn er de personen die het dichtst bij me staan. Pap, Mam, Broer. . . bedankt.

Rogier



# Curriculum Vitae

Rogier Hesselting was born on the 8th of August 1976 in Amsterdam, the Netherlands. In 1994, he finished his secondary education at the Damstede College in Amsterdam. Due to his interests in technology, he chose the study Mechanical Engineering at the Technische Universiteit Eindhoven, where he obtained his Master's degree in 1999. As a part of the study, he wrote the thesis entitled "Methode zur Optimierung von Rückhalte-systeme, unter Berücksichtigung variabler Lastfällen und Insassen", resulting from his research in close collaboration with the Advanced Safety Engineering Group of BMW, Munich, Germany. During the master project, it became clear that the feedback control for (design of) restraint systems could be effective. With this motivation, he became in 1999 a Ph.D. student under the supervision of prof. dr. ir. Maarten Steinbuch at the Technische Universiteit Eindhoven in the Netherlands. The Ph.D. project, conducted in close co-operation with BMW, resulted in this thesis.